DISSERTATION

INTEGRATED ASSESSMENT OF WATER SHORTAGE UNDER CLIMATE, LAND USE, AND ADAPTATION CHANGES IN THE CONTIGUOUS UNITED STATES

Submitted by

Ahmed AbdelTawab Fahmy AbdelMeged Gharib

Department of Civil and Environmental Engineering

In partial fulfillment of the requirements

For the Degree of Doctor of Philosophy

Colorado State University

Fort Collins, Colorado

Spring 2024

Doctoral Committee:

Advisor: Mazdak Arabi

Christopher Goemans
Sybil Sharvelle
Travis Warziniack

ABSTRACT

INTEGRATED ASSESSMENT OF WATER SHORTAGE UNDER CLIMATE, LAND USE, AND ADAPTATION CHANGES IN THE CONTIGUOUS UNITED STATES

Water scarcity is a critical global challenge. Water managers pursue water supply- and demand-side strategies, including construction or enhancement of water supply systems, conservation, and water reuse, to address water security driven by changes in climate, population, and land use. However, the effects of these strategies to mitigate future water shortages under dynamic climate and socioeconomic conditions at various spatial and temporal scales remain unclear. The overarching goal of this dissertation is to (1) improve understanding of the interconnections and interactions between climate, socioeconomic, hydrological, and institutional factors that influence water shortage at the river basin level, and (2) conduct an integrated assessment of water and land use management strategies. The dissertation is organized into three research studies. The first study explores water shortages in the South Platte River Basin (SPRB) and the potential benefits of investing in storage infrastructure and demand management strategies. The second study develops a methodology to understand the interactions between land use planning, water demands, shortage vulnerability, and effects on associated economic value. The third study expands the integrative assessment framework to assess changes in water demand, supply, and withdrawals, and identify effective mitigation strategies across river basins in the Contiguous United States over a range of climatic and socioeconomic pathways that are forecasted for the coming decades.

In the first study, we develop data analysis and modeling tools to project water demands, supply, and shortages in the SPRB by the mid and end of the 21st century, examine the efficacy of adaptation strategies to reduce water shortages, and explore conditions under which reservoir storage and demand management would serve benefits for reduction of the vulnerability of economic sectors to water shortages. We implement two demand modeling tools to simulate the current and future urban and agricultural water demand in the river basin. Water yield is simulated using calibrated and tested Variable Infiltration Capacity (VIC) model. The estimated water demands and supplies are integrated using the Water Evaluation and Planning (WEAP) model to simulate water allocation with a half-monthly timestep to 70 aggregate users in the basin. Population growth, climate change, reservoir operations, and institutional agreements were considered during the modeling. The study reveals that the vulnerability to water shortages across sectors would increase without adaptation strategies. Population growth tends to be the primary driver of water shortages in the river basin. Reservoirs in the basin can relieve the sequences of the earlier seasonal shift of the water supply by capturing water during the high flow to be used in the high-demand seasons. However, additional storage is only beneficial up to a threshold of storage capacity to the water supply mean ratio of 0.64.

The second study focuses on integrating the effects of land use planning and water rights institutions into the shortage analysis of the SPRB. The goal is to build a framework to understand the complex interactions between climate change, water rights institutions, urban land use planning, and population growth, and how they collectively impact the water shortage and economic analysis. We apply this framework to the SPRB simulate three water institutions, update the urban demand modeling to be a function of the population density, and test different scenarios of population locations throughout the basin. Results show that changing water rights institutions has a small impact on total shortages compared to climate change, but substantially impacts which users experience shortages. Land use policies influencing population locations have larger impacts on shortage and economic value compared to water rights. Finally, distributing the population more evenly between upstream and downstream regions reduces water shortages and increases associated economic value regardless of water rights institutions and climate conditions.

The third study employs an integrative modeling assessment framework to assess water shortage and effective mitigation strategies in river basins across the Contiguous United States. The goals are to improve the methodologies for estimation of water withdrawals, consumptive use, and water shortage, and explore the effectiveness of supply- and demand-side adaptation strategies. The simulated demands are integrated with the water supply components (groundwater, interbasin transfers, water yield, and reservoirs) into a water allocation model for simulating shortage under different scenarios. Results reveal that irrigation has the highest historical and future consumptive use, over 75% of the total consumptive use. Although the consumptive use ratio receives little attention in the literature, it appears to be the most significant parameter for shortage calculations. The allocation model provides comprehensive shortage analysis considering shortage volume, ratio, and frequency across multiple scenarios for the 204 sub-regions –Hydrologic Unit Code 4 watersheds– of the Contiguous United States. Water shortages concentrate between the boundaries of the West Region with both the Midwest and the South regions, in addition to Arizona, Florida, and the center valley of California. Relying only on sustainable groundwater pumping rates is essential to stop the ongoing groundwater depletion, but adds more pressure on demand reduction strategies.

The ongoing research examining water demand, supply, and shortage is important and requires further integration of the key influencing variables. This dissertation demonstrates the necessity of an integrated approach to fully understand the relative impacts of the main drivers of water allocation and shortage. We highlight that reservoirs play a vital role in balancing seasonal fluctuations in the water supply. However, their effect on the 30-year mean annual shortage is effective until the storage volume ratio to mean water supply exceeds 64%. Additionally, land use policies carry higher direct significance on water shortages compared to water rights. We find that distributing the population more evenly throughout the river basin provides the lowest shortage. Lastly, the approaches targeting shortage calculation and mitigation should analyze both regional and national scenarios under integrated frameworks comparing demand- and supply-side options.

ACKNOWLEDGMENTS

I would like to express my gratitude to my advisor, Dr. Mazdak Arabi, for everything he has done for me since we met five years ago. Dr. Arabi always supports, guides, encourages, and pushes his students to become better versions of themselves. I want to thank Dr. Arabi specifically for his friendly advising and knowledge delivery during my PhD program.

I extend my thanks to Dr. Christopher Goemans for serving as a mentor, friend, and committee member, and for his assistance throughout all my research components. Additionally, I appreciate the support and insightful comments from my committee members, Dr. Sybil Sharvelle and Dr. Travis Warziniack. Special thanks go to Dr. Dale Manning for his ideas and efforts that shaped my first publication. I am grateful to my co-authors Joey Blumberg and Dr. Alexander Maas, and I appreciate the support of my friends during challenging times.

The work presented in this dissertation would not have been possible without years of funding and support from the National Institute of Food and Agriculture award no. 2018-69011-28369, along with additional funding from the National Science Foundation grant no. 1444758 as part of the Urban Water Innovation Network (UWIN).

I am indebted to my parents, Dr. AbdelTawab Gharib and Dr. Mona Hussin, for inspiring in me the dream of obtaining my Ph.D. and for their ongoing, unaccountable help and support. A special thanks goes to my wife, Maryam, who endured more than I did during those five years. I appreciate Maryam for taking care of our children, Yosr, Omar, and Habiba, enabling me to continue working overnight and during weekends, and for managing my special, complicated diet. Most importantly, ‘All praise is due to Allah, to whom belongs whatever is in the heavens and whatever is in the earth’.

TABLE OF CONTENTS

CHAPTER 1.

INTRODUCTION

1.1. Research background

Over half of the global population faces water shortages for at least one month every year (Mekonnen & Hoekstra, 2016; Muratoglu et al., 2022). Climate change and population growth continue to place pressure on scarce water resources (Cook et al., 2014; Dai, 2013; Flörke et al., 2018; Martinsen et al., 2019; Richter et al., 2013), increasing the complexity of water resources management (Momblanch et al., 2019). Increasing demands driven by population growth, industrial expansion, and environmental considerations have intensified the competition for limited water resources, particularly in arid western US states (Brewer et al., 2008; Brown, 2006; Tidwell et al., 2014). Water managers are now working to find novel solutions that better balance water supply with demand (e.g. Golfam et al., 2021; Kolokytha & Malamataris, 2020; Sun et al., 2017; H. Wang et al., 2020).

Policymakers often address increasing water scarcity by managing the demand or supply sides. Managing demand includes employing water-efficient appliances and irrigation systems while reducing irrigated landscapes and improving water-use efficiency (Chinnasamy et al., 2021; Dieter et al., 2017; Hering et al., 2013; Ma et al., 2015; Paterson et al., 2015; Sharvelle et al., 2017). Despite demand reduction efforts, Brown et al. (2019) project that continued population growth coupled with changing water supplies will cause water shortages to increase across the US. Additionally, demand reduction strategies can impose costs on constituents (Neale et al., 2020; Russell & Fielding, 2010).

Water supply options include: building or upgrading reservoirs, groundwater pumping and recharge, desalination, rainfall harvesting, water reuse, and others (Blamey et al., 1999; Foti et al., 2012; Kim et al., 2019; Kirshen et al., 2018; Makropoulos et al., 2008; Rathnayaka et al., 2016; Sutherland & Fenn, 2000). Among adaptation strategies for water supply management, reservoirs are often found to bolster climate change resiliency by increasing water availability (Hallegatte, 2009; Iglesias & Garrote, 2015) and, in turn, economic activity (Biemans et al., 2011). Water availability is the location- and time-specific water available to be diverted from a stream. In that context, reservoirs increase the water availability, not the water supply. Contrasting these findings, Brown et al. (2019) conclude that additional reservoirs have minimal effect on decreasing future water shortages. However, reservoirs may be more effective at reducing shortages at finer spatial and temporal resolutions (Brown et al., 2019). In general, reservoirs have no effect if water is the limiting factor (Brown et al., 2019; Foti et al., 2012; Kim et al., 2019).

In several basins where water supply (e.g., reservoirs) and demand (e.g. increasing block rates) management strategies have traditionally been options to address water shortages, these methods have diminishing returns since the "low-hanging fruit" has already been picked (Barnett et al., 2008; Brown et al., 2019; Gutzler & Robbins, 2011; Seager et al., 2013). For example, most high-quality dam sites have already been developed; where options do exist, environmental objections to dams and reservoirs often preclude their construction (Glennon, 2005). Water conservation technologies, such as center pivot irrigation or low-flow toilets, have seen mass adoption in recent decades such that additional demand-side conservation is likely to require substantial behavioral and technological change (Fleck, 2016; Gilligan et al., 2018; P. H. Gleick, 2002; Sankarasubramanian et al., 2017).

Further, there is a limited understanding of how primary drivers of water scarcity—population location, land use, water institutions, and climate conditions—interact with each other at a basin level. Academics and practitioners have long argued for updating water rights institutions (water institutions) as a means of dealing with increased water scarcity (Grafton et al., 2013). However, explicit water institutions are not the only way to influence water scarcity. How populations grow, in terms of land use and housing density policies, also plays an important role in determining water demand patterns (A. Miller, 2023; Richter, 2023; Ty et al., 2012).

The importance of integrating land use and water management has been recognized by researchers and policymakers, though its implementation is still limited. Stoker et al. (2022) published a literature review on the integration of land use planning and water management and highlighted calls for better integration (Angelo, 2001; Carter et al., 2005; Lucero & Dan Tarlock, 2003; Mitchell, 2005; Plummer et al., 2011; Shandas et al., 2015; Stoker et al., 2022; X. Wang, 2001). Similarly, Colorado's Governor has acknowledged the need for intentional land use/housing density policy given its clear implications for, *inter alia*, water use and continued economic prosperity (A. Miller, 2023).

Research studies that focus on a single component of water resources assessments are way more than studies that integrate them. Several studies focused on the water supply sides (e.g. Archfield et al., 2016; Dudley et al., 2017; Hammond et al., 2022; Konikow, 2015; Megdal et al., 2015; Rateb et al., 2020). Other studies focused on water demand sides e.g. (Brown, 2000; Brown et al., 2013; Chinnasamy et al., 2021; Warziniack et al., 2022).

In the United States, water supplies are expected to face more extreme hydrologic events (Brown et al., 2019; Foti et al., 2014a; Leng et al., 2016; Naz et al., 2016) which can lead to more severe and protracted droughts (Wehner et al., 2017). Also, climate change had major consequences and is projected to continue affecting several river basins across the country (Dettinger et al., 2015; Haddeland et al., 2014; Palmer et al., 2008). The most obvious issue is the mega-drought that started in the year 2000 and still going on in the Colorado River Basin in the Southern Western US (O. L. Miller et al., 2021; Richter, 2023; Villarini & Wasko, 2021; Wheeler et al., 2022; Williams et al., 2022). According to the survey by Rudd & Fleishman (2014), the question of how much water is needed to sustain the future population and ecosystems is the most emerging among policymakers and scientists (Rudd & Fleishman, 2014).

Improving water demand forecasts will help planners understand and optimize future investments in water supply infrastructure and related programs (Ashoori et al., 2017). The increasing water demand contributes twice as much as the decreasing water availability to water shortage (Yan et al., 2006). Water scarcity is not just a supply problem, but also a demand problem, and is not truly scarce in most of the world at a national scale (Rijsberman, 2006). A recent U. S. Geological Survey water-use report suggests that increasing water-use efficiency could mitigate the supply-and-demand imbalance arising from changing climate and growing population (Sankarasubramanian et al., 2017). Population and economic growth alone would increase water stress in the United States through mid-century (Blanc et al., 2014). Water is at the center of a complex and dynamic system involving climatic, biological, hydrological, physical, and human interactions (Blanc et al., 2014).

1.2. Research objectives

The overall goal of this dissertation is to enhance the capacity for water demand and shortage calculations in an integrated water resources management framework under climate, socioeconomic, land use, institutional, and adaptation changes. Specifically, the objectives are to:

1. Predict future water demands and shortages in the South Platte River Basin (SPRB) under the effect of climate and land use changes and population growth.
2. Test the efficacy of demand reduction and additional strategies for reducing shortages in SRPB.
3. Generalize the finding of when and where investing in additional storage would reduce shortages compared to demand reduction
4. Develop an integrated land use planning and water management model.
5. Examine the effects of climate, water rights institutions, and land use on water shortage and economic values in the SPRB.
6. Analyze how the location of population across the basin changes water allocation patterns and identify the optimal setup to reduce shortages and increase economic benefits.
7. Provide improved water withdrawals and consumption projections with reproducible methodologies at the sub-region levels for the contiguous US.
8. Provide better estimates of groundwater mining historically, and required in the future.
9. Improve the water allocation simulations by considering updated demand projections along with the newest available water yield and inter-basin transfers.
10. Improve the water shortage calculations by considering shortage volume, ratio, and frequency across multiple scenarios.

Achieving these research objectives provides a more accurate water shortage vulnerability assessment under future conditions, which in turn could assist policy-makers and local water planners in their decision to adopt the best efficient adaptation strategies.

1.3. Organization of the dissertation

Chapter 1 presents a holistic research background and the main objectives and significance of this dissertation.

Chapter 2 focuses on projecting the water demands and shortages in SPRB, then applying a sensitivity analysis for demand and supply management strategies to identify general results of the conditions where additional storage and demand reduction would effectively reduce water shortages.

Chapter 3 develops a modeling framework that integrates the effects of land use policies, water rights, location of population, and climate change into a hydro-economic model. The methodology is applied to SPRB for providing the relative effects of these factors under the effect of climate changes on the water shortages and the economic values.

Chapter 4 changes the scale of the study from specific basins to national scale water management analysis for the United States. Demand and supply data are modeled and integrated into a water allocation model to simulate water shortage under several future conditions.

Chapter 5 combines important closing remarks, summaries of findings of the current research, and suggestions for future directions.

The second chapter of the dissertation has been published in the journal of "The Science of the Total Environment" with the following citation:

Gharib, A. A., Blumberg, J., Manning, D. T., Goemans, C., & Arabi, M. (2023). Assessment of vulnerability to water shortage in semi-arid river basins: The value of demand reduction and storage capacity. *The Science of the Total Environment*, *871*(January), 161964. https://doi.org/10.1016/j.scitotenv.2023.161964

The third chapter is under review in the journal of "Water Resources Research" with the title: “Integrated Land Use Planning and Water Management under Different Water Rights Institutions: Methodology and Application”

CHAPTER 2.

ASSESSMENT OF VULNERABILITY TO WATER SHORTAGE IN SEMI-ARID RIVER BASINS: THE VALUE OF DEMAND REDUCTION AND STORAGE CAPACITY

Interest in securing reliable water supplies has increased due to climate change and rapid population growth. This challenge is significant in growing areas with limited water supplies. To meet water demands, water managers are considering new storage infrastructure to increase the reliability of water supplies while also identifying opportunities to reduce water use per person. Although these strategies change water consumption patterns, their success at reducing shortages across space and time for different climate change scenarios remains unclear. In this paper, population- and climate-dependent future water supply and demand models are developed and integrated into a water allocation model calibrated for the South Platte River Basin of Colorado. Eight future climate scenarios are simulated using four statistically downscaled models from the Coupled Model Inter-Comparison Project Phase 5 (CMIP5) with two Representative Concentration Pathways (RCP). Lastly, findings from the water allocation model simulations are generalized beyond the study area using a novel approach by introducing dimensionless indices to characterize water shortage and basin conditions. Results reveal a threshold ratio of total storage capacity to mean water supply with a value of 0.64 above which additional storage has no effect on total water shortages. This threshold communicates the limitation of building storage infrastructure as a strategy to adapt to decreasing average water supplies for basins considering increasing storage capacity. However, basins with low current capacity are likely to fall below the threshold and could invest in reservoirs to mitigate future shortages.

2.1. Introduction

Over half of the global population face water shortages for at least one month every year (Mekonnen & Hoekstra, 2016; Muratoglu et al., 2022). Climate change and population growth continue to place pressure on scarce water resources (Cook et al., 2014; Dai, 2013; Flörke et al., 2018; Martinsen et al., 2019; Richter et al., 2013), increasing the complexity of water resources management (Momblanch et al., 2019). In the United States, water supplies are expected to face more extreme hydrologic events (Brown et al., 2019; Foti et al., 2014a; Leng et al., 2016; Naz et al., 2016) which can lead to more severe and protracted droughts (Wehner et al., 2017). Adaptation to increasing water scarcity can be achieved through a variety of demand- or supply-side strategies.

Demand-side strategies involve reducing total water use, which may include employing water-efficient appliances and irrigation systems, applying deficit irrigation, reducing irrigated landscapes, and improving industrial water-use efficiency (Chinnasamy et al., 2021; Dieter et al., 2017; Hering et al., 2013; Ma et al., 2015; Nouri et al., 2019; Paterson et al., 2015; Sharvelle et al., 2017). Despite demand reduction efforts, Brown et al. (2019) project that continued population growth coupled with changing water supplies will cause water shortages to increase across the US.

Regarding supply management, Brown et al. (2019) find that additional storage infrastructure has limited impacts on reducing water scarcity. However, increasing water availability through storage infrastructure investment continues to receive attention (Foti et al., 2012; Kim et al., 2019), in part because of the significant interest in maintaining agricultural production (Qin et al., 2020; Rosegrant & Ringler, 2000; P. Thornton et al., 2018). For example, the recently passed “Infrastructure Investment and Jobs Act” (HR 3684) in the US contains more than $1 billion for the construction of water storage and conveyance projects (P. Gleick et al., 2021). To ensure the efficacy of projects financed with scarce public funds, it is important to identify the conditions in which additional water storage can decrease the prevalence of water shortages.

Some recent studies have modeled climate effects on water supplies and demands across the US without explicitly testing adaptation strategies (Blanc et al., 2014; Foti et al., 2012, 2014b, 2014a; Roy et al., 2012; Strzepek et al., 2010). Brown et al. (2019) simulate the effectiveness of four alternative adaptation strategies in reducing expected water shortages across the US at the HUC-4 level, however return flows were not considered. Among adaptation strategies for water supply management, reservoirs are often found to bolster climate change resiliency by increasing water availability (Hallegatte, 2009; Iglesias & Garrote, 2015) and, in turn, economic activity (Biemans et al., 2011). Water availability is the location- and time-specific water available to be diverted from a stream. In that context, reservoirs increase the water availability, not the water supply. Contrasting these findings, Brown et al. (2019) conclude that additional reservoirs have minimal effect on decreasing future water shortages. However, reservoirs may be more effective at reducing shortages at finer spatial and temporal resolutions (Brown et al., 2019). In general, reservoirs have no effect if water is the limiting factor (Brown et al., 2019; Foti et al., 2012; Kim et al., 2019).

In this paper, a model of water supply and demand in the South Platte River Basin (SPRB) of Colorado is developed to examine if additional storage infrastructure reduces the vulnerability to water shortage -the probability of water demands exceeding water supplies- through the end of the 21st century. The model contains detailed information on water supplies, demands, and allocation rules at a half-monthly timestep. The Variable Infiltration Capacity (VIC) model is used to measure and project water supply, the Integrated Urban Water Model (IUWM) model to simulate urban water demand, and the DayCENT model to estimate agricultural water requirements, all of which depend on downscaled models of climate change projections. Water supplies are aggregated at the HUC-8 level, and 75 users represent both agricultural and urban water demands at different points along the stream system. A water allocation model is built and calibrated using the Water Evaluation and Planning (WEAP) system (Yates et al., 2005) for the historical period 1985-2014, and an uncertainty analysis is conducted to estimate the results' errors. Required water diversions, consumptive use, and water shortages are then simulated for four future climate models with two Representative Concentration Pathways (RCP) through the end of the 21^{st} century, and the effects of storage capacity and demand reduction on water shortage are examined through 150 model-scenario combinations. Two dimensionless indices are identified that characterize the system: the ratios of storage capacity and average water demand to average water supply. The indices reflect the conditions the drive the most effective policy decisions for a given basin. The indices convey whether policymakers should prioritize demand reduction strategies or additional storage based on the current state of their basin.

The present paper contributes to the relevant literature in several aspects. First, the model captures the climate's role in influencing water supply and demand at a fine spatial (HUC-8) and temporal (half-monthly) scale. The finer scale allows for the examination of shortages from both prolonged drought and short periods of high demand and low supply. Second, information is also disaggregated to the sector-level to examine how water scarcity impacts agricultural and municipal users located at different points along the South Platte River. Third, return flows are explicitly incorporated into the model. This innovation is particularly important in the SPRB because total water diversions are 200 percent of the average water supply (CWCB, 2015), implying that return flows are critical for meeting current and future water demands. Lastly, the presented generalized basins classification from their supply, storage, and demand conditions is an innovation in this study through the identified threshold.

2.2. Methods

2.2.1. Study Area and Model Overview

Colorado provides a relevant case study for many western US states due to its quickly increasing population and climate-change-driven changes to water supplies and demands. Colorado was one of the fastest-growing states during the last decade, with a 14.8% increase totaling 5.7 million people (United States Census Bureau, 2020). This population growth is estimated to continue in the future with an estimated total population of 10 million by 2050 (CWCB, 2019b). Climate models predict changes in annual streamflow by 2050 of between -5% and 8% (Lukas et al., 2014) and temperatures have increased since the beginning of the 20th century (Lukas et al., 2014; NOAA, 2021). Since 1980, the statewide average temperature has increased by 1.1°C (Lukas et al., 2014), a trend that is expected to accelerate with increases of 1.4 to 3.6 °C by 2050.

The SPRB, within Colorado, is a snow-dependent basin located in a semi-arid region with highly variable hydrology and The SPRB is one of the fastest-growing areas in the US, with dense agriculture and urban communities. The long-term mean annual water supply from native and transferred sources is 2.34 billion cubic meters (BCM) (CWCB, 2015). Surface water diversions totaled 4.93 BCM/y, with 2.59 BCM/y coming from return flows. The State Water Plan (CWCB, 2015) expects the gap between water demand and supply to range from 0.44 to 0.58 BCM/y by 2050 (CWCB, 2015), and it is estimated that the SPRB will face an 8.5% decrease in stream discharge for every 1°C increase in temperature in the worst-case climate scenario (Aliyari et al., 2021). Overall, examining strategies that decrease water shortages can produce significant benefits for the study area in this research as well as provide general insights into vulnerable basins throughout the western US.

Irrigated agricultural land is primarily located downstream of urban areas, and return flows from cities are often used to meet agricultural water demands (Figure 2.1a). Following Dozier et al. (2017), the SPRB in our simulation, is divided into five regions: North, North Central, Central, South Metro, and East, which creates a spatially heterogeneous distribution of water demands (Figure 2.1a). Each region represents one or more counties and has 15 stylized users. Twelve agricultural (Ag) users represent six staple crops using flood or sprinkler irrigation systems, and three urban users represent demands for (1) residential indoor, (2) commercial, industrial, and institutional indoor (CII), and (3) total (residential plus CII) outdoor water use. Fourteen nodes represent the model's water supply at the sub-regions' (HUC 8 level) headwaters (Figure 2.1a). Additionally, six main hydraulic structures are connected to the sub-regions, representing the water transferred to the SPRB from other watersheds. In each sub-region, existing reservoirs are aggregated into one representative reservoir.

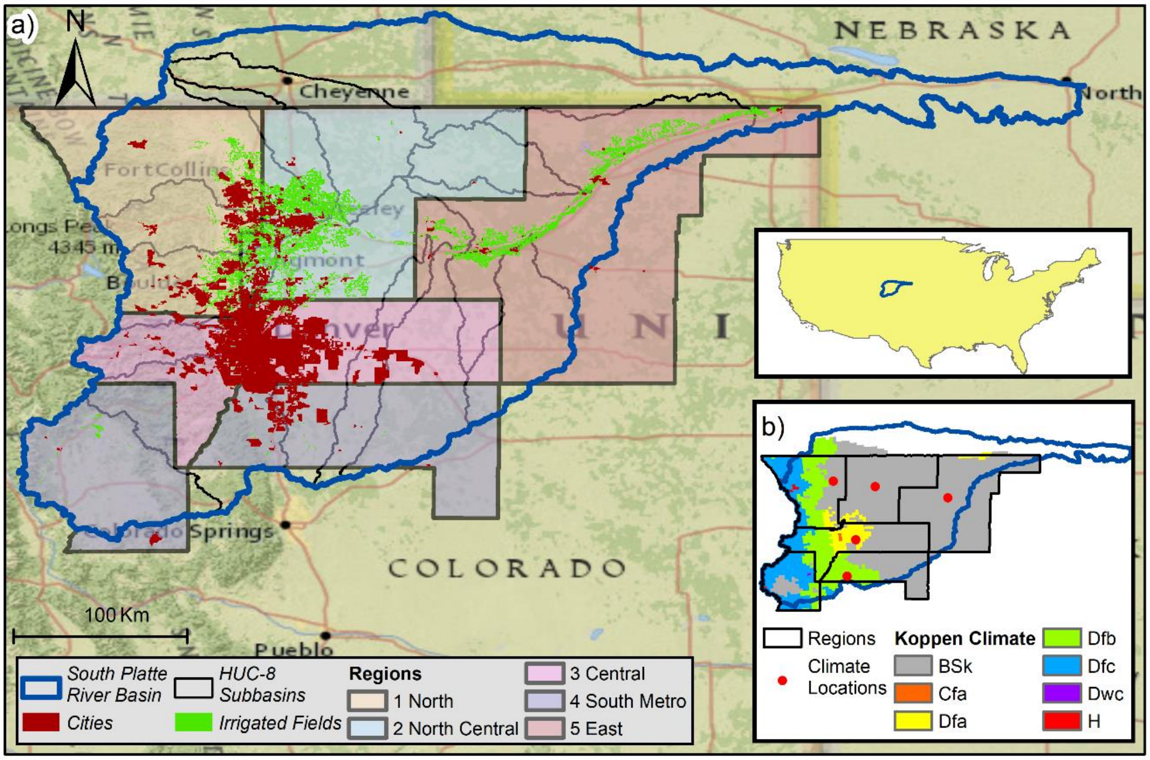

Figure 2.1: a) South Platte River Basin (SPRB) extent, cities and irrigated fields in SPRB, the five modeled regions, and the HUC-8 sub-regions. b) The study boundary with Koppen climate classification and the selected climate location in each region.

The modeling framework contains three main components (Figure 2.2). First, land use and population data are summarized at the annual level, and climate data are summarized at the daily level. These data are then used as inputs for the second component of the framework, the water supply and demand models, which provide output at the half-monthly timestep for the model regions and sub-regions described above. Lastly, water is allocated to users at each timestep using the WEAP model (Yates et al., 2005), hereinafter referred to as WEAP-SP. WEAP uses linear programming to solve the optimization function of maximizing water demand satisfaction subject to mass balances, allocation priority, water availability, and other constraints. The model runs at each timestep sequentially without foresight.

In total, WEAP-SP has 20 supply nodes, 60 Ag demand nodes, 15 urban demand nodes, ten reservoir nodes, one outflow requirement node, natural river links, diversion links from rivers to demand nodes, and return flow links from demand nodes to streams (Figure A1). WEAP-SP runs from 1981 to 2099, with the first four years to initiate the model, followed by 30 years for calibration from 1985 to 2014, defined as the historical period. Future water allocations from 2015 to 2099 are then simulated using eight climate scenarios. Two 30-year periods—the near-future period from 2025 to 2054 and the far-future period from 2070 to 2099—are compared with the historical results. Lastly, the relative effectiveness of several adaptation strategies at reducing expected shortage is examined. The following sections provide additional detail on each of the model components and the uncertainty analysis for results.

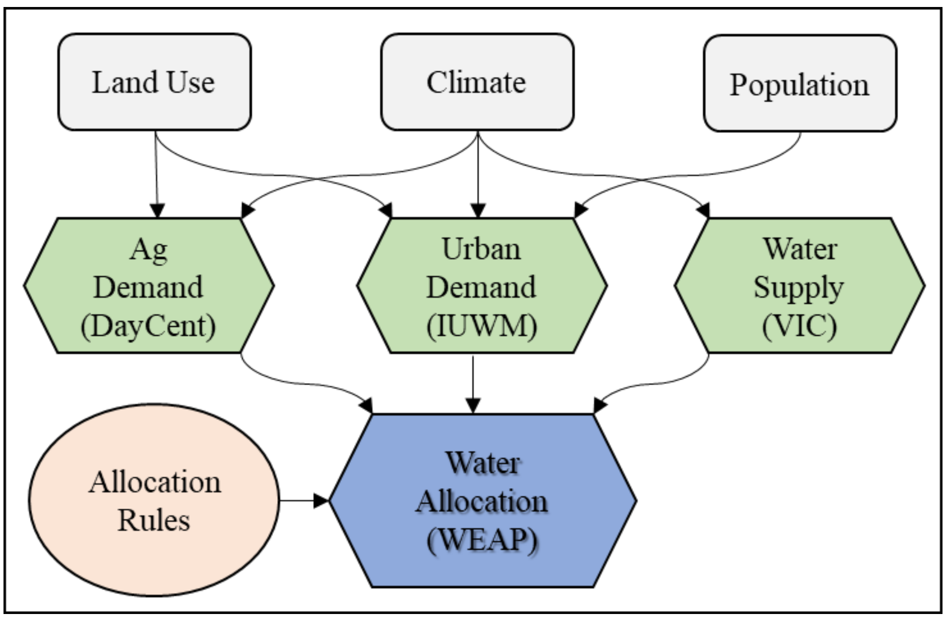

Figure 2.2: The integrated modeling framework

2.2.2. Climate Data

Climate data is essential for this study and is used in all three of the water supply and demand models (Figure 2). According to Koppen Climate Classification (Chen & Chen, 2013), the SPRB is primarily a cold semi-arid climate (BSK), humid continental climate (Dfa & Dfb), or Subarctic climate (Dfc) (Figure 2.1b), depending on seasonal temperature, precipitation patterns, and vegetation types (Chen & Chen, 2013). To capture the heterogeneity in climate classifications, one location near the centroid of each region is selected to represent the climate in the water demand models' simulations (Figure 2.1b).

Historical climate data from 1980 to 2015 is obtained from Naz et al. (2016), which is calculated using a combination of three datasets: the Parameter-elevation Regressions on Independent Slopes Model (PRISM) dataset (Daly et al., 2008), Daymet dataset (P. E. Thornton et al., 1997), and the North American Regional Reanalysis (NARR) dataset (Mesinger et al., 2006). Daily precipitation and minimum and maximum temperature estimates from Daymet are biased corrected at a monthly time scale using PRISM, and wind speed is obtained from NARR.

Several global climate models (GCM) predict the future climate at different scales. However, GCM estimates are inappropriate for high-resolution studies as they generally have a coarse grid resolution (roughly 150 to 200 km grids) (Heidari et al., 2020; Naz et al., 2016). Hence, the projected climate data from Abatzoglou & Brown (2012), that use Multivariate Adaptive Constructed Analogs (MACA) to downscale GCMs from coarse to high spatial resolution were used in this study. The MACA daily dataset has 20 climate models downscaled for the entire conterminous United States (CONUS) from 1950 to 2099 at approximately a 4 km grid under 4.5 and 8.5 Representative Concentration Pathways (RCP) scenarios from the Coupled Model Inter-Comparison Project Phase 5 (CMIP5). Joyce & Coulson (2020) selected five of the available climate models to represent five ranges of predicted future climate in CONUS: hottest (HadGEM2-ES365), driest (IPSL-CM5A-MR), wettest (CNRM-CM5), warmest (MRI-CGCM3), and a model representing the middle predictions. For this study, the four extreme models -HOT, DRY, WET, and WARM- under RCPs 4.5 and 8.5 are used for future projections, resulting in a total of eight climate scenarios from 2015 to 2099 (Refer to Appendix A section 3 for more details).

2.2.3. Water Supply

In the SPRB, total water supply is the water yield produced within the basin plus the water transferred from adjacent basins via hydraulic structures. The within-basin water yield, comprised of surface runoff and baseflow, was simulated by Heidari et al. (2020) using the Variable Infiltration Capacity (VIC) model (Liang et al., 1994). VIC is a semi-distributed macroscale scale model used to solve full water and energy balances and simulate land-atmosphere fluxes and flow routing (Heidari et al., 2020; Warziniack et al., 2022). Building on the work by Oubeidillah et al. (2014) and Naz et al.(2016) to set, calibrate, and evaluate the VIC model at a grid size of 4 km for CONUS, Heidari et al. (2020) ran the model using the five selected climate models by Joyce & Coulson (2020) and summarized the results at the sub-region level, as described in the previous section.

Although several studies have been published using Heidari et al. (2020) results (Heidari, Arabi, & Warziniack, 2021; Heidari, Arabi, Warziniack, et al., 2021; Warziniack et al., 2022), none of them checked the bias between the water yield simulations using historical and modeled climate data. To address this, the Kolmogorov-Smirnov test was performed to compare the statistical performance of the water yield in SPRB generated from the eight climate scenarios and the historical climate from 1985 to 2014. In seven of the eight scenarios, excluding the DRY-8.5 scenario, KS results suggest that their simulated annual water yield follows the same distribution of the water yield generated using the historical climate data. This finding supports the use of water yield generated from these seven scenarios without bias correction; additional analyses are available in section 13 of Appendix A. In this paper, the DRY-8.5 scenario is nevertheless included to represent an extreme drought scenario. This simulated water yield is referred to as the native water supply.

The transferred water from nearby basins, referred to as out-of-basin water supply, represents approximately 20% of the mean annual total water supply in the SPRB. The HydroBase database, maintained by the Colorado Division of Water Resources (CWCB, 2019a), provides daily streamflow from out-of-basin water sources downstream of the hydraulic structures. Six major structures are identified to represent the out-of-basin supply, which accounts for almost 98% of the historical transferred water. Future out-of-basin supplies at each hydraulic structure are forecasted using the 'forecast' package in R (Rob J. Hyndman & Yeasmin Khandakar, 2008), which performs an Auto-Regressive Integrated Moving Average (ARIMA) model with automatic parameter estimation and an external regressor. The ARIMA model predicts the future half-monthly out-of-basin supply extending from the historical out-of-basin supply time series. The native water supply from VIC is used as the external regressor.

2.2.4. Water demand

2.2.4.1. Land Use, Population, and Urban Water Demand

Climate, land use, population, and housing are the main components for estimating urban water demand. Land use data is acquired from the Multi-Resolution Land Characteristics (MRLC) consortium National Land Cover Database (NLCD) raster images and then processed for years 2001, 2006, 2011, and 2016 using ArcGIS to calculate the urban area in each region. In the NLCD, urban areas are represented by open space areas and low-, medium-, and high-intensity developed areas. MRLC also provides the 1992 NLCD, but with a different format, so the desired four urban categories for 1992 are estimated using the conversion factors suggested by Fry et al. (2009). Annual land uses are then linearly interpolated between observed years for each region.

In the SPRB, urban land use and population are projected to increase. The Integrated Climate and Land Use Scenarios (ICLUS) tool developed by the Environmental Protection Agency

(EPA) provides land use changes and population projections on a decadal basis from 2020 to 2100 for different scenarios (EPA, 2017). The "SSP5 RCP85 HadGEM2-ES" scenario is selected from the ICLUS V2.1.1 (EPA, 2020) database, because its 2050 projected population lies in the range of possible population projections of the Colorado Water Plan (CWCB, 2019b). Also, land use in this scenario represents the highest developed urban area. The ICLUS land use data is reclassified to the NLCD land use categories by estimating conversion parameters by matching the 2010 ICLUS with the 2011 NLCD datasets.

Historical annual population is obtained from the Colorado Department of Local Affairs (DOLA, 2020),ado and future population from ICLUS (EPA, 2020). ICLUS provides the decadal population projections at the county or multi-county level, so model regions 3 and 4 in this study are combined in the ICLUS dataset. To rectify this, a linear regression model is used to estimate the population in region 3 as a function of the population in region 4 using their annual historical records, achieving a fit of 0.96 R-squared. The same linear model is then used to split the future population of the two regions. The Colorado Department of Local Affairs also provides the number of households, which is required in the water demand model, so another linear regression model is used to estimate the number of households as a function of population (0.99 R-squared). It is then used to predict the future number of households from the projected population (equation 2.1), refer to Appendix A section 2 for details about all the regression models used in this study.

$$Number\ of\ Households = 0.4026 * Population \qquad 2.1$$

Using the variety of data described above, the Integrated Urban Water Model (IUWM), a municipal water use forecasting tool, is used to simulate urban water demand in each region (Sharvelle et al., 2017). IUWM uses a daily mass balance approach to estimate the water demand in three categories: residential indoor, CII, and outdoor residential (Sharvelle et al., 2017). IUWM inputs include daily precipitation, daily temperature, urban land use in the NLCD format, population, the number of households, and other model parameters -Net irrigation requirement met, plant factor, the minimum threshold temperature for which irrigation is applied, irrigation efficiency, and indoor demand power function parameters-. IUWM also can simulate the use of alternative water sources (i.e., wastewater, greywater, and stormwater) and water conservation for indoor and outdoor demands.

Five IUWM models are built to simulate the urban water demand in each of the five regions using the relevant climate data. IUWM requires many calibration parameters. Neale et al. (2020) and Sharvelle et al. (2017) calibrated models for the cities of Denver and Fort Collins, both located in the SPRB, and their reported calibration parameters are applied to the relevant regions in the present study. Historical and future annual urban water demands are presented in Figure 3, where climate is the only input that varies across the future scenarios.

2.2.4.2. Agricultural Consumptive Use (Net Water Irrigation Requirement)

This study simulates water demands for irrigated lands with access to surface water. Two trends are observed in the agricultural sector in the SPRB: declining total irrigated lands and the steady transition from flood to sprinkler irrigation. Six irrigated crops account for 99% of irrigated land in the SPRB: corn, alfalfa, grass pasture, wheat & small grains, sugar beets, and dry beans (CWCB, 2019a). In 1976, irrigated lands were 3,400 km^2 with 5% as sprinkler irrigation (CWCB, 2019a). In 2015, irrigated lands decreased to 2,589 km^2 with 43% as sprinkler irrigation (CWCB, 2019a). For this analysis, the irrigated crop area, crop mix, and irrigation technologies for future simulations are fixed at 2015 levels. Hence, only climate drives the variability in Ag water demands over time.

Net irrigation requirements for each crop in each region are estimated using the DayCENT model (Parton et al., 1998). DayCENT is a daily timestep version of the CENTURY model, which is used widely in agroecosystem studies to simulate terrestrial croplands, grasslands, forest lands, and savannas (Del Grosso et al., 2000). Inputs for DayCENT include daily temperature, daily precipitation, soil classification, land use, cultivation schedules, planting, and nutrient amendments. The model simulates several of ecosystem parameters including soil carbon, water balance, plant productivity, methane emissions, nitrous oxide, and nitrogen dynamics (Del Grosso et al., 2006; Dozier et al., 2017; Ogle et al., 2010; Robertson et al., 2018; Stehfest et al., 2007; Zhang et al., 2020). The output used in this study is the irrigation depth, defined as the depth of water required to produce 100% crop yield.

The calibrated DayCENT model used in this study is provided by Zhang et al. (2020), with 293 calibrated sites distributed across the SPRB. The model is run for the calibrated sites for the six crops using the historical and future climates of each region. The mean irrigation depth is then calculated for each crop in each region and multiplied by the irrigated area of each crop to obtain Ag consumptive use (Figure 2.3) over time. Additionally, section 4 in Appendix A shows the comparison of the simulated results from VIC, IUWM, and DayCENT compared to their monitored values for the study area.

2.2.5. Water Allocation Model Parameterization and Calibration

This section presents the integration of the water supplies and demands into WEAP-SP and describes the parameterization and calibration of the WEAP-SP. WEAP-SP is manually calibrated from 1985 to 2014 by trial-and-error sequential model runs. Calibration parameters include delivery efficiency, irrigation application efficiency, percent of consumption uses in the urban indoor and CII users, percent of consumptive losses from return flow, and reservoir parameters.

Three model outputs are used as main calibration targets: (1) annual water diversions, (2) monthly storage, and (3) annual outflow from the basin. The calibration process starts with comparing the calibration targets' results with their observed values from HydroBase (CWCB, 2019a). WEAP-SP is re-tuned and re-estimated until it imitates the SPRB current conditions.

2.2.5.1. Required Water Diversion and Model Efficiencies

The required water diversion is the total water necessary to be diverted from a stream to fulfill a water demand. Hence, required water diversions needed to achieve the water demands from DayCENT and IUWM are estimated considering delivery and irrigation application efficiencies (Figure 2.3). Application efficiency is already a component of IUWM and is set at 71% for the outdoor demand, while the indoor and CII consumption ratios are estimated at 20%. During the calibration process, delivery efficiencies are set at 80% for Ag users and 75% for urban users. The application efficiency for sprinkler irrigation is assumed to be 25 percentage points greater than the flood application efficiency, and flood irrigation efficiency is chosen independently for each year to predict the historical required diversions during the calibration process. A linear regression model of the annual flood application efficiency as a function of the annual Ag consumptive uses per unit area is estimated with an R-Squared value of 0.98. Annual flood and sprinkler application efficiency are then projected for each future scenario. Lower and upper limits for the calculated flood application efficiency are estimated at 35% and 65%, so sprinkler application efficiency ranges from 60% to 90%.

Figure 2.3 summarizes the annual urban water demand from IUWM, the Ag consumptive use from DayCENT, and the estimated required diversion from the calibration process for the historical period and the eight climate scenarios. Urban water demand has an increasing trend over the total simulation time, largely driven by population growth. There are minor annual fluctuations reflecting the effects of different climate scenarios on outdoor demands. Ag consumptive use has a slightly declining trend during the historical period reflecting the reduction in irrigated lands and the transition from flood to sprinkler irrigation during the historical period. In the future, the annual mean of Ag consumptive use across the scenarios remains relatively stable as total irrigated land and irrigation technology are fixed after 2015. In general, population growth drives the upward trend in required diversions, while climate effects are represented by the shaded area around each curve (Figure 2.3).

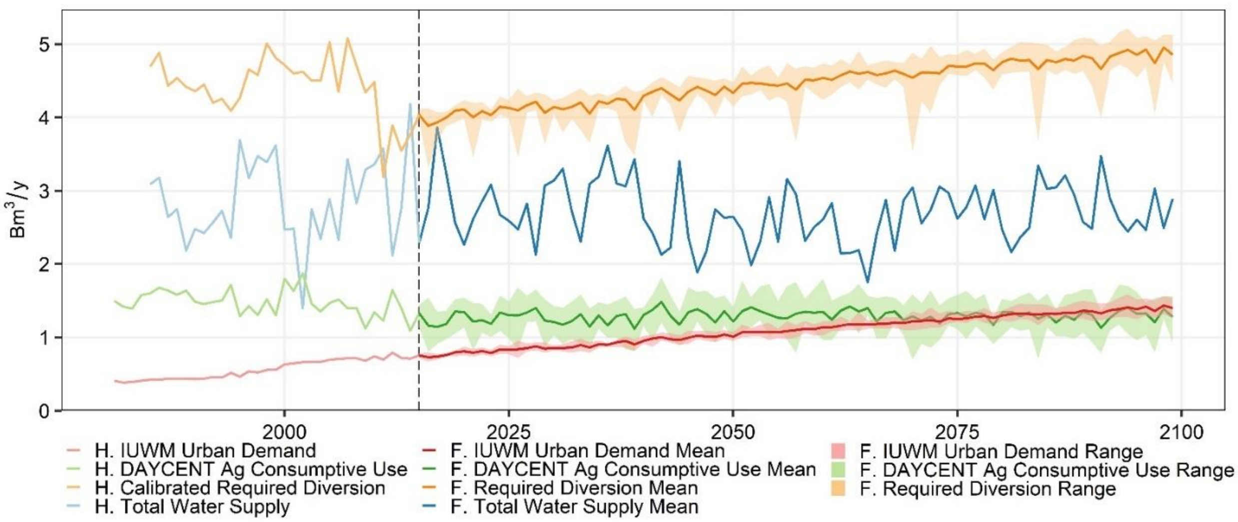

Figure 2.3: Annual estimated required water diversion, simulated ag consumptive uses, simulated urban water demands, and simulated total water supply. The lighter lines are the historical values, and the darker lines are the means of the future baseline scenarios. The areas around the means present the maximum and minimum values of the future baseline scenarios; this range is not shown for the water supply (blue curve) because it covers the entire plot area. Refer to figure A10 for the inflow range.

In WEAP-SP, as application or delivery efficiencies decrease, more water must be diverted from a stream to satisfy a given demand. The difference between diverted and consumed water is the return flow, a portion of which is lost from the system while the rest re-renters the streams. All water in WEAP-SP is accounted for through consumptive demands, losses from return flow to streams, reservoir evaporation (discussed in the following section), and outflow from the basin. From the calibration process, the percent of water lost from the return flow is estimated at 10%

and 13% for Ag flood and sprinkler irrigation, 35% for urban outdoor users, and 15% for indoor and CII users. The parameter uncertainty is further discussed in section 2.2.6.

2.2.5.2. Representing Reservoirs

The SPRB has several reservoirs that store water from high flow season to high demand season and from wet to drought years. Total storage in each sub-region is aggregated to a single reservoir located downstream of the headwater. This representative reservoir is allowed to store all the water supplies connected to this sub-region. Total storage is estimated using recorded monthly reservoir levels from 1975 to 2018 in HydroBase (CWCB, 2019a), which are aggregated to the sub-region level. At the Basin level, the maximum total quantity of stored water was 1.97 BCM, observed in May 1985 (Figure 2.4). The sum of the stated maximum storage of each individual sub-region yields 2.25 BCM, implying that the full storage capacity was not reached. In reality, it is difficult to for all reservoirs to reach maximum capacity at the exact time due to physical limitations and operational difficulties. Therefore, each sub-region's maximum storage capacity is modified to match the maximum observed storage. Empirical cumulative distribution functions (ECDF) of the monthly stored water in each sub-region are calculated, and the maximum storage capacity for each sub-region is specified at the non-exceedance probability of 0.97, aggregating to 1.97 BCM storage capacity for the entire study area.

The dead storage (i.e., stored water below the outlet level of the reservoir) is estimated at 28% during the calibration process, leaving the active storage at 1.42 BCM. As a secondary calibration target, the simulated mean annual evaporation from 1993 to 2013 is compared to the simulated evaporation of the South Platte Decision Support System (SPDSS) (CWCB, 2017). The models have similar evaporation volumes, with values of 0.18 BCM/y and 0.22 BCM/y for WEAP-SP and SPDSS reports, respectively.

2.2.5.3. Simulating Outflow from the SPRB

The South Platte River Compact between Colorado and Nebraska (State of Colorado & State of Nebraska, 1923) regulates the minimum flow of the South Platte River at Julesburg in Colorado, near the states' border. From April 1st to October 15th, the flow is not to drop below 3.4 m^3/s on any given day which accounts for at least 0.06 BCM. For the remainder of the year, the volume of water released to Nebraska should be at least 0.04 BCM with a daily minimum not to drop below 0.28 m^3/s. Although the compact requires only 0.1 BCM/y to be released to Nebraska, the water released is 0.49 BCM on average (CWCB, 2015). According to data from HydroBase (CWCB, 2019a), Julesburg station's annual flow from 1925 to 2017 has a mean, median, and standard deviation of 0.49, 0.36, and 0.48 BCM/y.

The difference between the actual and compact outflow results from several components, including the released water from a reservoir when it is full, the un-stored water when water supplies are expected to be very high, or the return flow of the most downstream users. To combine the compact regulations with the natural flow process, an exponential regression model is estimated to predict the half-monthly outflow discharge as a function of the previous ten months' aggregated native water supply volume and the following six months' aggregated native water supply volume (Equation A1). This model has an R-Squared value of 0.94. The exponential model predicts the outflow for each future scenario using the VIC native water supply independently from WEAP-SP (Figure 2.4). Then, lower and upper bounds of the estimated outflow, 3.4 and 56.6 m^3/s, are used to satisfy the minimum flow requirements and imitate the historical annual outflow to preserve the same environmental conditions.

2.2.5.4. Water Allocation Rules

For the baseline scenario, priority numbers are estimated for each demand node using data on actual water rights to best approximate the current makeup of the SPRB. To emulate how water is administered under a prior appropriation doctrine, WEAP allocates water to the nodes with high priority before those with lower priority. Once water is allocated to a particular node, return flows and remaining natural flows are available to downstream nodes. Reservoirs have the lowest priorities, preceded by the outflow from the SPRB with the second-lowest priority.

To estimate priorities for the remaining nodes, priority numbers are aggregated for relevant water rights using data from HydroBase (CWCB, 2019a). The priority number communicates a ranking within the hierarchy of all water rights in Colorado, which is determined by a right's appropriation and court adjudication date. For urban demand nodes, all water rights within a region with relevant uses (e.g., domestic, commercial, or municipal) are identified, and a mean priority number, weighted by each right's decreed flow rate, is calculated. A similar process is used for agricultural nodes, however after isolating agricultural water rights within a region, a weighted-mean priority must first be calculated for all associated irrigation ditches. Priorities are then generated for each agricultural node using the mean priority across irrigation ditches weighted by the area of each crop with flood and sprinkler irrigation. Every demand node has a fixed priority number during the entire simulation time and across simulations.

In the SPRB, most urban communities are upstream of the agricultural communities in all regions. In WEAP-SP, the three urban users exist upstream of the 12 Ag users in each region, where each user has access to the return flow from the upstream users. In each region, the urban users are arranged such that indoor users are upstream, followed by the CII and outdoor users. The outdoor priority number is estimated from HydroBase data, while the priorities for CII and indoor are increased as they are upstream of the outdoor user. Regarding the Ag users, they are located in each region according to their priority numbers; the highest priority crop is located upstream, followed by the lower crops, maximizing the availability of return flows.

2.2.5.5. Water Allocation Calibration Evaluation

The main calibration target is the annual water diversions, which is the most important variable in the water allocation process (Figure 2.4b). The modeled values have less than 0.5% Bias, with 0.82 Nash Sutcliffe Efficiency (NSE) and 0.91 Kling-Gupta Efficiency (KGE), which indicates very good model performance (Knoben et al., 2019; Moriasi et al., 2015). Monthly storage (Figure 2.4a), the secondary calibration target, also performs well with less than 4% Bias and 0.53 KGE. Annual outflow from the model is also evaluated (Figure 2.4c), which is overestimated in the model compared to the monitored values (blue line) and the outflow generated from the regression model (dotted line). Higher outflow values likely occur because the demand models estimate net irrigation requirements. In practice, farmers may not know these requirements with certainty. It would therefore be rational for risk-averse farmers to hedge against downside risk by applying water more intensely (Finger, 2013). This behavior could lead to slightly more losses and slightly lower outflows. Despite the difference in predicted outflows, the WEAP-SP successfully imitates the historical water allocation in the SPRB (Figure 2.4) and can be meaningfully used in simulations of future scenarios.

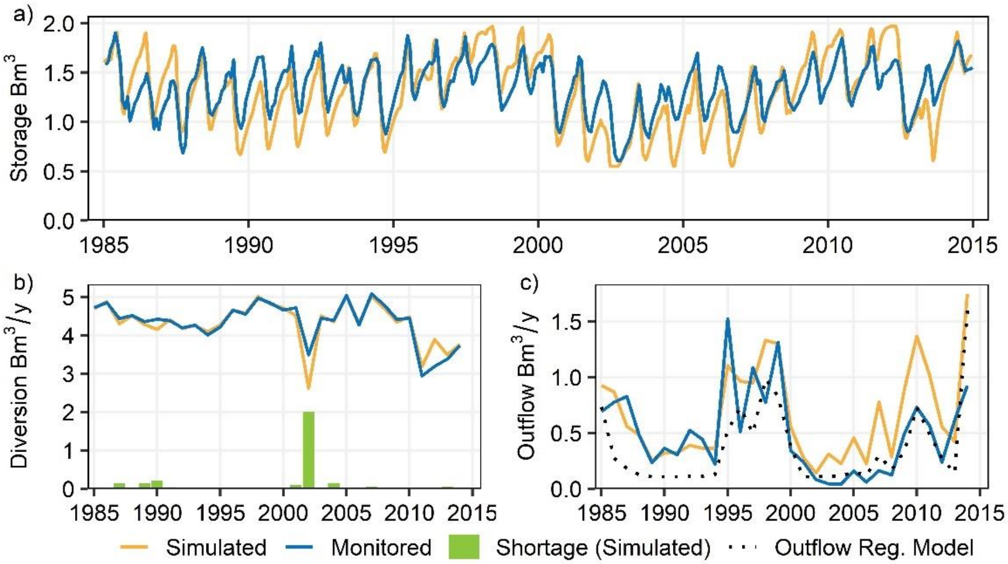

Figure 2.4: The three calibration targets of the WEAP-SP calibration process, (a) monthly storage, (b) annual diversions and the simulated shortage, and (c) annual outflow.

2.2.6. Uncertainty Analysis

Three primary levels of uncertainty exist in each modeling system: input, structural or model, and parameter (Cibin et al., 2014; Herrera et al., 2022; Renard et al., 2010; Song et al., 2015). In this analysis, input uncertainty is handled by using eight climate scenarios in the four models used in this framework. Additionally, the effectiveness of alternative strategies and the index-based approach analyses in sections 3.2 and 3.4 represents uncertainty in the model inputs of water supply, storage capacity, and required diversions as previously described. The structure or model uncertainty occurs because of model simplifications. It could be addressed by using more than one model to simulate the same outputs, which is out of the scope of this manuscript. Additionally, only calibrated models are used in this study.

Parameter uncertainty (Arabi et al., 2007) is then fully addressed by performing Sobol uncertainty analysis for WEAP-SP. Sobol is a variance-based method that uses Monte Carlo methods to perform global sensitivity analysis. Eight parameters are selected to represent the majority of WEAP parameters. The most significant parameters are determined using the SALib python package (Herman & Usher, 2017; Iwanaga et al., 2022) through 2304 runs in WEAP-SP for the historical period, where each run represents a parameter set. Then, a multi-objective optimization for maximizing the three calibration targets KGE is performed to determine the non-dominated parameter sets through Pareto front analysis (Bastidas et al., 1999). The non-dominated sets represent the sets where no other sets are better than them in all dimensions of the maximization problem (Khanmohammadi et al., 2021). Finally, these non-dominated sets are simulated for the future conditions of the DRY4.5 scenario to estimate the confidence interval of the results.

2.2.7. Scenarios, Strategies, and Metrics Calculation

In this paper, a 'scenario' refers to all simulated baseline results associated with one of eight climate scenarios. A 'strategy' defines a percentage increase to the current storage capacity or decrease in the future baseline required diversions, and an 'alternative starting condition' generalizes the strategies by considering any applied change to the storage capacity or the future baseline required diversions. According to water availability and priority, a simulated diversion is equal to or less than the required diversion. 'Shortage' is defined as the deficit between the required and simulated water diversions.

Section 2.3.1 presents the model outputs for the baseline scenarios without any changes to the storage capacity or the required diversions. For the baseline scenarios, the gap between the water supply and aggregate consumptive use (if all water requirements were met), annual shortages by model regions and users, and 30-year annual and half-monthly results summaries are all reported.

In section 2.3.2, three adaptation strategies of 10% and 20% demand reduction across all users and 25% increase to the current storage are implemented to test their impact on shortages. The demand reduction strategies represent a range of possible future management actions as described in the Colorado Water Plan (CWCB, 2015), such as enhancing water use technologies or reducing irrigated lands. Differences between demand reduction strategies are beyond the scope of this study but warrant attention in future research. Regarding reservoir infrastructure, a 25% increase in storage capacity, corresponding to 0.49 BCM, represents an arbitrary but achievable goal in the SPRB. The 30-year half-monthly mean shortage is the metric used to compare strategies for future baseline scenarios.

Section 2.3.3 shows the uncertainty analysis results, and section 2.3.4 presents a more generalized analysis of the impact of alternative starting conditions on shortages. Three scenarios and 48 alternative starting conditions of storage and required diversions are examined to generalize results. The DRY-8.5, DRY-4.5, and WET-4.5 represent the worst-case, middle, and optimistic scenarios, respectively (Table A3). Then for these scenarios, storage capacity is varied from 40% to 160% of the current storage by 20% increments and required diversions from 40% to 130% of the future baseline demands by 15% increments, resulting in 147 total simulations. The metrics used in this analysis are dimensionless to facilitate the generalization of results to other basins, as discussed in detail in the results section.

2.3. Results and Discussions

2.3.1. Baseline Scenarios

2.3.1.1. Consumptive Uses and The Water Balance Gap

The 10-year running annual mean aggregate consumptive use and water supply across the baseline scenarios are compared to examine how climate change and population growth affect the overall water balance in the SPRB (Figure A11). The aggregate consumptive use is the total of consumptive demands, losses from return flow, and mean historical reservoir evaporation. The 10-year annual mean provides an overview of the water balance by reducing the effects of extreme single wet or drought years. In SPRB, the consumptive uses plus the mean outflow are expected to continually exceed the mean water supply, on average, after the 2040s without effective adaptation strategies. This gap confirms that population growth substantially impacts potential water shortages more than climate change, as indicated in Figure 2.3. This simulated shortage is consistent with the results of previous studies (Brown et al., 2019; Foti et al., 2012; Heidari, Arabi, & Warziniack, 2021; Jaeger et al., 2017; Warziniack & Brown, 2019; Yigzaw & Hossain, 2016) that water shortage is predicted to increase in the areas projected to increased water demands and more variable water supplies.

2.3.1.2. Annual Spatial Shortages

WEAP-SP also provides the spatial distribution of expected shortages to help decision-makers prepare specific management plans for the study region. Shortages depend on the spatial location of each user, the priority of allocation, and overall water availability. Given the distribution of water rights, shortages are nearly shared equally between Ag and urban sectors. The annual aggregate urban shortages increase with time as population grows, while Ag shortages are more climate-dependent as irrigated areas are constant across the future simulations. The largest urban shortages occur in the Central region, followed by the North and the South Metro regions, where most urban required diversions exist. Ag shortages also mainly occur in North, East, and North Central regions where most Ag required diversions exist. Appendix A section 7 provides the annual required diversions and shortages by aggregate users, model regions, and basin total.

2.3.1.3. 30-Year Mean Results

In addition to the spatial distribution, WEAP-SP provides results at a half-monthly timestep to better understand the effect of climate change on water allocation within a year. Figure 2.5 provides the 30-year half-monthly average water supply, storage, outflow, reservoir evaporation, required diversion, and shortage for historical, near-future, and far-future baseline periods. Warming climate trends beget an earlier stream discharge hydrograph with lower future-period means across the scenarios (Figure 2.5a). The 30-year annual mean water supply is mostly greater than historical under the WET and WARM scenarios, and it is lower than historical for the HOT and DRY scenarios (Table A3). The simulated outflow from SPRB highly depends on the existing water supply with a wide range across the scenarios. Although the near- and far-future outflow means are close to the historical mean (Figure 2.5c), some scenarios (e.g., DRY-8.5) have low outflow (Table A3), meaning that in addition to water shortage, environmental problems from low stream flows could be likely.

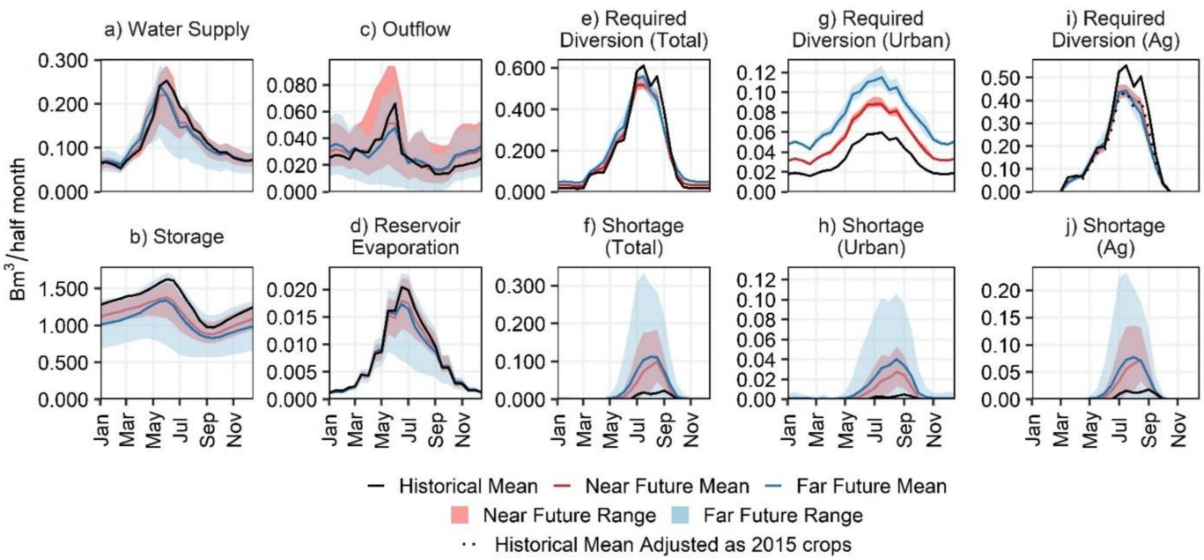

Figure 2.5: 30-year half-monthly water supply, storage, required diversions, and shortage means. The solid lines represent the mean across the eight climate scenarios, and the areas represent the maximum and minimum values at each timestep.

Historically, reservoirs in the SPRB store water from the high-flow season to the high-demand season (Figure 2.5b). This pattern remains the same in both future periods, allowing for the mitigation of the consequences of earlier water supplies but with lower storage means due to the changes in water supplies and required diversions (Figure 2.5b). Less stored water means that the mean evaporation from reservoirs will be lower in the future than in the historical period (Figure 2.5d).

Required diversion patterns have a lower peak and thicker tails in both future periods (Figure 2.5e) due to less irrigated land compared to the historical mean (Figure 2.5i) and increased urban requirements (Figure 2.5j). Figure 2.5i also shows the mean historical Ag required diversion assuming the same crops of the year 2015 as simulated in the future simulations. Despite the within-season required diversion change, the required annual mean diversions in the near-future are very close to the historical mean (Table A3). However, the far-future required annual mean diversions are much higher than the historical mean (Table A3). Additionally, the near- and far-future shortages have much higher and earlier peaks with a wide range across the climate scenarios (Figure 2.5f). The shortage distribution between Ag and urban is shown in Figure 2.5h and Figure 2.5j. The anticipated summer and early fall shortages indicate that urban outdoor conservation strategies are likely to be effective mitigation strategies (Figure 2.5h). Ag shortages increased and shifted earlier following the shift in water supply (Figure 2.5j).

Table A3 provides the 30-year mean shortage ratio, a ratio between the annual shortage divided by the annual required diversions. These values indicate that the shortage ratio: (1) is 2.2% during the historical period, (2) ranges between 0.5% and 9.9% in the WARM and WET scenarios that are considered the optimistic scenarios, (3) ranges between 10.7% and 13.5% in HOT-4.5 and DRY-4.5, (4) and ranges from 13.9% to 41.3% in the HOT-8.5 and DRY-8.5 scenarios (Table A3).

2.3.2. Effectiveness of Alternative Adaptation Strategies for Reducing Shortages

Adaptation for future resilience is the desired goal for decision-makers. This section presents the results of three adaptation strategies and the sensitivity of shortages to them. For comparison purposes, Figure 2.6a shows the baseline 30-year half-monthly shortage mean for the historical, and near- and far-future periods. The first tested strategy of 25% additional storage shows modest or negligible effects on decreasing shortages in both future periods (Figure 2.6b). However, demand reduction strategies directly diminish the shortages (Figure 2.6c and Figure 2.6d).

Overall, demand management strategies outperform storage infrastructure investment strategies because increasing demands affect the water balance more than changing the timing of water yields (Figure 2.6). Thus, a 10% demand reduction strategy lets the near-future mean shortage almost match the historical mean except from June to August (Figure 2.6b). Additionally, a 20% demand reduction strategy lets the near-future mean shortage be less than the historical mean and the far-future mean shortage be close to the historical mean except from May to August (Figure 2.6d). However, 25% additional storage has limited effects on decreasing the shortage (Figure 2.6b). Moreover, the performances of adaptation strategies do not vary across the climate scenarios (Figure A16).

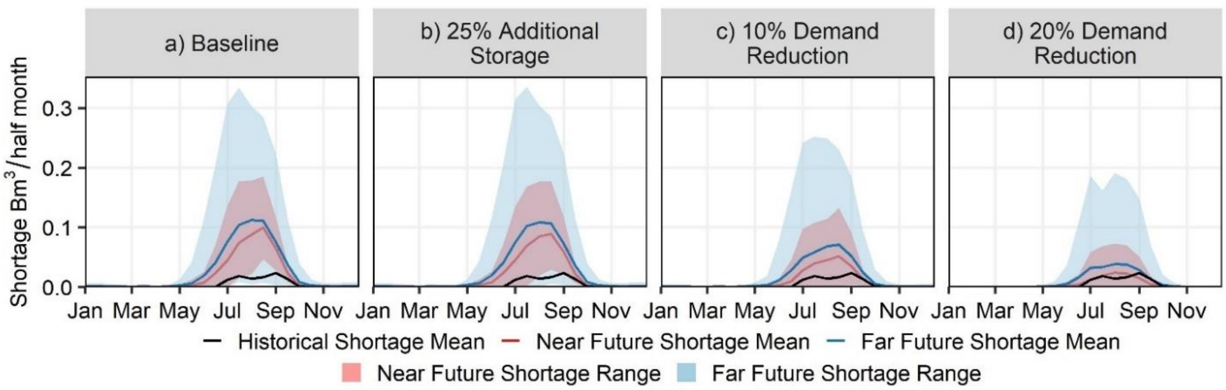

Figure 2.6: 30-year half-monthly shortage means of future baseline scenarios and the three alternative adaptation strategies with the historical mean. The solid lines represent the mean across the eight climate scenarios, and the areas represent the maximum and minimum values at each timestep across the scenarios. The results for each climate scenario is presented in figure A16.

2.3.3. Uncertainty Analysis

The two most significant WEAP-SP parameters from the Sobol analysis are the return flow losses and the flood irrigation consumption factor, indicating that they must be precisely estimated. The urban delivery efficiency and the residential indoor consumptive use come next in importance, while the others have limited impacts on the model performance. The calibration targets goodness of fitness for the total Sobol runs are calculated, and sets are reduced to the sets with NSE and KGE greater than 0.1 and Bias less than 40%. The Pareto front analysis for the reduced sets yields 108 non-dominated parameter sets through maximizing KGE values. The manual calibration results, as presented earlier, exist within the 95% confidence interval of the Pareto front sets (refer to Appendix A section 10 for more details).

The DRY-4.5 is simulated with the 108 sets, and the annual shortage ratio, calculated as the annual shortage divided by the annual required diversions, exists within the 95% confidence interval of the Pareto front sets. Finally, the coefficients of variation of the annual shortage ratio for the near future and far future are 0.07 and 0.1, respectively, indicating the low error range for the 108 model results and the feasibility of generalization.

2.3.4. Generalizing Results: An Index-based Approach

To generalize the results from the present case study, a range of required diversions and storage capacities across three climate scenarios are explored to determine thresholds when adaptation strategies will perform well. Results can inform the likelihood of shortages and how changes in demand and storage capacity may affect shortages in other basins with different initial conditions. Three indices are identified that drive the water allocation process: (X_1) the 30-year annual required diversion mean normalized by the 30-year annual water supply mean (WS), (X_2) the storage capacity normalized by WS, and (X_3) the 30-year annual return flow mean normalized by WS. The four components in these three indices can be measured for any water basin and describe more than 99% of the variance of the 30-year annual shortage ratio mean (Y); refer to Appendix A section 11 for more details. X_3 has a significant role in meeting the required diversions, which describes water use efficiency and ranges from 0.75 to 1.2 in the future baseline scenarios (Figure A21).

Figure 2.7 shows the relationship between X_1, X_2, and Y during the near and far future shortage for the WET-4.5, DRY-4.5, and DRY-8.5 scenarios. Looking at the horizontal axis, demand reductions always diminish shortage regardless of storage and inflow conditions. Also, all subplots in Figure 2.7 share the same trend of contour lines being almost vertical when the values of X_2 exceed a threshold of approximately 0.64, above which changes in storage capacity do not affect shortage. However, the contours display curvature below this threshold, reflecting non-linear relationships between Y and X_1 and highlighting the sensitivity of shortages to storage in this condition. Y decreases as X_2 increases until it reaches 0.64 (corresponding to 0.46 considering only active storage), as X_2 becomes insignificant -refer to Appendix A section 12 of statistical evidence of this threshold existence-. However, if X_2 exceeds 1.2, Y increases as X_2 increases because of more evaporation from a larger storage area, because dead storage volume and surface area increase when storage volume increases, leading to more evaporation losses. The current storage conditions in the SPRB are at or above the identified threshold in the dry scenarios, explaining why additional storage has negligible effects on shortages as discussed in Figure 2.6b.

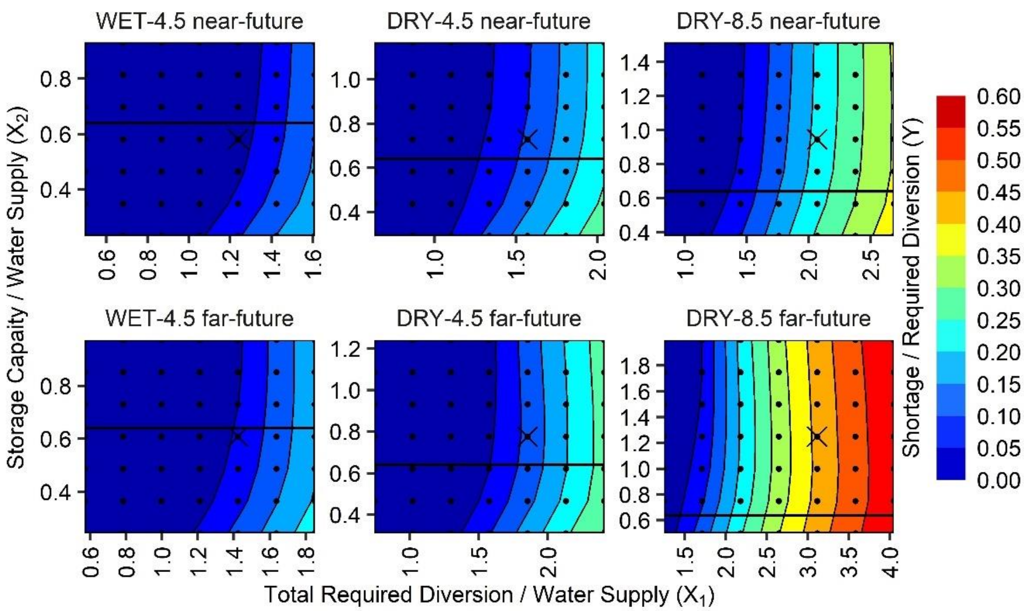

Figure 2.7: Shortage (Y) at different starting conditions -the dots- of required diversion (X_1) and storage (X_2); each subplot represents one 30-year period; the cross represents the future baseline conditions for each scenario.

Figure 2.8a shows the predicted Y at the mean of X_1 with a 95% confidence interval (Arel-Bundock, 2022) using the regression model shown in equation 2.2 (R-squared = 0.94). For the group with D = 0 ($X_2 < 0.64$), Y decreases as X_2 increases, while it is almost horizontal for the other group with a narrower confidence interval (Figure 2.8a). Additionally, the marginal effect of

X_2 on Y is almost zero for the D = 1 group (X_2 >= 0.64), highlighting that increasing X_2 has a negligible effect on Y (Figure 2.8b). This result implies, perhaps counterintuitively, that additional storage has more significant benefits as water inflows increase relative to current capacities (Lower X_2).

$$Y_{c,t,i} = \alpha + \beta_1 * X_{1\ c,t,i} + \beta_2 * X_{2\ c,t,i} + \beta_3 * D + \beta_4 * X_{2\ c,t,i} * D \quad 2.2$$

where c, t, and i represent the climate scenario, simulation period (near or far future), and starting conditions, respectively.

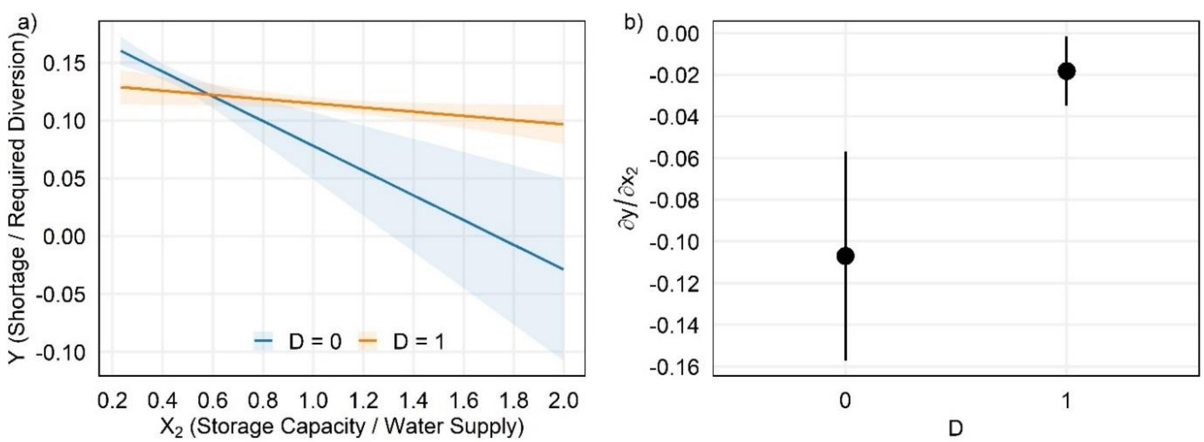

Figure 2.8: a) Conditional Adjusted Predictions of Y. b) Marginal effect of X_2 on Y. Both are for the groups above and below the threshold with 95% confidence intervals (Arel-Bundock, 2022).

From this generalization approach, basins above the 0.64 storage threshold would need to focus on demand reduction strategies to reduce shortages. In this case, investments in storage may not help reduce overall basin shortages. It is important to note, however, that additional storage may impact the shortages of specific users even if total shortages are not affected. While this distributional impact does not appear to occur in the current setup of WEAP-SP, it may be an important consideration for other basins considering expansion of storage capacity. This may be especially true if additional storage is accompanied by other strategies, such as purchasing the water rights of downstream users and storing the water.

2.4. Conclusions

In this study, a water allocation model (WEAP-SP) was developed and calibrated for the SPRB driven by population growth and climate change through 2100 with a half-monthly time step. The main goals are to predict the spatial and temporal future water shortage, test the effectiveness of demand reduction and additional storage strategies on reducing shortages, and identify generalized conditions under which each strategy may be beneficial to similar basins. Results indicated that although the reservoirs in SPRB reduce the consequences of the temporal shift of the water supply timing, a continuous shortage nevertheless exists after the 2040s.

In SPRB, the two tested strategies showed very different effects on water shortage mitigation. In all eight simulated climate scenarios, additional storage showed insignificant effects on reducing water shortages. Conversely, a 20% demand reduction strategy diminished the near- and far-future shortage mean across all eight climate scenarios to be close to the historical half-monthly shortage mean.

To generalize the effect of the two strategies to other basins, 147 scenarios were simulated at different starting conditions of required diversions and storage capacity. A threshold of the ratio between the storage capacity and the 30-year annual mean water supply of 0.64 was identified, above which additional storage does not affect water shortages. This suggests that areas expected to experience increased water inflows (or those with low current storage capacity) are most likely to benefit from additional water storage infrastructure. In contrast, demand reduction strategies always reduce expected shortages.

Although illustrating the impact of storage investment and demand reductions on water shortages is necessary to inform policy decisions, it is insufficient to recommend pursuing a specific strategy. Policymakers should consider the costs of candidate strategies compared with their effectiveness in reducing water shortage and the associated environmental impacts.

CHAPTER 3.

INTEGRATED LAND USE PLANNING AND WATER MANAGEMENT UNDER DIFFERENT WATER RIGHTS INSTITUTIONS: METHODOLOGY AND APPLICATION

Water supply systems are heavily influenced by the location and type of users within a watershed, which impact the timing and quantity of water demanded, as well as the availability of supplies to downstream users through heterogeneous rates of return flows. While numerous studies have investigated demand management policies as a means of mitigating the impacts of climate change and population growth, little attention has been given to how land use policies and water institutions interact in addressing these challenges. In this article, we develop a methodology to evaluate land use planning for population growth under alternative water institutions and climate scenarios by integrating the impacts of population locations and densities on water demands, water shortages, and economic values. We apply this methodology to the South Platte River Basin (SPRB) in Northeastern Colorado under three scenarios with ~2,700 simulations. Results suggest that a change to water rights institutions has a negligible impact on total shortages relative to climate change, but substantially impact the distribution of shortages across water users. Results also suggest that continuous population growth in upstream cities yields the lowest water shortages if per capita use decreases with urbanization. However, if we assume that cities have constant per capita demand, an equal distribution of population to upstream and downstream regions yields the lowest water shortage and highest economic value. These findings indicate a need for central planning efforts that account for return flows and development patterns throughout a watershed to reduce water shortages and promote economic prosperity.

3.1. Introduction

Sufficient freshwater supplies are crucial for food production, economic prosperity, and ecosystem functions. While the total amount of water present on Earth doesn't vary substantively from year to year, its temporal and spatial location has shifted over the past half-century (IPCC, 2022). These changes in the water availability over time and space have led to shortages in many basins (Degefu et al., 2018; Liu et al., 2018) that developed institutions and infrastructure for historical population densities, climate conditions, and hydrologic expectations which no longer exist. Increasing demands driven by population growth, industrial expansion, and environmental considerations have intensified the competition for limited water resources, particularly in arid western US states (Brewer et al., 2008; Brown, 2006; Tidwell et al., 2014). Water managers are now working to find novel solutions that better balance water supply with demand (e.g., Golfam et al., 2021; Kolokytha & Malamataris, 2020; Sun et al., 2017; H. Wang et al., 2020). Academics and practitioners have long argued for updating water rights institutions (water institutions) as a means of dealing with increased water scarcity (Grafton et al., 2013). However, explicit water institutions are not the only way to influence water scarcity. Urban planning policies that determine how populations grow, in terms of land use and housing density, also play an important role in determining water demand patterns (A. Miller, 2023; Richter, 2023; Ty et al., 2012).

While water supply (e.g., reservoirs) and demand (e.g., increasing block rates) management strategies have traditionally been options to address water shortages, these methods have diminishing returns since the "low-hanging fruit" has already been picked (Barnett et al., 2008; Brown et al., 2019; Gutzler & Robbins, 2011; Seager et al., 2013). For example, most high-quality dam sites have already been developed; where options do exist, environmental objections to dams and reservoirs often preclude their construction (Glennon, 2005). Water conservation technologies, such as center pivot irrigation or low-flow toilets, have seen mass adoption in recent decades such that additional demand-side conservation is likely to require substantial behavioral and technological change (Fleck, 2016; Gilligan et al., 2018; P. H. Gleick, 2002; Sankarasubramanian et al., 2017). Further, there is a limited understanding of how primary drivers of water scarcity—population location, land use, water institutions, and climate conditions—interact with each other at a basin level to cause water shortages.

Water markets have been proposed as institutional mechanisms for reallocating water among competing users that would improve economic efficiency (Garrick et al., 2013). However, the effectiveness of water markets in the western United States has been limited by high transaction costs and legal barriers imposed by the region's water laws (Womble & Hanemann, 2020). Historically, water trades that have occurred predominantly involve transfers from agriculture to urban areas (Payne et al., 2014). While changing water allocation institutions may provide substantial benefits, this suggestion has traditionally been met with strong political opposition, such that land use planning may be a more palatable institutional approach to balancing water supplies with demands.

Past literature contributes in part to the integration of those primary drivers— population location, land use, water institutions, and climate conditions —but no existing work has examined how spatial population locations interact with other primary drivers to affect water shortages and economic values. Miller et al. (1997) highlight the need to modify water institutions under a changing climate in order to mitigate extreme water shortages and economic losses. Ty et al. (2012) found that land use changes have greater impacts on water stress than climate change and Räsänen et al. (2018) reported that water and land use policies need tighter integration to minimize water-related risks (e.g., floods, droughts, and poor water quality). Wang (2020), as well as numerous technical papers (Belete & Gezie, 2017; Chhipi-Shrestha et al., 2017; Shandas & Parandvash, 2010; Stoker et al., 2019), suggest densifying the population through zoning and land-use regulations as an effective tool for improving water use efficiency and reducing per capita water demand.

The importance of integrating land use and water management has been recognized by researchers and policymakers, though its implementation is still limited. Stoker et al. (2022) published a literature review on the integration of land use planning and water management and highlighted calls for better integration (Angelo, 2001; Carter et al., 2005; Lucero & Dan Tarlock, 2003; Mitchell, 2005; Plummer et al., 2011; Shandas et al., 2015; Stoker et al., 2022; X. Wang, 2001). Similarly, Colorado's Governor has acknowledged the need for intentional land use/housing density policy given its clear implications for, *inter alia*, water use and continued economic prosperity (A. Miller, 2023).

This study builds on the modeling framework by Gharib et al. (2023) and provides a new framework for evaluating integrated water and land use management strategies under alternative climate and institutional settings. First, the methodology is presented; then it is applied to a representative watershed, the South Platte River Basin in Colorado. Specifically, we consider three water institutions, update Gharib et al.'s (2023) urban demand modeling to account for population density, and explore varying population location scenarios and land use policies. Lastly, we describe the distribution of population within the water basin that maximizes economic value or minimizes the water shortages that would occur.

3.2. Methodology

This section outlines novel methods for evaluating integrated land use planning and water management. The next section discusses the application of this method by parameterizing and calibrating the models used for simulations. Figure 3.1 provides an overview of the model framework developed for this analysis. Model drivers (in grey) include irrigated area, climate, urban land use density, population, and water institutions. These are used to generate model inputs (in green) that include water supply, agricultural demands, and urban demands. Based on this information, the water allocation model generates half-monthly water deliveries and calculates water shortages (yellow) for each user throughout the basin. Simulated water deliveries are then input into an economic model to estimate the generated economic value (also in yellow) from water across different runs.

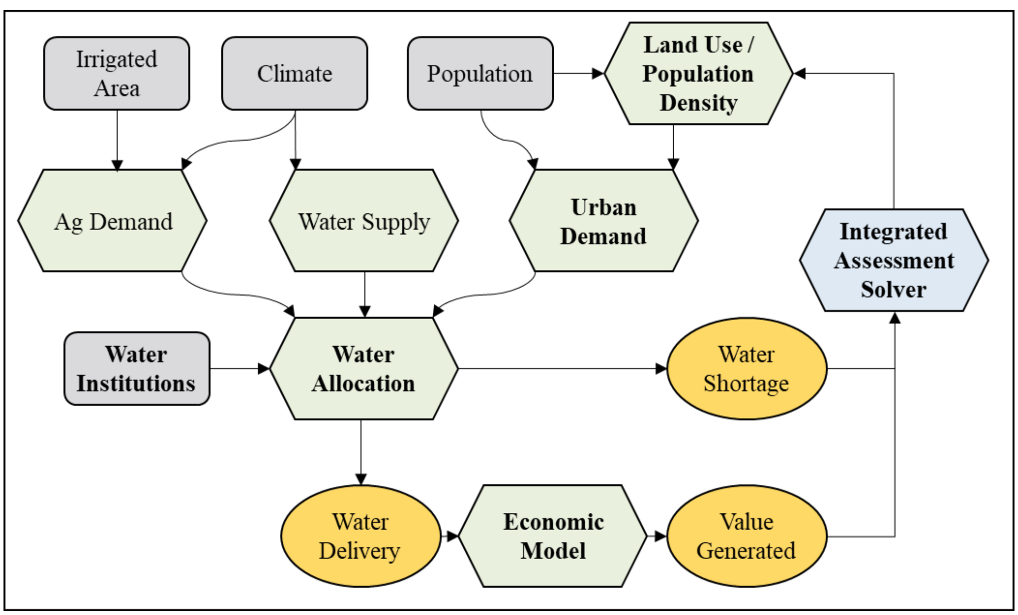

Figure 3.1. Integrated land use planning and water management Framework. Model Drivers in grey, modeling tools in green, outputs in yellow, and the integrated assessment solver in blue.

For water right institution θ and climate scenario δ, the objective of this framework is to provide the shares of population (x_r) in each region, r, within a basin that yields the lowest basin-wide volumetric water shortage ($Z|\theta, \delta$) or that generates the maximum basin-wide economic value ($\mathrm{P}|\theta, \delta$) under dynamic modeling of water demand and shortage. Both objective functions are solved independently, and optimal solutions may differ. The objective functions are:

$$\underset{x}{\text{Minimize}}\ (Z|\theta, \delta) = E\left[\sum_{i}\sum_{r}\sum_{t_1}^{t_2} D_{i,r,t}(x_r, \theta, \delta) - Y_{i,r,t}(x_r, \theta, \delta)\right] \quad \text{3.1}$$

Water shortage objective function

$$\underset{x}{\text{Maximize}}\ (\mathrm{P}|\theta, \delta) = E\left[\sum_{i}\sum_{r}\sum_{t_1}^{t_2} V_{i,r,t}(x_r, \theta, \delta)\right]$$

Economic value objective function

Subject to:

$$\sum_{r} x_r = 1$$

Population shares constraints

$$Z|\theta, \delta \geq 0$$

Shortage constraints

$$Y_{i,r,t}(x_r, \theta, \delta) \leq D_{i,r,t}(x_r, \theta, \delta)$$

Water delivery constraint

$$\sum_{i}\sum_{r} Y_{i,r,t}(x_r, \theta, \delta) \leq W_t(\delta)$$

Water balance constraint

Where $E[.]$ denotes the expected values of a response, $Z|\theta, \delta$ is the expected value of the annual total shortage between years t_1 and t_2 for all users i in all regions r conditional on the water right institution θ and the climate scenario δ, $\mathrm{P}|\theta, \delta$ is the expected value of the annual total economic value between years t_2 and t_1 for all users i in all regions r simulated under the water right institution θ and the climate scenario δ, x is a vector of ratios of the population in each region r, x_r is the share of population in region r, $D_{i,r,t}$ is the water demand for user i in region r in year

t, $Y_{i,r,t}$ is the water delivered for user i in region r in year t, solved through a water allocation model, W_t is the water supply available for delivery in year t under climate scenario δ, and $V_{i,r,t}$ is the value generated for user i in region r in year t, solved through a model of economic value. Specifically, $V_{i,r,t}$ is the integral of the marginal willingness to pay for water, $p_{i,r,t}$, equal to the inverse demand function for water as presented by Maas et al. (2016):

$$p_{i,r,t} = \begin{cases} \left(\frac{Y_{i,r,t}(x_r,\theta,\delta)\,\eta_{ir}}{c_{i,r}}\right)^{\frac{1}{\epsilon_i}} & if\ \ Y_{i,r,t}(x_r,\theta,\delta) \geq \tilde{Y}_{i,r,t} \\ p_i^{max} & Otherwise \end{cases} \tag{3.2}$$

where $Y_{i,j,t}$ is the quantity of water delivered to aggregate user i in region r at time t, $c_{i,r}$ is a calibrated constant, $p_{i,r,t}$ is the marginal value of water, ε_i is the price elasticity of demand for water, and η_i represents water use efficiency. Determination of a maximum marginal value is necessary for this model specification; otherwise, the inverse demand function (p) in equation 3.2 goes to infinity as water delivery goes to zero. Therefore, we define a parameter, p_i^{max}, as the maximum marginal willingness-to-pay (mWTP) for each user i that represents the marginal value of water when water deliveries fall below a threshold level, $\tilde{Y}_{i,r,t}$. In reality, the mWTP for water would not go to infinity, particularly for agricultural water users who would face negative profits at high water prices. Non-agricultural users would have opportunities to use alternative sources, implying that the benefits of water are finite.

The effect of land use policies arises from the population density, which is affected by the population's location. The urban demand $D_{i=urban,r,t}$ is calculated by multiplying the population $\varphi_{r,t}$ in each region r by the per capita demand in urban use $j \in \{\text{indoor}, \text{outdoor}\}, \mathrm{U}_{j,r,t}$. $\mathrm{U}_{j,r,t}$ is a function of population density, $S_{j,r,t}$ such that:

$$D_{i=urban,r,t} = \sum_j \varphi_{r,t} \, \mathrm{U}_{j,r,t} = \sum_j \varphi_{r,t} \left[\alpha_j \, {S_{j,r,t}}^{\beta_j}\right] \qquad 3.3$$

where $D_{i,r,t}$ is the demand for user i ∈ {urban} in region r and year t, $\varphi_{r,t}$ is the total population of region r in year t, $\mathrm{U}_{j,r,t}$ is the per capita demand for urban use j in region r in year t, $S_{j,r,t}$ is population density per 10,000 m^2, α_j and β_j are calibrated model parameters for sub-users j. Total population $\varphi_{r,t}$ in each region r in year t is calculated by one of the following equations:

$$\varphi_{r,t} = \begin{cases} \varphi^H_{r,t_o} + x_r \, \varphi^G_t & \text{if reallocating only population growth} \\ x_r\left(\varphi^H_{t_o} + \varphi^G_t\right) & \text{if reallocating the total population} \end{cases} \qquad 3.4$$

where $\varphi_{r,t}$ is the total population of region r in year t, x_r is the share of population in region r, φ^H_{r,t_o} is the historical population in region r at the baseline year t_o, φ^G_t is the basin-wide population growth from the baseline year t_o to year t, and $\varphi^H_{t_o}$ is the basin-wide historical population the baseline year t_o.

Finally, the statistically coherent probabilistic Dirichlet Distribution (Frigyik et al., 2010; Wong, 1998), a common probability distribution in Bayesian statistics, is selected to generate random samples x of the population shares across the model regions. The Dirichlet Distribution is specifically chosen as it ensures that the components of the sample vector x are non-negative and sum to one, which is essential since the elements of x represents shares of total population (or population growth). It takes the form:

$$f(x;\gamma) = \frac{\Gamma\left(\sum_{k=1}^{r} \gamma_k\right)}{\prod_{k=1}^{r} \Gamma(\gamma_k)} \prod_{k=1}^{r} x_k^{\gamma_k - 1} \qquad 3.5$$

where γ is the shape parameter, f is the probability mass function, and x is the vector of population shares in each region. The concentration of the distribution varies based on a shape parameter, γ. When γ is greater than 1, the density concentrates in the center of the probability simplex, defined as the set of all non-negative vectors whose components sum to one (Frigyik et al., 2010; Legaria et al., 2023). If γ is between 0 and 1, the concentration shifts to the vertices of the simplex (Frigyik et al., 2010). The distribution becomes uniform when γ equals 1 (Frigyik et al., 2010). Equations 3.1 to 3.5 present the mathematical formulation of the framework and the newly developed methods. In the next section, we introduce the study area and methods for parameterizing the model.

3.3. Application

3.3.1. Study Area

This paper focuses on Colorado, USA, a state with well-developed water laws and active water markets (Brewer et al., 2008; Womble & Hanemann, 2020), which makes it an ideal venue for studying the role of water and land use planning institutions. Specifically, the methodology is applied to the South Platte River Basin (SPRB) in Colorado, which is in the Northeastern portion of the state and is a critical water source for irrigation, municipal use, and recreation. We chose SPRB because it represents many basins throughout the western US that are facing water shortage challenges largely driven by rapid population growth and climate change. It is semi-arid and snow-dominant with no upstream flow, relies partly on inter-basin transfers, has an active water market, and has mixed agricultural and urban communities. Around 20% of the basin water supply comes from inter-basin transfers from the Colorado River Basin, which is experiencing a 23-year-long severe drought (Wheeler et al., 2022). The SPRB contains 71% of the state's population. However, only 9% live in the downstream regions (Regions 3 and 4 in Figure 3.2b), and 63% reside in Region

2b, around Denver (Figure 3.2b). Although the total population of the basin is projected to double by the end of the century, only 11.2% of the population growth is expected to occur in the downstream regions (CWCB, 2019b), reinforcing current population concentrations in upstream regions.

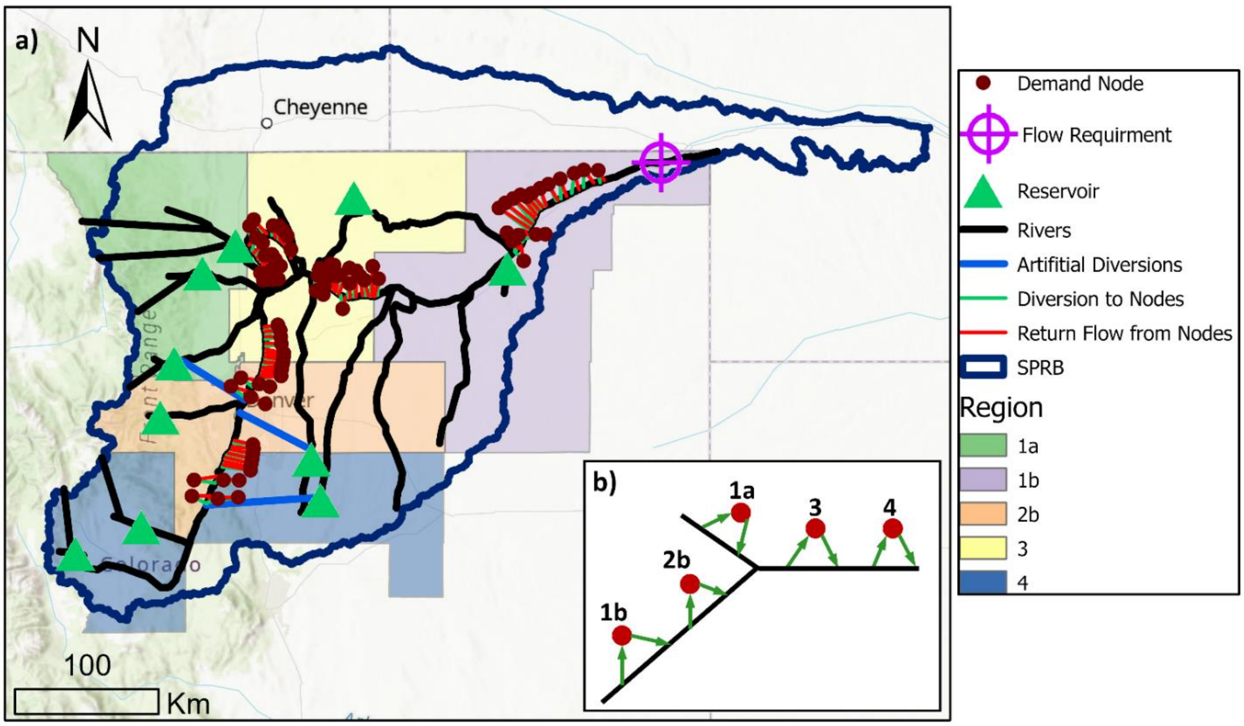

Figure 3.2. a) SPRB layout in the water allocation model (WEAP) showing the model links and nodes. b) simplified WEAP schematic for the regions in SPRB. Region 1a presents Boulder, Broomfield, and Larimer Counties. Region 1b presents Douglas, Elbert, and Park Counties. Region 2b presents Adams, Arapahoe, Clear Creek, Denver, Gilpin, and Jefferson Counties. Region 3 presents Weld County. Region 4 presents Logan, Morgan, Sedgwick, and Washington Counties

3.3.2. Data and model parameters

A calibrated water allocation model for the SPRB was developed by Gharib et al. (2023) using the Water Evaluation and Planning (WEAP) Model (Yates et al., 2005). WEAP attempts to maximize deliveries to users throughout the basin using linear programming iteratively for each priority in each timestep without foresight. Figure 3.2a illustrates the spatial layout of the model which includes 14 water supply nodes representing HUC8 catchments with 6 water supply nodes representing inter-basin transfers that provide water to agricultural and urban demands across five demand regions. Urban demands are split into indoor and outdoor demand nodes representing commercial, institutional, and industrial (CII), and residential water demands. Agricultural demand is modeled to reflect the main crop types in the SPRB under flood and sprinkler irrigation, represented separately.

3.3.2.1. Water Rights Institutions

WEAP allocates water to satisfy water demands based on the priority of the individual users, with higher demand priorities fulfilled first. Return flows and other natural flows become available to downstream users with lower priorities. WEAP iterates until all demands are met, or water is fully allocated (denoting a shortage). Colorado, like seventeen other western states, allocates water under the Doctrine of Prior Appropriation (PA) (Brown, 2006; Leonard & Libecap, 2019). Under this doctrine, individuals and entities who first diverted water for “beneficial use” are granted “seniority”. In times of shortage, if senior water users are unable to receive their total allotment due to diminished flows, they can “call” junior water rights holders, forcing them to cease diversions until the senior users’ full allotments are met. In practice, this generally results in a seniority date, below which junior users must reduce or pause withdrawals (Womble & Hanemann, 2020). PA does not broadly include any determination of the economic value of water use when allocating flows during times of shortage (Burness & Quirk, 1979). Most prior appropriation rights were established between 1850 and 1920 when water was valued primarily as an input to irrigated agriculture (Brewer et al., 2008). As such, it is feasible—and indeed frequent—that low-value users have senior water rights (Howe et al., 1982), though water rights sales from agriculture to urban users have occurred (Payne et al., 2014; Womble & Hanemann, 2020).

For this analysis, we consider three alternative water rights institutions (θ) including prior appropriation (PA) with fixed water rights, prior appropriation with a functioning water market (WM), and equal sharing (ES). The PA institution with fixed water rights simulates the historic water rights of the Doctrine of Prior Appropriation (as reported by the Colorado Decision Support System database up to the year of 2015) without the ability to reallocate water rights based on changes in demands. Specifically, in the model, each (aggregated) user's priority was assigned based on the weighted mean of the appropriation dates and the decreed flow rate for the portfolio of water rights held by the respective user, as reported by the Colorado Decision Support System database up to the year of 2015. Under PA, water demands associated with new population growth are assigned to a new node and – consistent with the Doctrine of Prior Appropriation - assumed to have a lower priority than all other existing demand nodes.

The WM institution simulates a case of prior appropriation while allowing water rights reallocation from agricultural to urban users. Under WM, all urban users are assumed to have higher priorities than all Ag users, with upstream urban users having higher priorities than downstream users to maximize return flow benefits. Lastly, the ES institution represents a proportional allocation of shortages, where all nodes in the basin have the same priority. WEAP then allocates an equal percentage of delivered water to each node based on its marginal demand.

3.3.2.2. Climate, Water Supply, and Agricultural Water Demand

The model relies on climate data, which drives both water supply and demand. Historical climate data from 1980 to 2015 are sourced from Naz et al. (2016). Future climate projections through the end of the century come from Abatzoglou and Brown (2012), who used Multivariate Adaptive Constructed Analogs (MACA) to downscale Global Climate Models (GCMs) of the Coupled Model Inter-Comparison Project Phase 5 (CMIP5) to high spatial resolution. Four climate models are selected based on Joyce & Coulson's (2020) definitions of the hottest (HadGEM2-ES365), driest (IPSL-CM5A-MR), wettest (CNRM-CM5), and warmest (MRI-CGCM3) average over the US. These definitions are based on precipitation and temperature changes over time as described by Joyce and Coulson (2020). Also, two Representative Concentration Pathways (RCPs), 4.5 and 8.5, are considered for each climate model, resulting in eight total climate scenarios, $\delta = \{$hottest 8.5, hottest 4.5, driest 8.5, driest 4.5, wettest 8.5, wettest 4.5, warmest 8.5, warmest 4.5$\}$.

The water supply, $W_t(\delta)$, represents the summation of the water yield and the inter-basin transfers to the basin from neighboring basins. Water yield, from Heidari et al. (2020), refers to the contribution to renewable supply from recent precipitation, available as surface or groundwater (Brown et al., 2019). It equals the sum of surface runoff and base flow estimated by the Variable Infiltration Capacity (VIC) model (Liang et al., 1994). VIC is a semi-distributed macroscale scale model that solves full water and energy balances to simulate land-atmosphere fluxes and flow routing (Liang et al., 1994).

Historical and future agricultural water demands, $D_{i=Ag,r,t}$, come from Gharib et al. (2023), where 6 crops (corn, alfalfa, grass pasture, wheat & small grains, sugar beets, and dry beans) and two irrigation technologies (flood and sprinkler), under both historical and the 8 future climate scenarios were simulated (Gharib et al., 2023). Gharib et al. (2023) simulated the irrigation water requirements of each of the 5 regions in SPRB using the DayCENT model (Del Grosso et al., 2000). DayCENT is a daily timestep version of the CENTURY model, which is used widely in agroecosystem studies to simulate crops, grasslands, forests, and savannas (Del Grosso et al., 2000). Similar to Gharib et al. (2023), irrigated crops and irrigation technology —flood or sprinkler irrigation— are assumed to remain constant in all future scenarios. Although this assumption may not entirely reflect reality, it allows us to isolate the role of climate and institutions.

3.3.2.3. Urban Water Demand

Historical urban water demands, $D_{i=Urban,r,t}$, also come from Gharib et al. (2023), which used the Integrated Urban Water Model (IUWM) (Sharvelle et al., 2017). The main inputs of the model are population, climate, and land use. IUWM simulates residential indoor, CII indoor, and total outdoor demands. We aggregate them into indoor and outdoor urban water demand for each region. Using the IUWM results from Gharib et al. (2023), we estimate the historical per capita demand $U_{j,r,t}$ of indoor and outdoor water uses in each of the model regions.

We analyze monthly data on the total billed residential and CII water from Denver, Fort Collins, and Pueblo municipalities from 2010 to 2017 to parameterize equation 3.3, and to calculate $U_{j,t}$. Average data for the months of December to March are used to represent the indoor per capita demand $U_{j=indoor,t}$ in liters per capita per day (lpcd) for the entire year. Outdoor per capita water demand $U_{j=outdoor,t}$ is calculated by subtracting the annual indoor per capita water demand from municipalities' total annual per capita demand. The monthly outdoor demand patterns come from the historical monthly average of the years 2010 to 2014 for each region of the IUWM simulations. The population density, $S_{j,r,t}$, is calculated as the total population divided by each city area and expressed in population per 10,000 m^2. These values were used to calibrate the power function in equation 3.3 for the indoor and outdoor per capita water demand, $U_{j,t}$. Indoor parameters are α_{indoor} = 748.93 and β_{indoor} = -0.348 with 0.88 R-squared value (Figure B2). While the outdoor parameters are $\alpha_{outdoor}$ = 4008.3 and $\beta_{outdoor}$ = -1.25 with 0.86 R-squared values (Figure B2). Both β parameters are negative meaning that as population density increases, the per capita demand decreases, with the outdoor declining more rapidly.

The future population projections, $\varphi_{r,t}^{G}$, were accessed from the Integrated Climate and Land Use Scenarios (ICLUS) tool. ICLUS provides population projections from 2020 to 2100 for all US counties (EPA, 2017). The SSP5 scenario is selected from the ICLUS V2.1.1 (EPA, 2020) to present the highest expected growth. As described in equation 3.3, the population $\varphi_{r,t}^{G}$ is multiplied by the per capita demand $U_{j,t}$ to get the indoor and outdoor total urban demand $D_{i=urban,r,t}$.

Finally, water use efficiencies and losses were estimated during the calibration of the water allocation model by Gharib et al. (2023) to calculate the required diversions. Required diversion is the consumptive plus return flow and losses. For simplicity, required diversions will be referred to hereafter as water demand. In 2014, agricultural demands represented 75% of the total demands with over half in Region 1a and 38% in the downstream regions (Figure B1). Urban demand was 69% in Branch B and 20% in Branch A, leaving 11% of urban demand in the downstream regions (Figure B1).

3.3.2.4. Economic Model Parameter

Demand curves as presented in equation 3.2 are developed for agricultural and urban users in each region following Maas et al. (2016). In this economic analysis, we aggregate the agricultural users in each region by the irrigation type as Ag Flood and Ag Sprinkler. Also, the indoor and outdoor urban users are combined and then disaggregated by the season into Urban Winter and Urban Summer. The maximum mWTP, p_i^{max} for urban and agricultural nodes are assumed as \$405/1000m^3 and \$81/1000m^3, respectively. Ag elasticities, $\varepsilon_{i\,\in\{Ag\ Flood, Ag\ Sprinkler\}}$, are estimated from the literature at -0.6 for Ag (Maas et al., 2016; Scheierling et al., 2006; Schoengold et al., 2006). Urban elasticities $\varepsilon_{i \in \{Urban\ Summer, Urban\ Winter\}}$, are assumed to be -0.7 and -0.2 for summer and winter periods, respectively (Dalhuisen et al., 2003; Espey et al., 1997; Olmstead et al., 2007). Efficiencies, η_m, are assumed as 0.5, 0.8, and 0.9 for Ag flood, Ag sprinkler, and both urban users based on SPRB WEAP assumptions.

The demand curve for each user (i) (flood-irrigated agriculture, sprinkler-irrigated agriculture, summer-time urban, and winter-time urban) has a unique kink point, $\tilde{Y}_{i,r,t}$, when the demand function reaches p_i^{max}, calculated through the calibration of the demand curve, (Figure 3.3). To calibrate the demand curves (equation 3.2) and calculate $c_{i,r}$, the initial price, $p_{i,r,t}$ is set to the lease price of \$33.25/1000m^3 based on historical climate and hydrologic averages, suggested by Maas et al. (2016) relevant to SPRB. All dollar amounts are in 2016 nominal values. The calibration constant $c_{i,r}$ is then calculated separately for each region under each simulation to get the kink point $\tilde{Y}_{i,r,t}$. The baseline demand curves of the baseline year 2014, the last year of the historical water allocation model simulations, are presented in Figure 3.3. Finally, the generated economic value from water $V_{i,r,t}$ is calculated by integrating the demand curves from zero to the water delivery $Y_{i,r,t}$ for each user and region and normalized by the generated values in the baseline year of 2014. Qualitative results are consistent but exact monetary values are sensitive to the choice of p_i^{max}. It is important to note that the generated values do not reflect any transfer payments associated with water rights transfers that would occur with a water rights market within the prior appropriation institution.

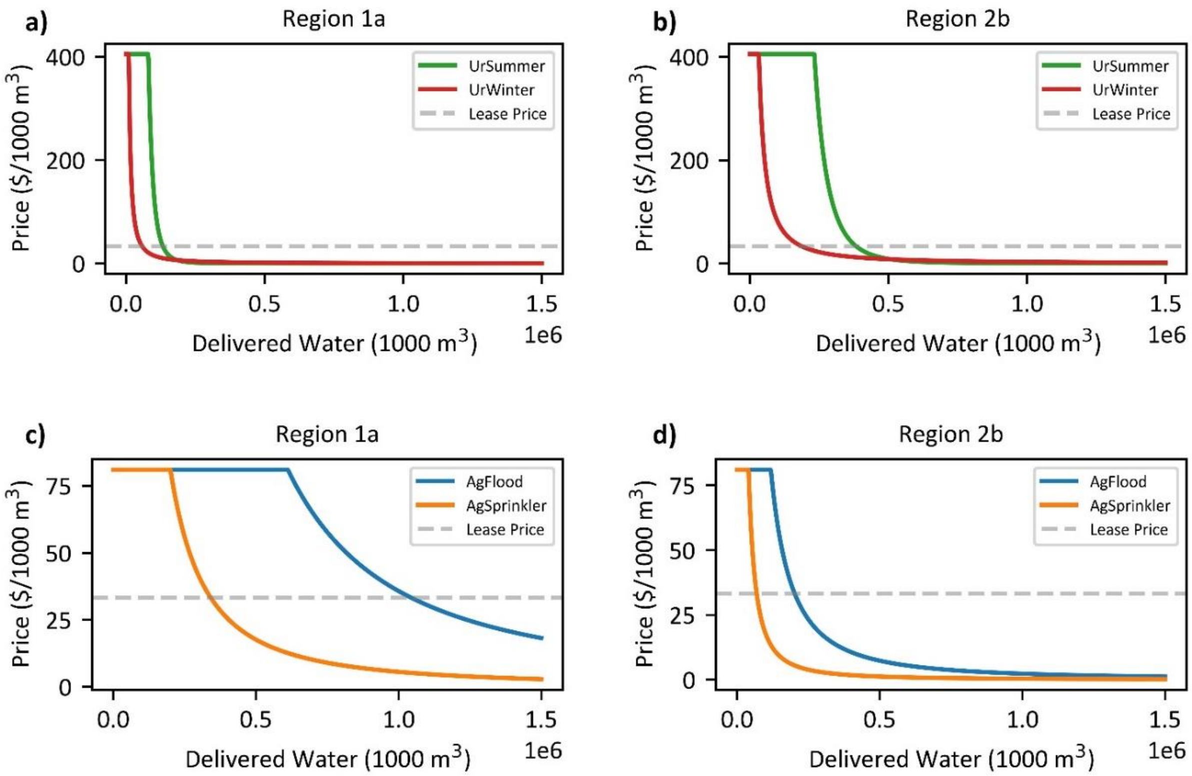

Figure 3.3. Demand functions for each water demand sector in Region 1a —largest Ag user— and Region 2b —largest Urban user— calibrated to the year 2014. (Refer to Figure B3 for the functions of the five regions)

3.3.3. Alternative Water Rights and Land Use Policies Scenarios

This section outlines the three key modeling scenarios applying the framework developed here (Table 3.1) to get approximate solutions to the water shortage and economic value objective functions. Thousands of simulations are implemented under these three scenarios to isolate the effects of changing climate, population location, land use patterns, and water institutions on water shortages and economic value using the water allocation model, WEAP. The first scenario compares the effect of water institutions and climate on the water shortages and generated values from water based on projected population growth locations and densities. The second scenario tests the effects of population growth reallocation in SPRB by considering alternative spatial distributions of new population in the SPRB, allowing density to differ based on location. The last scenario is intended to isolate the effect of population location from the effect of the density of urban growth, by holding the population density constant across space and testing the significance of only population locations within the basin. In this third scenario, we test two sets of moving only future population and both historical and future population. These scenarios are not designed to provide explicit policies to move current cities but to provide better options for future land use and housing policies.

Table 3.1. Alternative Water Rights and Land Use Policies Scenarios

	Scenario 1 **Baseline Future Scenarios in SPRB**	**Scenario 2** **Population growth reallocation under SPRB land use patterns**	**Scenario 3** **Effects of population locations to the water allocation under constant per capita demand**	
Water Institutions	3	3	3	
Climate Scenarios	8	1	1	
Population Locations	As Projected by ICLUS.	300 reallocation scenarios of the population growth	300 reallocation scenarios of population growth	300 reallocation scenarios of the total population
Population Density	Increases in upstream regions but constant in the downstream regions; urban per capita demand is like the region's historical values	Increases in upstream regions but constant in the downstream regions; urban per capita demand is like the region's historical values	Constant in all regions; urban per capita demand is the same across all the regions	
Number of Simulations	24	900	1800	

A few key modeling assumptions are applied consistently across scenarios. Irrigated crop areas, crop types, and irrigation technologies are held constant throughout the future time horizon. These assumptions control for agricultural demands so that the scenarios focus specifically on the effects of changing climate, population, and urban land use factors. The three alternative water institutions—prior appropriation, water markets, and equal sharing—are applied to all simulations.

The first scenario provides an initial reference point to compare the three institutions and eight climate scenarios before manipulating population densities and locations. We first assume that the projected locations of the population come directly from the ICLUS dataset without any changes to their locations. Second, the urban per capita demands $U_{j,r,t}$ for regions 3 and 4, with predominantly agricultural water use, are assumed to be constant into the future, equal to their historical values. This is mainly due to their low-density patterns in cities. Third, the urban per capita demands $U_{j,r,t}$ for the upstream regions 1a, 1b, and 2b are predicted based on population density using the power function presented in equation 3.3. These regions are more urbanized areas and are assumed to experience increased housing density that decreases the urban per capita demand.

The target of the second scenario is to test how the population density and location of the population affect water shortages, and the economic value generated. We assume that urban land use patterns hold as described in the previous scenario; the downstream regions grow with historical per capita demand, and the upstream regions grow with declining per capita demand. However, we vary the locations of the population growth across the regions rather than relying on the values reported by ICLUS in each region. We employ two shape parameters in the Dirichlet Distribution (equation 3.5), $\gamma \in \{0.1, 0.7\}$, to generate two-150 random variable sets x using the gtools R package (Bolker et al., 2022). The generated total of 300 samples covers a broad range of population combinations across the regions, as demonstrated in the results section. Equations 3.3 and 3.4 are then applied to calculate the total population $\varphi_{r,t}$ in each region and its urban water demand $D_{i=urban,r,t}$ for each population shares sample x. These simulations are carried out under the driest 4.5 climate scenario and three different water institutions, with a total of 900 simulations.

The last scenario focuses on the effects of population location within the basin while assuming constant future per capita demand across all regions and future years to highlight the effect of population locations on water allocation and value calculation. We assume all regions in the future have the same per capita urban demand, similar to Region 2b's historical per capita demand. Region 2b is selected as the majority of the population resides in it, and it has the highest efficiency of current water use. This approach allows us to isolate the impact of population location on water allocation and the importance of their return flow while holding other factors constant. Using this approach, we test how redistributing (1) only population growth and (2) total population (including existing plus new population) affects the water shortages and value. The same distribution (equation 3.5) with the same parameter values as the second scenario is used to generate the sample vectors x of the population shares in each region.

3.4. Results and Discussions

In this section, the results of each scenario are presented separately. To simplify presentation, the five regions are aggregated into two main regions: downstream regions (DS) representing Regions 3 and 4, and upstream regions (US) representing the other three regions (see Figure 3.2). The results are presented for the mean of the far future period from 2090 to 2099 to give average conditions not related to specific one-year climate data. Two key metrics are used to assess scenario performance: the mean annual shortage ratio (annual shortage divided by annual demand) and the mean annual generated economic value (generated economic value from mean annual water delivery divided by total generated value of the year 2014). These represent the values of the objective functions described in equation 3.1. Comparison of objective function values at all randomly drawn values of x reveals approximate solutions to the optimization problems.

3.4.1. Comparison of Climate Scenarios and Water Institutions under Baseline Population Growth and Land Use Policies

Overall, water institutions do not appear to have a substantial effect on total shortages at the river basin level compared to climate scenarios, but they influence the distribution of shortages across users and the total economic value generated (Figure 3.4). This section presents the results of the first scenario (Table 3.1) which focuses on investigating the effects of climate scenarios and water institutions on water shortages and economic value under baseline population growth and land use projections in the SPRB for the far future period. Figure 3.4 illustrates the mean annual far future shortage ratios and generated economic values relative to the baseline year of 2014 (both total and by sector) across each water institution and climate scenario. First, total shortage amounts vary little across water institutions (maximum of 2 percentage points), in contrast to the significant variations observed across climate scenarios (above 35 percentage points, Figure 3.4a). Second, while institutional changes have a relatively minor impact on total shortage amounts, they have a significant effect on who gets shorted (Figure 3.4a,b).

The total economic value increases in the wet and warm climate scenarios regardless of the water institution (Figure 3.4c), driven by population growth, as the average annual shortages are less than 4% (Figure 3.4c). For the dry and hot climate scenarios, the generated value decreases in all except for Dry4.5 and Hot8.5 under WM institution (Figure 3.4c), where water is allocated to urban users that have higher marginal value. Despite ES resulting in the highest total shortage under each climate scenario (Figure 3.4a), it exhibits two positive aspects: it efficiently distributes shortages between agriculture and urban sectors (Figure 3.4b) and generates higher total economic values than PA by allocating water from low-value users (e.g. flood irrigators) to high-value users (e.g. urban)" (Figure 3.4c).

As expected, the agricultural sector faces lower shortages and generates higher agricultural value under the PA institution compared to the other two institutions (Figure 3.4b,d). On the other hand, the urban sector faces lower shortages and generates higher value under the WM institution compared to the other two institutions (Figure 3.4b,d). Figure 3.4d also reveals that all urban users under the WM institution generate more economic value compared to 2014, irrespective of the climate scenario. These results collectively imply that altering water institutions can influence which sectors experience water shortages and generate more value, but the overall shortage and magnitude of value generated are primarily determined by climate changes, which are inherently uncertain and not controlled by local policymakers.

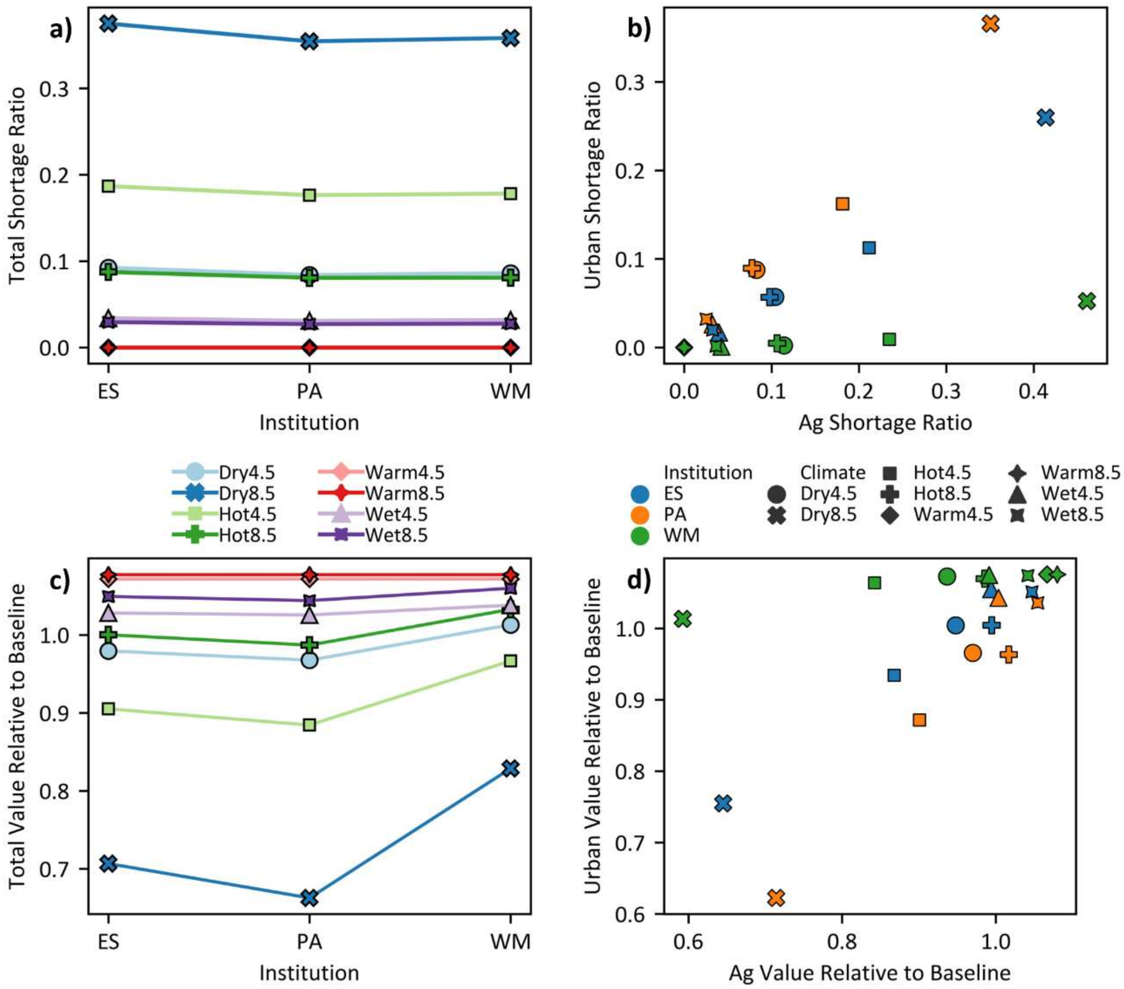

Figure 3.4. Baseline Mean Annual Shortage Ratio and Mean Annual Value Generated (relative to the baseline year of 2014) for the far future period 2090 to 2099. A) Mean Annual Total Shortage Ratio. B) Ag and Urban Mean Annual Shortage. C) Mean Annual Total Value Generated. D) Ag and Urban Mean Annual Value Generated.

3.4.2. Population Growth Reallocation under SPRB Land Use Patterns

In SPRB, the lowest water shortage is observed as more population growth joins the upstream regions, which reduces the total water demand because of the densification effect on urban water demand. As illustrated in Figure 3.4, climate plays a pivotal role in determining water availability, serving as the primary driver of total shortages, while other policies influence who experiences shortages and the extent of those shortages. Hence, to facilitate interpretation of the effects of population growth location, we present results for the Dry 4.5 climate scenario, which is the middle range of the simulated shortage and economic values (Figure 3.4a,c). The results of the second scenario (refer to Table 3.1) of reallocating the population growth with different patterns of per capita demands are summarized in Figure 3.5, with the share of downstream population growth occurring downstream on the x-axes. In each plot, 900 points are presented for each simulation under different population growth distributions and water rights with lines for the fitted second-degree polynomial.

The mean total annual shortage for the far future period increases as the share of population growth that is downstream increases (Figure 3.5a). This is mainly due to the constant (and relatively high) per capita urban demand assumed in downstream regions, and the limited ability to reuse return flows. On the other side, as more population joins the upstream regions, the urban per capita demand decreases as population density increases (Figure 3.5c), which decreases the shortage ratio (Figure 3.5a). The share of the projected population growth to the downstream regions is 9%. This suggests that projected growth is likely to lead to a relatively low overall shortage. Interestingly, the same trend applies across all water institutions, with equal sharing providing the highest shortage, similar to the results of the first scenario (Figure 3.4a, Figure 3.5a). Prior Appropriation tends to provide lower shortages compared to the water market institution as more population joins the downstream regions as seen by the increasing distance between the green and orange curves in Figure 3.5a.

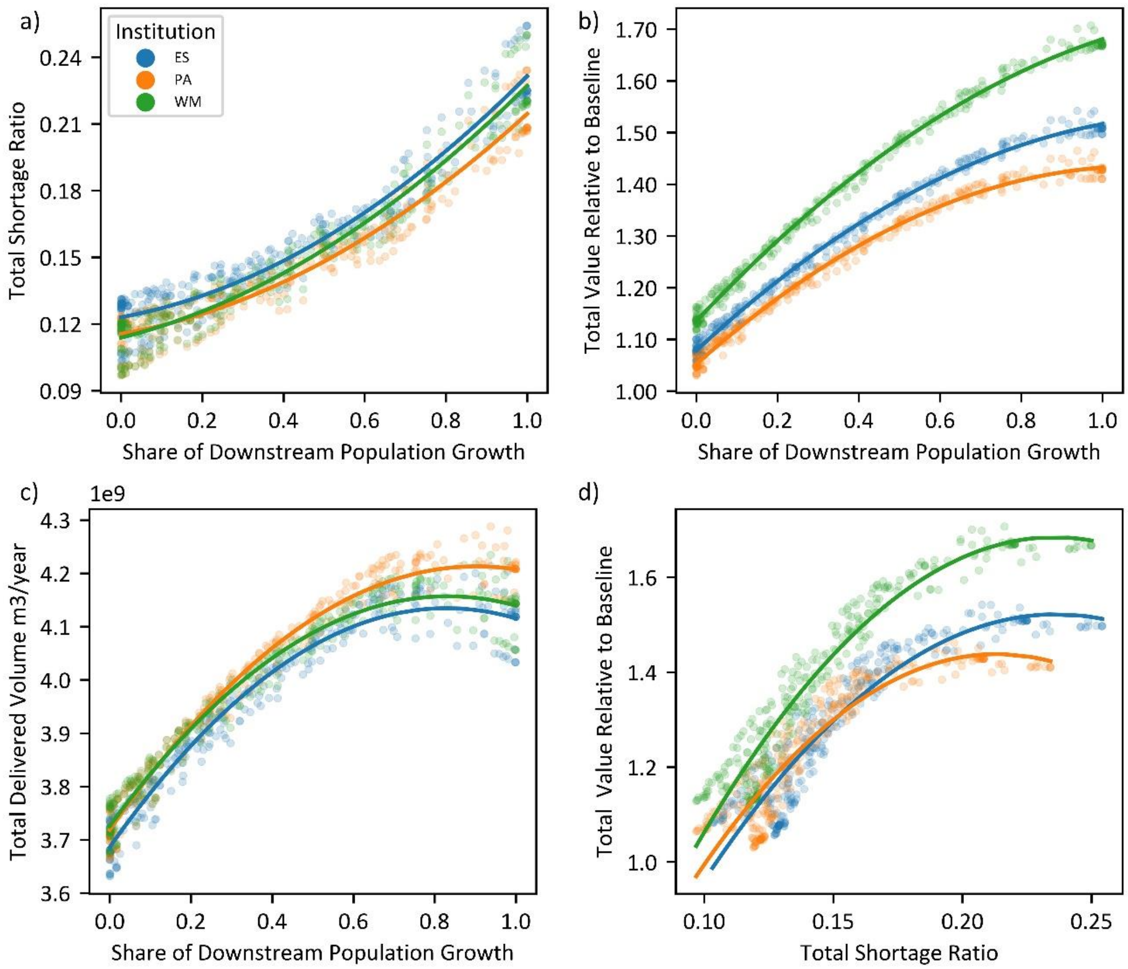

Figure 3.5. Far future mean annual results for the second scenario which reallocates population growth in SPRB with constant urban per capita demand for the downstream regions and declining per capita demand for the upstream regions under the dry4.5 climate scenario a) total shortage ratio, b) total generated economic value relative to 2014, c) total delivered volume, and d) total shortage ratio and generated economic value relative to 2014. Each dot represents one of the 900 simulations and the lines show second-degree polynomial fit.

The mean annual value generated in the far future shows a different story, highlighting the importance of including both metrics in water management studies (Figure 3.5b). The economic model generates more value as more water is delivered to the sectors with high marginal WTP for water, specifically, to the urban sector. Figure 3.5b shows that as the population growth share in downstream regions increases, more value is generated, mainly because of increased water deliveries for the urban users that derive relatively large benefits from using water. The total urban water demand is almost double when 100% of population growth is located downstream compared to 100% located upstream (Figure B4). Urban demand has lower consumptive use compared to Ag which generates more return flow that can be used more than once allowing for an increased amount of overall water delivery (Figure 3.5c, Figure B4). This result occurs because downstream households have larger lawns and other outdoor uses for water that have high value. On the other side, densifying people in upstream regions reduces the urban marginal WTP for water as people have smaller lawns and fewer outdoor uses for water. This lowers the total economic benefits from water used by urban households (Figure 3.5b).

Figure 3.5d shows the tradeoffs between the shortage ratio and the economic value generated across the population growth reallocation scenarios. This analysis does not suggest that sprawled growth that generates more value is preferred to dense growth, but it highlights that both metrics are important to inform decisions and tradeoffs associated with water allocation.

3.4.3. Effects of Population Locations to the Water Allocation Under Constant Per Capita Demand

If all cities in the basin grow with the same urban water demand pattern, an even distribution of population between upstream and downstream regions provides the lowest shortage and the highest economic value. For more generalizable results that are not specific to the growth conditions in the SPRB, this third scenario (refer to Table 3.1) assumes a constant per capita urban demand across all the regions in the basin and highlights the effects of only varying the location of the population within the basin. Two sets are tested under this scenario of reallocating the population growth and the total population of the SPRB. The first set – the left column of Figure 3.6 – shows the reallocation of population growth in SPRB assuming all cities in the basin will grow with the same urban pattern. The second set – the right column of Figure 3.6 – shows the results if all population is reallocated across the basin holding the per capita demand constant. It is important to highlight that these results are conditioned on the locations of Ag demands across the basin (Figure 3.2).

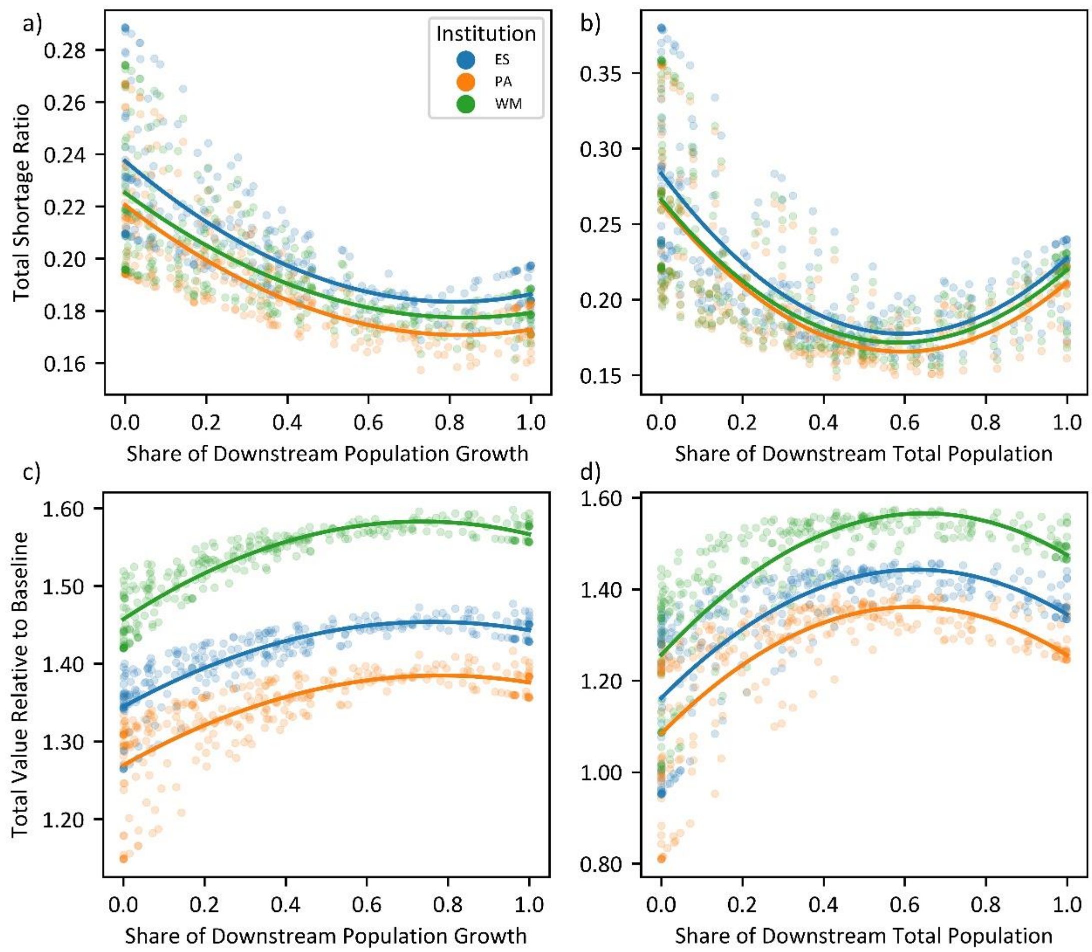

Figure 3.6. Mean annual total shortage ratios (top panels) and mean annual total economic value generated relative to 2014 (lower panels) for the far future period 2090 to 2099 under PA, ES, and WM institutions and the dry4.5 climate scenario. Each point represents one of the 900 simulations under the third scenario, which reallocates population growth (a, and c) or total population (b, and d) in SPRB with constant urban per capita demand for all regions. The lines show second-degree polynomial fit.

Total shortages decrease and then increase as the share of downstream population growth increases (Figure 3.6a). At the same time total value increases and then decreases (Figure 3.6c). These qualitative results hold under all water institutions. The lowest shortage and the highest economic value take place when around 80% of the population growth occurs in the downstream region (Figure 3.6a,c). The highest economic values also occur when 80% of population growth is in the downstream regions (Figure 3.6c). It is important to note that this allocation equates to nearly 50% of the total population in those regions. These findings emphasize the importance of spatially distributing populations within a basin to effectively manage water resources, taking into account the competing demands for local water resources and return flows associated with each use.

Across the 300 model runs for each institution, the total shortage ratio spans from 15.5 to 28.9% (Figure 3.6a). The range of economic values relative to the values of the year 2014 across all simulations is from 1.16 to 1.6 which reflects that economic value increases as more population exists regardless of the institutions (Figure 3.6c). Similar to the previous scenarios, the water market institutions yield the highest values, followed by equal sharing and finally prior appropriation.

Figure 3.6b and 6d display the result of the total population reallocation scenario with constant per capita demand to eliminate the effect of the distribution of the current population of SPRB. It is apparent that the most favorable outcomes, characterized by the lowest water shortages and highest economic values, emerge when populations are distributed more evenly across both upstream and downstream regions under all institutions, assuming all cities have the same water use pattern, with 50% to 70% of the total population located in the downstream regions (Figure 3.6b,d).

This finding emerges because urban water users typically have relatively low consumptive use rates, resulting in a large return flow that can benefit downstream users. The advantage (from a water shortage perspective) of distributing the total population between downstream and upstream regions is that the upstream population generates high return flows that become available to the downstream populations. If all population is upstream, this leads to high return flows but low downstream demand, diminishing the benefits from the return flows. Similarly, if the population is concentrated downstream, no users in the basin could benefit from the generated return flows. Further, concentrating the population downstream or upstream has other drawbacks, such as intensifying competition for local water resources and increasing vulnerability to climate extremes. One advantage of downstream population allocation is their ability to use all water infrastructure (e.g., reservoirs) and access more of the water inflows into the basin. This reduces their vulnerability to climate extremes, similar to California in the Colorado River Basin. The introduction of new land use policies governing where and how populations grow emerges as an effective strategy for impacting water shortages and value, highlighting the significant impact of population locations and their per capita use on water shortages and economic values.

3.5. Conclusions

This study develops an integrated assessment framework for dynamic water allocation and economic value calculation considering climate scenarios, land use policies/population locations, and water institutions. Then the framework is applied to the SPRB and three main scenarios are tested to provide several insights into factors influencing water shortages and economic values. The first scenario involves the impact of climate scenarios and water institutions on water shortages and economic value under baseline population growth assumptions in the SPRB. The second scenario explores the effects of population growth location and density on water demand, water shortage, and the generated economic value under varying water institutions. The last scenario isolates the effects of current and future population locations on water shortages and the economic value generated.

Results from the first scenario reveal that while water institutional changes influence the distribution of shortages among sectors, climate (together with population growth) remains the primary driver of total shortage. Despite notable increases in shortages under some climate scenarios, the total economic value increases, as the urban sector has increasing demands and willingness to pay for water, leading to higher economic values. While these results are intuitive—more people demanding water leads to a higher marginal and total value for water—welfare implications should be interpreted with caution since per capita water use is still lower. Notably, water markets (WM) and equal sharing (ES) institutions exhibit higher value generation due to the reallocation of water from agriculture to urban users where the marginal value of water is higher. Population growth is identified as a factor likely to amplify the economic value generated, particularly in the context of water markets. In the SPRB, the lowest water shortage is observed as more population growth occurs in the upstream regions, which reduces the total water demand because of the densification effect on urban water demand.

Assuming the current urban land use of SPRB continues, the second scenario suggests that as more population growth occurs in upstream regions, water shortages decrease, but the generated economic value also decreases. This shows the tradeoffs associated with densifying urban communities that decrease water shortages but also decrease the value generated from water. While this result initially seems counterintuitive, it manifests largely because less dense communities have equal or higher marginal values for a given level of water use. For example, a residential water user in downtown Denver gets very little value from additional units of water beyond what is needed for domestic purposes, whereas a user in a more rural community can use additional water for lawn irrigation or to fill pools. In this case, allocating people to the upstream denser communities is better from the perspective of reducing water shortages.

The third scenario examines population reallocation under constant per capita demand, emphasizing the significant influence of population location on total and sector-specific shortages and economic values. Minimum shortage and maximum economic value occur when a population is distributed more evenly between upstream and downstream regions, representing a favorable strategy for minimizing water shortages while maximizing value. Furthermore, the downstream population has advantages in terms of return flow availability, infrastructure utilization, and climate resilience.

The presented scenarios highlight tradeoffs between water allocation institutions. The equal sharing institution causes the highest total shortage but allocates water more evenly between Ag and urban users, which yields an intermediate economic value. The water market institution, on the other hand, generates the highest value as water is allocated first to urban uses that have higher marginal values and higher return flows, but provides an intermediate water shortage. Lastly, the prior appropriation institution yields the lowest water shortage under most conditions but also generates the lowest economic value.

Ultimately, this study demonstrates the robustness of strategies that focus on land use policies and the location of urban development as tools to address water scarcity, irrespective of climate uncertainties or challenges associated with water rights institutions. Our findings do not call for sprawling growth as denser housing communities lead to lower water shortages. However, we highlight that both how and where communities grow matter in water management and assessment. As policymakers seek reliable solutions to water resource challenges, the insights from this study offer valuable guidance toward achieving sustainable water management through strategic land use planning.

3.6. Nomenclature

CII	commercial, institutional, and industrial
Ag	Agriculture
$E[Z\|\theta,\delta]$	expected value of the annual total shortage between years t_2 and t_1 for all users $i \in$ {Agriculture, Urban} in all regions r simulated under the water right institution θ and the climate scenario δ
$E[P\|\theta,\delta]$	expected value of the annual total generated value between years t_2 and t_1 for all users i in all regions r simulated under the water right institution θ and the climate scenario δ
$D_{i,r,t}(x_r)$	water demand for user i in region r at year t,
$Y_{i,r,t}(x_r,\theta,\delta)$	water delivered for user i in region r at year t solved through the water allocation model
$V_{i,r,t}(x_r,\theta,\delta)$	value generated for user i in region r at year t solved through the economic value model
x	ratio of the basin wide population in region r
x_r	vector of the ratios of the basin's population in each region r
$W_t(\delta)$	water supply available for delivery at year t under climate scenario δ
θ	Water institution
δ	Climate scenario
i	Demand users i
r	Model regions
t	Time step or year
p	marginal value of water
mWTP	marginal willingness-to-pay
p_i^{max}	maximum marginal willingness-to-pay
ε_i	price elasticity
$c_{i,r}$	calibrated constant
η_i	Water use efficiency
$Y_{i,r,t}(x_r,\theta,\delta)$	the quantity of water delivered to user i
$\tilde{Y}_{i,r,t}$	threshold water delivery level
$\varphi_{r,t}$	total population of region r at time t

$U_{j,r,t}$	per capita demand for urban sub-uses $j \in$ {indoor, outdoor} in region r at year t
$S_{j,r,t}$	population density per 10,000 m^2
α_j	Calibrated parameter
β_j	Calibrated parameter
φ^H_{r,t_o}	historical population in region r at the baseline year t_o,
$\varphi^G_{r,t}$	population growth of region r from the baseline year t_o to year t
γ	shape parameter of the Dirichlet Distribution
f	probability mass function of the Dirichlet Distribution

CHAPTER 4.

EFFECTS OF GROWING WATER-SUPPLY-DEMAND GAP ON GROUNDWATER DEPLETION ACROSS U.S. RIVER BASINS

Water supply, demand, and shortage projections profoundly influence future growth strategies, especially as some cities curb new housing projects due to limited water resources. However, studies that comprehensively address the entire water balance, particularly integrating allocation aspects, are still limited. In this study, we present a monthly water allocation model spanning from 1985 to 2070 across sub-regions in the Contiguous United States (CONUS). First, we forecast water withdrawal and consumptive use under four socioeconomic scenarios and ten climate models. Integrating these projections with available data on water yield, reservoirs, and inter-basin transfers under various climate scenarios, second, we model water shortages and their implications on groundwater depletion. Findings reveal that irrigation dominates consumptive use, exceeding 75% historically and in future projections. Despite its significance in water shortage calculations, the consumptive use ratio has received limited attention in the literature. Water shortage calculations show that although groundwater mining is not sustainable in the future as its volume diminishes, additional demand reduction strategies are required in the future to mitigate water shortage. Finally, relying only on renewable groundwater pumping would increase the requirements for demand reduction strategies, however, more sustainable.

4.1. Introduction

Adaptation to the future is a critical aspect of governance globally, particularly in the water sector, as it impacts our lives and survival (Huang et al., 2021). The growing challenges of climate change and population growth continually pressure water managers to seek to balance supply and demand. Global water withdrawals fueled by rapid population growth and urbanization have tripled in the past five decades (Ferrara, 2008; Stoker & Rothfeder, 2014). Climate change is a major factor that affects social and economic outcomes (Carleton & Hsiang, 2016). It threatens the rise of agricultural yields and the profitability of agriculture (Bareille & Chakir, 2023; Moore & Lobell, 2015), may inflate electricity demand, and may trigger population movements within and across national borders (Carleton & Hsiang, 2016). Baldos et al. (2023) highlight that no individual is exempt from contributing to the climate change issue (Baldos et al., 2023).

In the US, climate change had major consequences and is projected to continue affecting several river basins across the country (Dettinger et al., 2015; Haddeland et al., 2014; Palmer et al., 2008). The most obvious issue is the mega-drought that started in 2000 and still going on in the Colorado River Basin in the Southern Western US (O. L. Miller et al., 2021; Richter, 2023; Villarini & Wasko, 2021; Wheeler et al., 2022; Williams et al., 2022). According to the survey by Rudd & Fleishman (2014), the question of how much water is needed to sustain the future population and ecosystems is the most emerging among policymakers and scientists (Rudd & Fleishman, 2014). Stackpoole et al. (2023) highlight the importance of the integration between the components of the national-scale water resources trend assessments. According to Stackpoole et al. (2023), the domains are the surface and groundwater quality and quantity, and the uses consist of human and ecological, and finally the drivers are climate, land use, and human use (Stackpoole et al., 2023). Additionally, Groundwater aquifers' depths are declining across the United States and should be treated more wisely as a non-renewable water resource (GebreEgziabher et al., 2022; Thaw et al., 2022).

Improving water demand forecasts will help planners understand and optimize future investments in water supply infrastructure and related programs (Ashoori et al., 2017). The increasing water demand contributes twice as much as the decreasing water availability to water shortage (Yan et al., 2006). Population and economic growth alone would increase water stress in the United States through mid-century (Blanc et al., 2014). Water scarcity is not just a supply problem, but also a demand problem, and is not truly scarce in most of the world at a national scale (Rijsberman, 2006). A recent U. S. Geological Survey water-use report suggests that increasing water-use efficiency could mitigate the supply-and-demand imbalance arising from changing climate and growing population (Sankarasubramanian et al., 2017). Water is at the center of a complex and dynamic system involving climatic, biological, hydrological, physical, and human interactions (Blanc et al., 2014).

Research studies that focus on a single component of water resources assessments are way more than studies that integrate them. Several studies focused on the water supply sides (e.g. Archfield et al., 2016; Dudley et al., 2017; Hammond et al., 2022; Konikow, 2015; Megdal et al., 2015; Rateb et al., 2020). Other studies focused on water demand sides e.g. (Brown, 2000; Brown et al., 2013; Chinnasamy et al., 2021; Warziniack et al., 2022). Very few studies model the water allocation across the entire United States while considering most of the components. For example, Brown et al. (2019) and Warziniack & Brown (2019) project the water withdrawals for the 204 sub-regions (HUC4) in the Contiguous United States (COUNS) using the proposed methods by Brown et al. (2013) and Foti et al. (2012), and simulate the water allocation to calculate water shortage under varying conditions (Brown et al., 2019; Warziniack & Brown, 2019).

In this analysis, we build on the previous water allocation model for the CONUS provided by Brown et al. (2019) and Warziniack & Brown (2019) which serve as a starting point. We then (1) develop a new water demand model for each water sector (n = 5) in each CENSES region (n = 4), (2) better represent the groundwater using the groundwater depletion dataset, (3) update the water yield and inter-basin transfers (IBT) with recently available data, and (4) enhance the water shortage calculations. Most importantly, this study considers two scenarios of groundwater pumping. The first scenario assumes that the groundwater pumping rate is limited to the amount of groundwater recharged, providing sustainable groundwater strategies. The second scenario considers groundwater depletion is the amount of groundwater mining from non-renewable resources to supplement the available water sources. Both scenarios are modeled under two water demand scenarios to provide a wider range of future estimates.

4.2. Materials and Methods

4.2.1. Overview

The modeling framework contains three main components: water supply, demand, and allocation modeling (Figure 4.1). The water yield and inter-basin transfers (IBT) were obtained from existing literature with minimal modeling effort (Heidari et al., 2020; Siddik et al., 2023). The groundwater pumping estimates from the non-renewable resources (mining) come from the USGS groundwater depletion report.

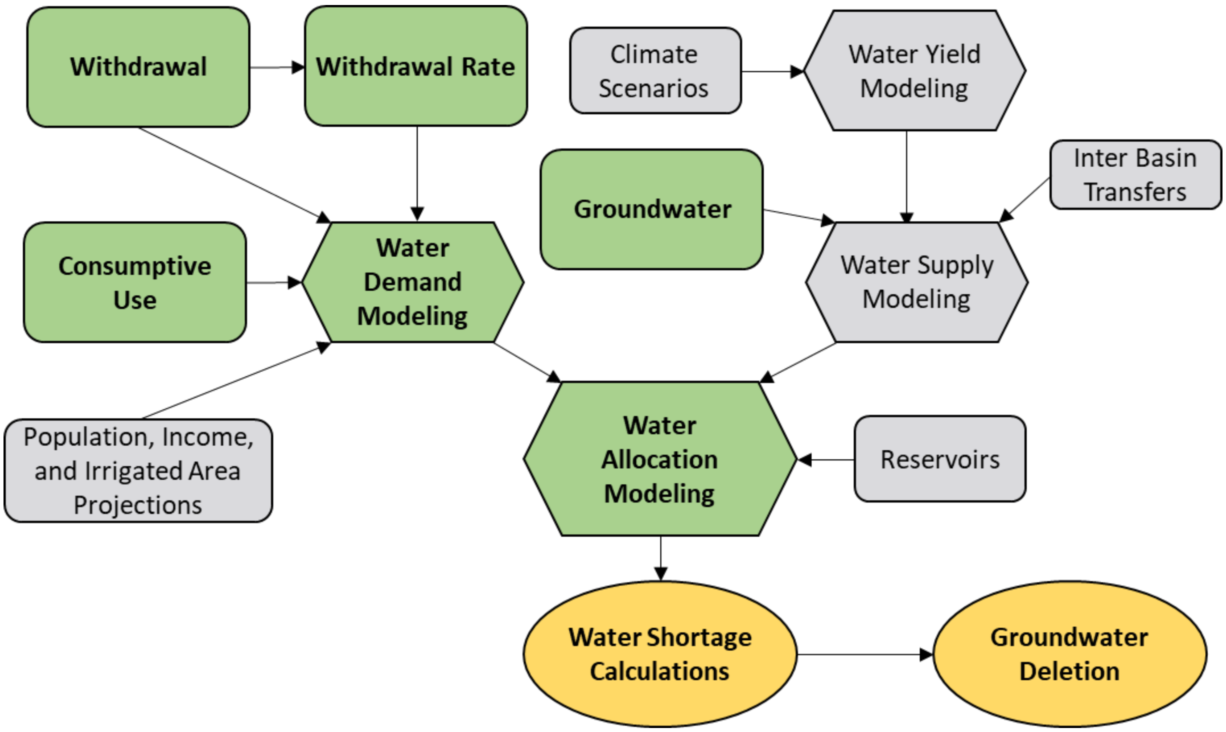

Figure 4.1. The study framework. In bold with a green background is the main contribution of this study. The light text with a grey background is taken from literature with minimal modeling effort. The yellow ovals are the framework outputs.

The demand modeling starts by analyzing the historical USGS water withdrawal datasets for all counties in CONUS, excluding island counties, from 1985 to the latest available year of 2015 across five water sectors. We then calibrate an auto-regressive exponential model to predict changes in withdrawal rates (i.e., liters per capita) at the CENSUS region level (Midwest, Northeast, South, and West), hereinafter referred to as regions. Next, we project future water withdrawals for the 204 sub-regions in CONUS, based on the 4-digit hydrologic unit code of the USGS. After that, we estimate the consumptive use ratios for the four regions and apply them to the withdrawal projections to get the consumptive use, which is used to define the demand in the allocation model. Both water supply and water demand in addition to reservoir data were integrated into a Water Evaluation and Planning (WEAP) model (Yates et al., 2005) that serves as the core water allocation model for this study. WEAP simulates water delivery to each demand node and calculates shortage volume at each time step.

4.2.2. Climate and socioeconomic scenarios

Climate scenarios are chosen based on Joyce's and Coulson's (2020) recommendations, covering a wide range of climate conditions for the entire United States, from driest and hottest to the wettest and least warm, with one model representing intermediate conditions (Table 4.1). Joyce's and Coulson's (2020) definitions are based on calculations involving temperature and precipitation percent changes across the United States. These scenarios utilize representative concentration pathways (RCPs) 4.5 and 8.5 based on the fifth Intergovernmental Panel on Climate Change (IPCC) assessment report (IPCC, 2014).

Table 4.1. Climate models (Joyce & Coulson, 2020)

Climate Model	RCP	Description	Model agency
MRI-CGCM3	4.5 and 8.5	Least Warm	Meteorological Research Institute, Japan
HadGEM2-ES365	4.5 and 8.5	Hot	Met Office Hadley Center, U.K.
IPSL-CM5A-MR	4.5 and 8.5	Dry	Institute Pierre Simon Laplace, France
CNRM-CM5	4.5 and 8.5	Wet	National Centre of Meteorological Research, France
NorESM1-M	4.5 and 8.5	Middle	Norwegian Climate Center, Norway

The USDA Forest Service 2020 RPA Assessment (Langner et al., 2020) evaluated future scenarios combining RCPs and Shared Socioeconomic Pathways (SSPs). RCPs model greenhouse gas trajectories and radiative forcing. While, SSPs describe socioeconomic development pathways characterized by population, economic growth, technology, and governance. This assessment suggested a total of 20 scenarios as a combination of five climate models, two RCPs, and four SSPs that provide a range of potential climate and socioeconomic futures within the United States (Table 4.2). Specifically, RCP 4.5 was linked with SSP1, and RCP 8.5 was linked with SSPs 2, 3, and 5, resulting in 20 total scenarios (Langner et al., 2020).

Table 4.2. Main Assessment Scenarios (RCPs and SSPs)

Scenario	Global scenario links	Climate model
Lower warming and moderate US socioeconomic growth	RCP4.5-SSP1	5 models
High warming and low US socioeconomic growth	RCP8.5-SSP3	5 models
High warming and moderate US socioeconomic growth	RCP8.5-SSP2	5 models
High warming and high US socioeconomic growth	RCP8.5-SSP5	5 models

4.2.3. Water withdrawals Modeling

Three main components formulate the water demand modeling as described in this section. The first component is water withdrawal, defined as the total water diverted from water streams or groundwater sources to beneficial use. It is also important to note that this study focuses on freshwater withdrawals, excluding saltwater. The second component is the consumptive use ratio, defined as the potion of the withdrawals that are consumed and don't return to the surface water or groundwater (e.g. evapotranspiration). The last component is the withdrawal rate that is used for modeling withdrawals (e.g. irrigation depth).

4.2.3.1. Water withdrawals (WD)

The most recent 7 USGS withdrawal datasets at 5-year intervals from 1985 to 2015 at the county level (Dieter et al., 2017; Hutson et al., 2004; Kenny et al., 2009; Maupin et al., 2014; Solley et al., 1988, 1993, 1998) are the data used for modeling the water demand. Over the years, some counties had different names, split, or merged. We apply Wear & Prestemon (2019) suggested changes to county codes, summing values for matches (Wear & Prestemon, 2019). We then aggregate counties into the sub-regions for each water sector. The water demand sectors were: domestic (DOM), industrial/commercial/mining (ICM), irrigated agriculture (IR), livestock/aquaculture (LA), and thermoelectric (TH).

Significant differences exist between data sets before and after 2000, specifically in identifying public water supply (PS) deliveries to different sectors. The first 3 years split PS withdrawals into deliveries to domestic, industrial, commercial, thermoelectric, and losses. However, later years only reported total PS and domestic deliveries. We use data sets from 1985 to 1995 to estimate PS delivery ratios to each withdrawal sector and apply them to later years. Additionally, DOM and ICM in 2000 are assumed to be the average values from the 1995 and 2005 datasets as they were missing 2000 from this dataset.

From these datasets, irrigated agriculture is the primary withdrawal sector, comprising nearly 40% of total withdrawals over the years (Figure 4.2). Thermoelectric withdrawals follow closely at around 38% of the total. Livestock and aquaculture represent approximately 2% of withdrawals, while the remainder is split between domestic and industrial uses.

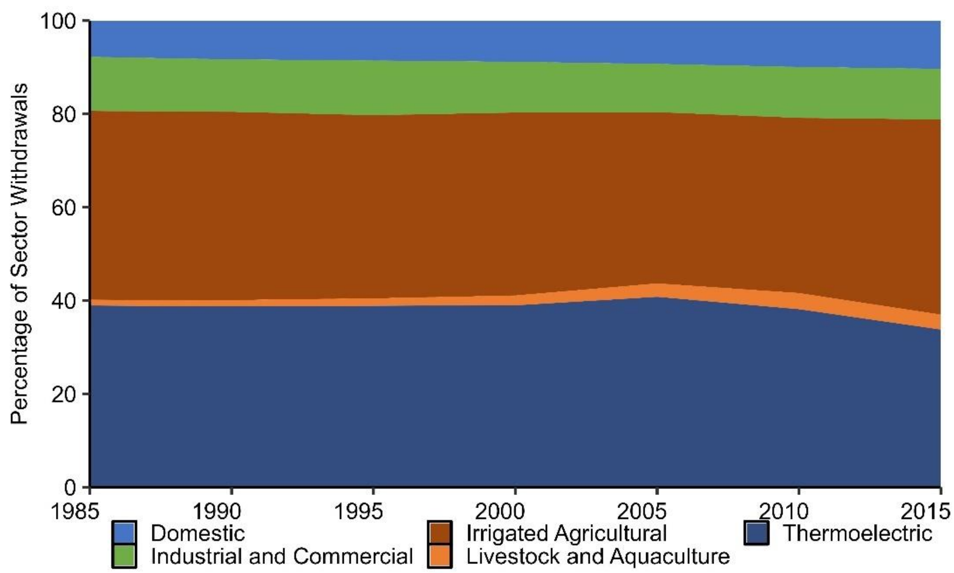

Figure 4.2. Total withdrawals by percentage of each demand sector.

4.2.3.2. Consumptive Use (CU) Ratios

Consumptive use (CU) ratio refers to the portion of water withdrawn that is consumed and not returned to the water system, thus unavailable for reuse (Dieter et al., 2017; Solley et al., 1998). Major consumptive uses include evaporation, transpiration by plants, incorporation into products or crops, and consumption by humans or livestock. Estimates of return flows and consumptive use were discontinued after 1995 from the USGS datasets, primarily due to resource and data constraints (Dieter et al., 2017). In 2015, estimates for thermoelectric and irrigation consumptive use were generated again. Thermoelectric estimates relied on internal USGS data and U.S. Department of Energy power plant models, while irrigation estimates relied on satellite-derived evapotranspiration data at the state level (Dieter et al., 2017). In 2015, total consumptive use for irrigation and thermoelectric was 62% and 3% of their total withdrawals (Dieter et al., 2017). The estimated values of consumptive use ratios in the 1995 USGS report – the latest available consumptive use for all sectors – are estimated based on coefficients rather than precise measurements in many cases (Solley et al., 1998).

Although the consumptive use ratio is the most important factor in the water allocation model, previous studies have investigated it the least. To model it, we estimate the weighted average consumptive use ratio for all regions whenever data is available for both consumptive use and withdrawals (Figure 4.3). We then assume that the latest sectoral consumptive use ratios per region remain constant in the future due to limited data points for modeling. All sub-regions are assumed to have the consumptive use ratio from their corresponding region.

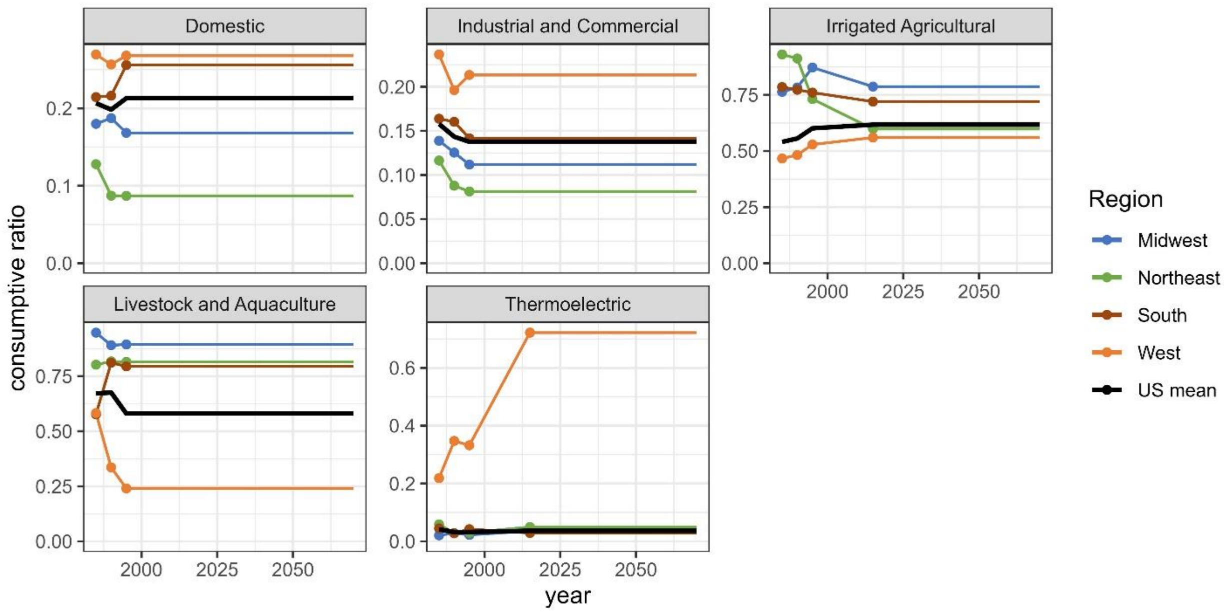

Figure 4.3. Consumptive use ratios by demand sector in each region. The dots represent the reported data and the lines represent the assumed values. The thick black color presents the weighted mean across the United States.

In the latest available data, the CU ratio for DOM ranges between 9% in the Northeast to 27.3% in the West with a weighted average across the United States of 22.2% for the latest available year (Figure 4.3). Similarly, the ICM ranges from 7.8% in the Northeast to 20.9% in the West with a 13.4% weighted average across the United States (Figure 4.3). Livestock and aquaculture have some of the highest CU ratios as high as 94.8% in 1985 in the West, but it didn't contribute much to the consumptive user as the withdrawal of this sector is 2% of the total withdrawals (Figure 4.3). On the other hand, thermoelectric has a 3% weighted average CU ratio that significantly reduces its effect on consumptive use (Figure 4.3 and Figure 4.4). Lastly, irrigated agriculture with a weighted average of 61.8% in 2015 (Figure 4.3), makes it the outstanding consumptive water user with more than 75% of the consumptive uses (Figure 4.4). The other four sectors have very close values to each other representing 25% of the consumptive use.

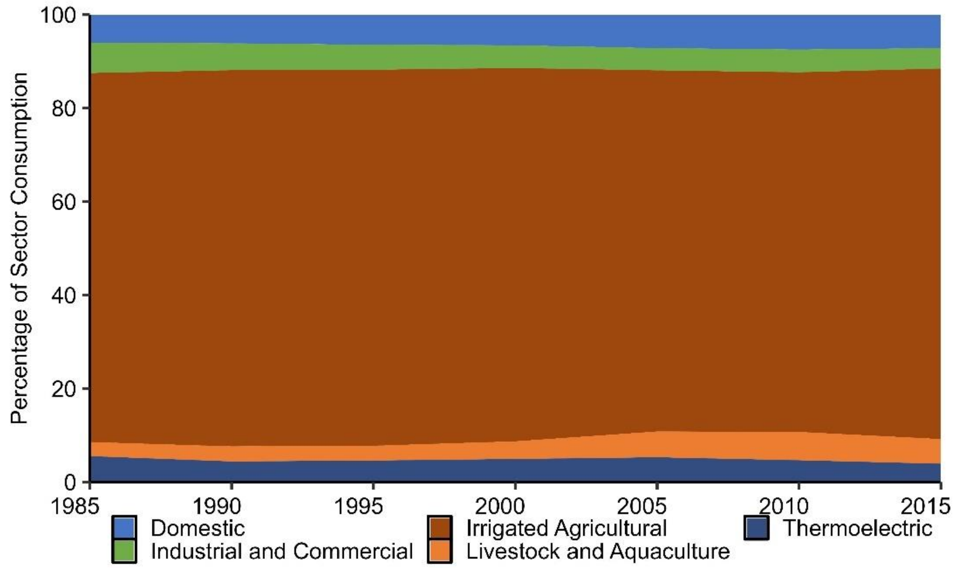

Figure 4.4. percentage of demand sectors' consumptive use to the total consumptive uses.

4.2.3.3. Withdrawal Rate

Withdrawal rates, defined as withdrawal per unit, have been identified as effective metrics for projecting future water withdrawals (Brown et al., 2019; Warziniack & Brown, 2019). In Table 4.3, one primary factor is assumed to be the key driver for the withdrawal of each demand sector. We use irrigation area as the driver for irrigated agriculture, measured in cm/year as the withdrawal rate. For the industrial group, the driver is liters per day per $1000 of total personal income (2005 dollars). For the other three sectors, liters per capita per day (lpcd) is used as the withdrawal rate. Although using liters per capita for thermoelectric is a simplification, it has a low consumptive ratio of 3% (Dieter et al., 2017), minimizing the estimation errors in our estimation. Personal income data are obtained from the Bureau of Economic Analysis, while irrigated areas and population data are sourced from the USGS withdrawal datasets mentioned earlier.

Table 4.3. Demand sectors with the driver and withdrawal rate for each.

Sector	Driver	Withdrawal rate
Irrigated Agricultural (IR)	Irrigated Area	cm/year
Industrial, Commercial, and Mining (ICM)	Total Personal Income	l/1000$/d*
Domestic (DOM)	Population	lpcd
Livestock and Aquaculture (LA)	Population	lpcd
Thermoelectric (TH)	Population	lpcd

* 2005 US dollars

We model the regions' withdrawal rates and then apply calibrated models to the sub-regions. Firstly, we aggregate withdrawals and drivers to the regions and calculate the withdrawal rate for each sector. Subsequently, we fit an auto-regressive exponential model (equation 4.1) for each sector in each region that minimizes the root mean square error (RMSE) between the modeled and observed withdrawal rates. The model takes the form:

$$\emptyset_{r,s,t} = \emptyset_{r,s,t-5} * \left(1 + \alpha_{r,s}\right)^5 \quad 4.1$$

where $\emptyset_{r,s,t}$ is the withdrawal rate for sector s in region r at year t and $\alpha_{r,s}$ is the calibrated parameter. Each simulated withdrawal rate at 5-year intervals takes into account the previous timestep withdrawal rate, capturing the changes in climate, technology, and policies during the historical period.

Observed and modeled withdrawal rates are presented in Figure 4.5. Additionally, calibrated parameters, RMSE, coefficient of variation (R-Squared), and percentage bias are reported in Table 4.4. DOM, ICM, and THERM exhibit decay rates in all regions with R-Squared values from 0.55 to 0.99 and less than 4% bias (Figure 4.5, Table 4.4). On the other side, LA shows a growth rate in all regions with R-squared values ranging from 0.22 to 0.66 and a bias lower than 2% except for the Northeast which reports a 9.2% bias. IR shows variation, with a decline in the

West and Midwest (Bias percent of 1.12% and 1.06%, respectively) but an increase in the South and Northeast (Bias percent of 1.62% and 4.03%, respectively).

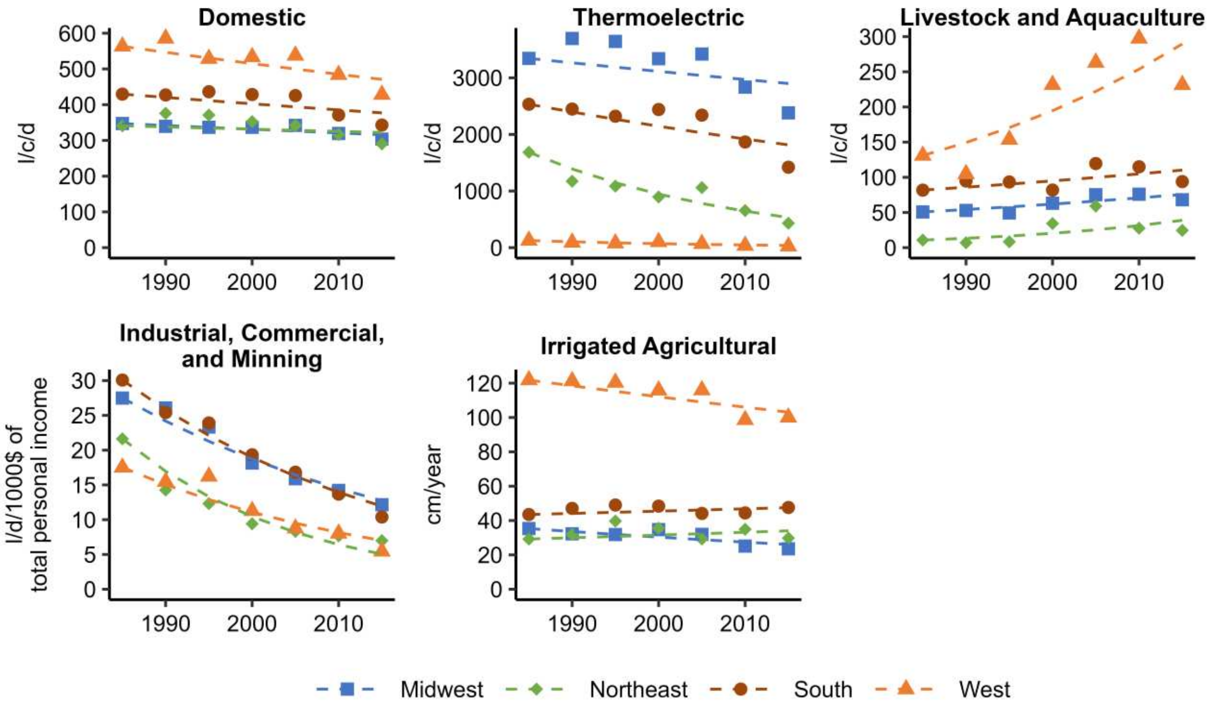

Figure 4.5. Withdrawal rate calibration for the five demand sectors in each region. The points present the weighted average region withdrawal rate and the dotted lines represent the calibrated model.

Table 4.4. The withdrawal rate calibration summary.

Sector	Region	Parameter	RMSE	R^2	Percent Bias
Domestic (DOM)	Midwest	-0.00298	20.7	0.71	0.33
	Northeast	-0.00149	69.5	0.55	2.97
	South	-0.00453	59.8	0.65	1.37
	West	-0.00598	71.8	0.77	1.36
Industrial, Commercial, and Mining (ICM)	Midwest	-0.02487	3.9	0.96	1.74
	Northeast	-0.04882	4.5	0.91	-1.99
	South	-0.03119	2.0	0.99	0.39
	West	-0.03026	3.7	0.91	1.82
Irrigated Agricultural (IR)	Midwest	-0.00895	7.7	0.58	1.06
	Northeast	0.00781	10.4	0.03	4.03
	South	0.00280	5.9	0.01	1.62
	West	-0.00580	12.8	0.81	1.12
Livestock and Aquaculture (LA)	Midwest	0.00987	11.2	0.66	-0.14
	Northeast	0.04487	40.4	0.22	9.22
	South	0.01106	33.1	0.34	1.57
	West	0.02713	104.6	0.66	0.30
Thermoelectric (TH)	Midwest	-0.00631	900.8	0.66	3.49
	Northeast	-0.03546	303.8	0.90	-1.05
	South	-0.01062	578.0	0.67	1.41
	West	-0.03597	41.5	0.79	-0.65

Sub-regions future withdrawal rates are modeled by substituting $\emptyset_{region}$ with $\emptyset_{sub-region}$ to obtain the future withdrawal rate for each sub-region (equation 4.1). To address errors from individual sub-region data or projections, upper and lower boundaries are consistently applied after calculating projected withdrawal rates for each sector. California, known for high water efficiency as of 2022 (Alliance for Water Efficiency, 2023), aims to reduce indoor residential water use to 190 lpcd by 2030 (State of California, 2018). Considering outdoor residential water use and source-to-home losses, we assume 250 lpcd as the minimum withdrawal rate for DOM. For ICM, a minimum of 4 l/1000$/d is assumed based on suggestions by Brown et al. (2019) and Warziniack & Brown (2019). Regarding LA, with increasing withdrawals, each sub-region is assumed not to exceed 120% of its maximum historical LA withdrawal. We don’t assign minimum or maximum bounds for IR and TH due to insufficient data and inconsistent trends.

Data on future drivers—population, personal income, and irrigated area—are obtained from Wear & Prestemon (2019) at the county level for the four selected SSPs (Figure C2 to Figure C5). Drivers are multiplied by withdrawal rates to calculate sub-regions' future withdrawals. Subsequently, withdrawals are multiplied by the consumptive use ratios to estimate sub-regions consumptive uses. Finally, monthly withdrawal patterns for each sector in each sub-region are adopted from Brown et al. (2019) to estimate the monthly consumptive uses that present the water demand in the modeling framework.

4.2.4. Water Supply Modeling

The water supply is comprised of three main components: water yield, inter-basin transfers (IBT), and non-renewable groundwater abstraction, as described below.

4.2.4.1. Water Yield

Heidari et al. (2020) utilized the Variable Infiltration Capacity (VIC) model (Liang et al., 1994) to simulate water yield over the CONUS, employing the climate scenarios presented earlier. VIC is a semi-distributed macroscale model solving full water and energy balances to simulate land-atmosphere fluxes and flow routing (Liang et al., 1994). Water yield represents the renewable water supply, occurring as surface runoff or baseflow (Brown et al., 2019), representing also the groundwater pumping from renewable resources. Water yield is obtained at a monthly time step for each sub-region in CONUS from Heidari et al. (2020). Figure 4.6a depicts the mean annual historical (1991 to 2015) water yield, and Figure 4.6b illustrates the percentage change between the mean annual mid-future (2046 to 2070) under 10 climate scenarios compared to historical levels.

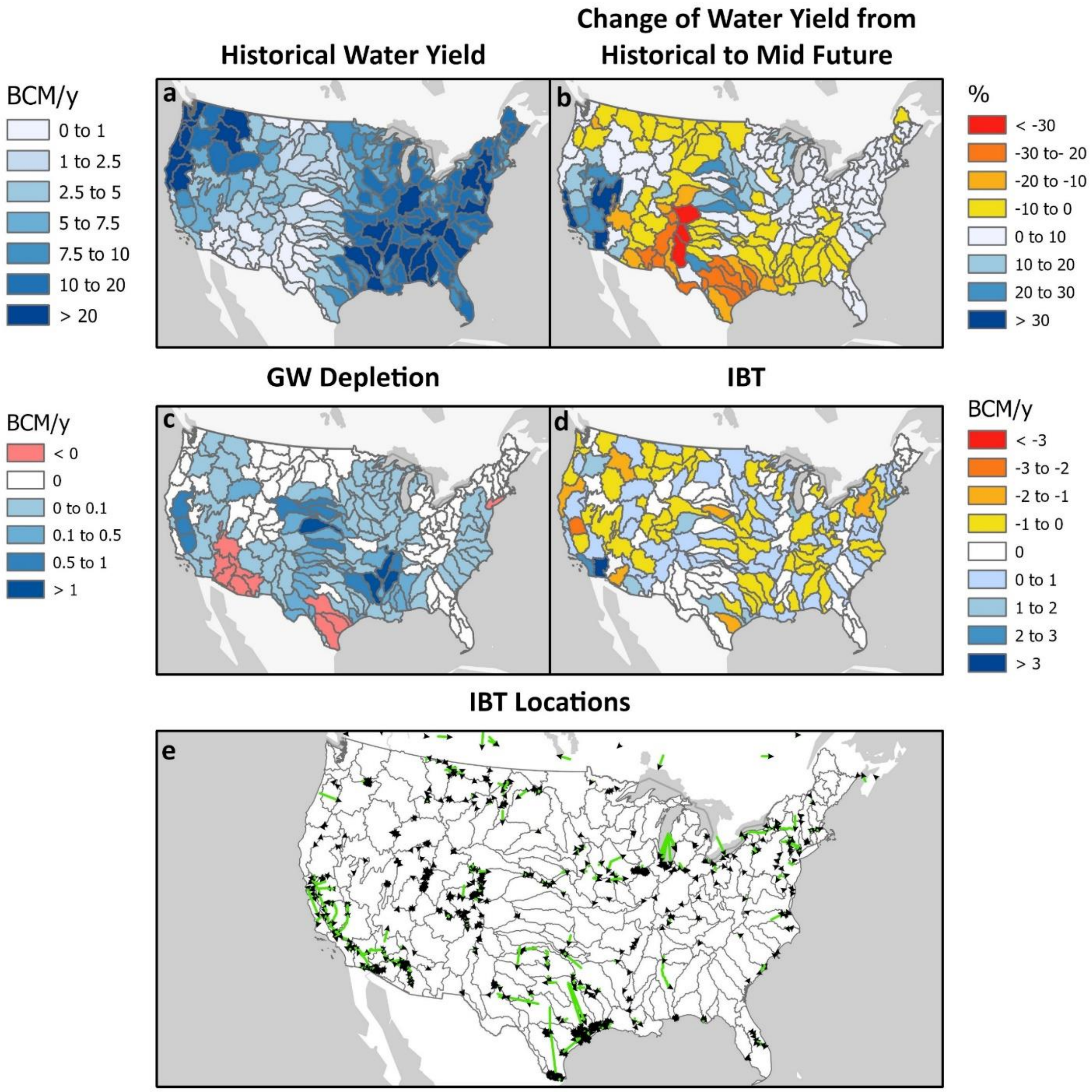

Figure 4.6. Water supply components in CONUS. a) Historical mean annual water yield. b) Water yield annual mean of 10 climates mid-future mean percentage change to the historical mean annual water yield. c) estimated groundwater annual Depletion. d) annual inter-basin transfers IBT. e) location of IBT.

4.2.4.2. Inter-basin transfers (IBT)

Surface water supply in a watershed relies on local water from precipitation and connections with other watersheds (Duan et al., 2019). Inter-basin water transfers (IBT) involve conveying water from one watershed to another through engineering projects like pipelines, aqueducts, or canals (Siddik et al., 2023). IBT data from Siddik et al. (2023) are incorporated into our water allocation modeling with the highest priority of allocation. This means that water is transferred through IBT before fulfilling demands. Figure 4.6d summarizes the annual volume of IBT for each sub-region, where negative values indicate the donor basin and positive values indicate the receiving basin. Figure 4.6e displays the locations of all IBT across the CONUS and Southern Canada.

4.2.4.3. Groundwater Depletion as Water Supply

Groundwater pumping comes from renewable and nonrenewable sources. Renewable groundwater which is sustainable groundwater pumping is already accounted for in the VIC water yield simulations. Nonrenewable groundwater is the groundwater pumping rate beyond percolation rates that recharges the aquifers. In a previous study for shortage adaptation in the United States by Brown et al. (2019), the groundwater was accounted for in the allocation modeling using the term groundwater mining. They defined groundwater mining as prolonged groundwater overdraft, causing a long-term drawdown of the water table or reduction in the hydraulic head of a confined aquifer (Brown et al., 2019). Their estimate of past groundwater mining volume equals past groundwater withdrawal minus the amount of mean annual yield that is likely to recently have infiltrated and become available for pumping and relies heavily on recent estimates of groundwater depletion (Brown et al., 2019).

In this analysis, the nonrenewable groundwater is represented by the volume of depleted groundwater from the aquifers as estimated by Konikow (2011, 2013). Groundwater depletion is defined as a reduction in the volume of groundwater in storage in the subsurface (Konikow, 2011, 2013). Konikow (2011, 2013) reported the mean annual groundwater depletion each decade from 1950 to 2008 for 40 main aquifers in the United States through extensive modeling and calculations. We map this depletion to sub-regions in CONUS and estimate the annual groundwater depletion. Then we apply the monthly demand shares to get the monthly estimated historical groundwater depletion for the historical period of this study (Figure 4.6b). The aggregate amount of groundwater depletion across CONUS has a minimum of 10 BCM/y between 1991 and 2000, while the peak is reported between 2001 and 2008 at 25 BCM/y (Figure 4.7). We assume that 2008 rates will continue until 2015. In the water allocation model, we add the volume of the groundwater depletion to the water yield in the corresponding sub-region to represent the total water supply.

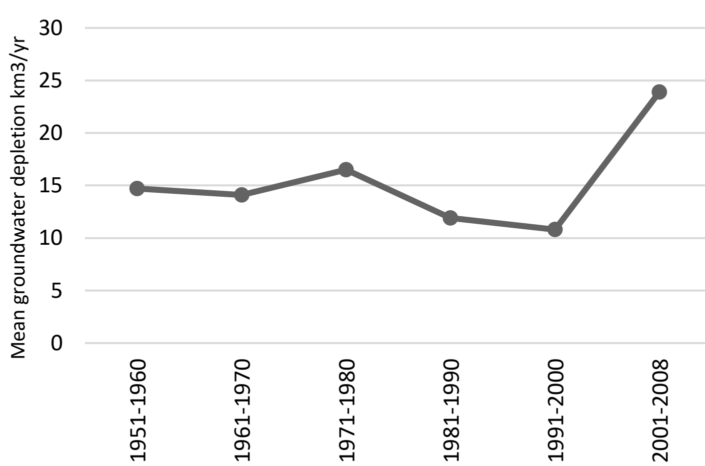

Figure 4.7. Historical annual mean groundwater depletion in the principal aquifers of CONUS (Konikow, 2011, 2013).

4.2.5. Water Allocation Modeling

Water allocation modeling is conducted using the Water Evaluation and Planning (WEAP) model (Yates et al., 2005). The model employs linear programming to address the water allocation problem, aiming to maximize the satisfaction of demands within the constraints of allocation priorities and water availability. The model prioritizes demands sequentially, addressing high-priority demands first without foresight into future months. The WEAP model, initially provided by Brown et al. (2019), serves as the foundation before applying the updates described earlier (Figure 4.9). In the water allocation model, the water supply is the water yield plus the groundwater depletion, and the water demand is the consumptive use.

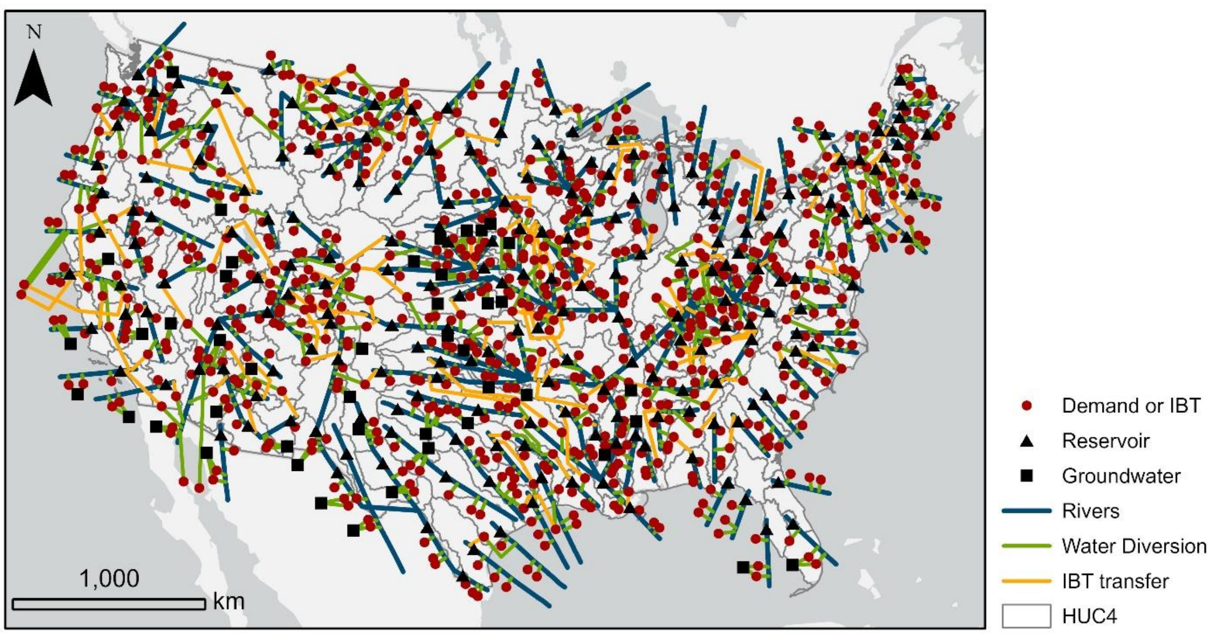

Figure 4.8. WEAP Layout

In our WEAP implementation, IBT nodes are assigned the highest priority, ensuring water moves from donor basins to receiver basins before other calculations. Once IBT allocation is complete, the model maximizes demand coverage –the percentage of demand satisfaction– for all demand nodes. Reservoirs, assigned the lowest priority, only fill up after all demands are met if possible. The model then progresses to the next time step, repeating the procedure. Because all nodes of the same category (IBT, reservoir, or demand) share the same priority, the allocation is an equity-based distribution of available supplies each time step. WEAP runs monthly from 1985 to 2015 as the historical period, and from 2015 to 2070 representing the future.

4.2.6. Scenarios and Water Shortage Metrics

Four main future scenarios are presented in this study (Table 4.5). The first two scenarios simulate the future water shortage relying only on sustainable groundwater (no groundwater depletion occurring in the future). However, they differ in the demand calculation. The first one uses the modeled withdrawal rates as presented early on in this analysis, and the latter assumes constant withdrawal rates as the year of 2015. The third and fourth scenarios apply also both demand models but assume that the historical groundwater depletion trend will continue as the latest available of the year 2008 (groundwater will continue depletion into the future).

Table 4.5. Scenarios Definition

Scenario	Water Demand	Groundwater
1) Baseline future: Modeled withdrawal rates with sustainable groundwater	Modeled withdrawal rates	Sustainable groundwater is only presented from VIC simulations
2) Constant withdrawal rates with sustainable groundwater	Historical withdrawal rates as of the year 2015	Sustainable groundwater is only presented from VIC simulations
3) Modeled withdrawal rates with sustainable groundwater and groundwater mining	Modeled withdrawal rates	Sustainable groundwater from VIC simulations and groundwater mining like the latest available estimate of annual mean of years from 2001 to 2008
4) Constant withdrawal rates with groundwater mining	Historical withdrawal rates as of the year 2015	Sustainable groundwater from VIC simulations and groundwater mining like the latest available estimate of annual mean of years from 2001 to 2008

It's crucial to point out that simulating water demands in our study is based on actual withdrawals and consumptive use estimates, which may not precisely align with the actual required water demand. Therefore, our water shortage calculations might underestimate the total water shortage. In simpler terms, the simulated water shortage in this analysis should be added to any existing shortages.

Water shortage in this analysis is defined as the deficit between the required demand and the delivered demand, calculated monthly using WEAP (equation 4.2). In addition to the shortage volume, we report the mean and 95th percentile of the annual shortage ratio over 25-year periods, which is the shortage volume divided by the demand volume (equation 4.3). We also report the shortage frequency, calculated as the sum of the months with shortage within 25 years divided by 300, the total number of months in 25 years (equation 4.4).

$$Shortage\ Volume = \ Required\ Demand - Delivered\ Demand \tag{4.2}$$

$$Annual\ Shortage\ Ratio = \frac{\sum_{month=1}^{12} \text{Shortage Volume}}{\sum_{month=1}^{12} Required\ \text{Demand}} \tag{4.3}$$

$$\text{Mean Shortage Frequency } = \sum_{year=1}^{\text{n}} \#\ of\ months\ with\ shortage\ \ / \left(12 * \text{n}\right) \tag{4.4}$$

4.3. Results and Discussions

4.3.1. Water withdrawals and consumptive use projections

Following the calibration of each region's exponential model on water withdrawal rates, the model was applied to the sub-region withdrawal rates of the year 2015 to project their future values. As reported in Figure 4.9 and Table 4.6, the weighted average domestic withdrawal rate is projected to decrease, ranging from 268 to 322 lpcd in 2070, while the ICM rate is anticipated to nearly reach its minimum within the range of 4 to 4.4 l/1000$/d. Thermoelectric rates are also expected to decrease in all regions with the range of 4.3 lpcd to 1566 lpcd. The maximum irrigated agriculture withdrawal rate in 2070 is projected to be 72 cm/year in the West, and the minimum is 14 cm/year predicted in the Midwest.

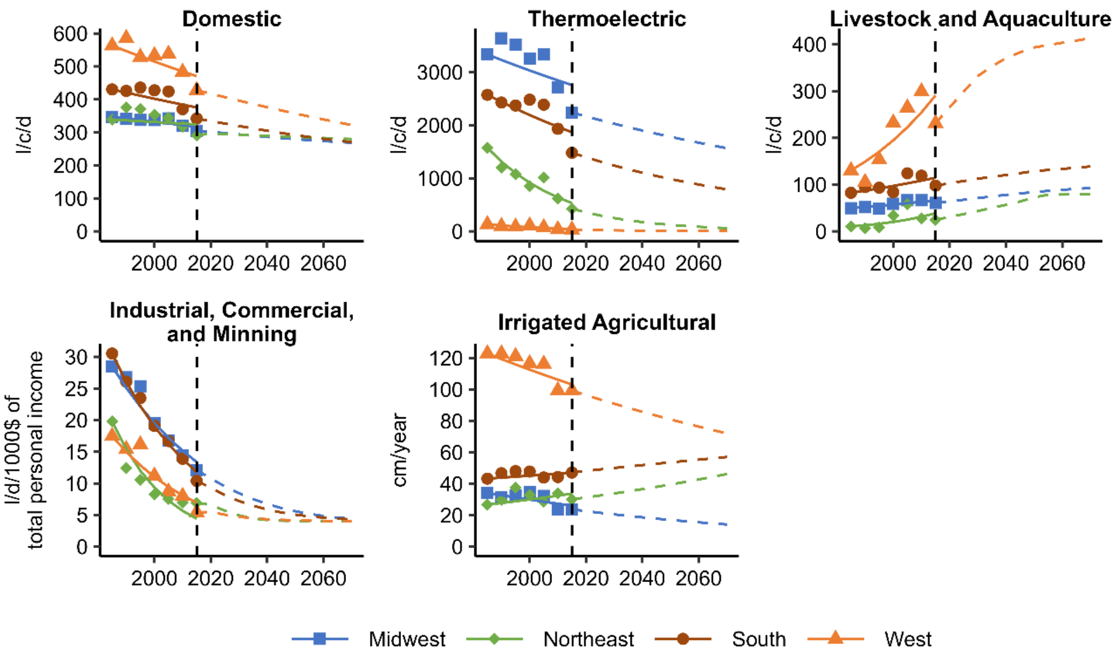

Figure 4.9. Weighted Average region withdrawal rates projection for each water sector of ssp1. The dots are the weighted mean of each region's data. The solid lines present the model of each region and sector. The dashed lines present the weighted mean projected withdrawal rate for each region starting from the data of the year 2015 estimated.

Table 4.6 Weighted Average region withdrawal rates projection for each water sector of ssp1 in 2070.

Region	DOM	ICM	IR	THERM	LA
	lpcd	l/1000$/d	cm	lpcd	lpcd
Midwest	268.84	4.42	14.11	1566.58	92.52
Northeast	279.91	4.00	46.22	59.49	79.20
South	270.56	4.31	57.07	789.93	138.82
West	322.22	4.02	72.07	4.30	413.35

Figure 4.10 illustrates the total withdrawal (a) and consumptive use (b) projections in CONUS for historical and future Shared Socioeconomic Pathways (SSPs). The historical peak of CONUS withdrawals occurred in 2005 at 1,324 MCM/y, while estimated consumptive use peaked in 2000 at 396 MCM/y (Figure 4.10). By 2070, total withdrawals in CONUS are projected to range

from 847 MCM/y for SSP3 to 1,317 MCM/y in SSP5, approaching the highest recorded historical withdrawals. Following the withdrawal trend, consumptive use projections range from 330 to 403 MCM/y, with the latter surpassing the maximum estimated historical consumptive use. Compared to 2015, the future consumptive use in 2070 increase by 5% to 16%. SSPs 1 and 2 total withdrawal and consumptive use projections closely align with the observed values in 2015. Figure C6 to Figure C13 provide a detailed breakdown of withdrawals and consumptive use by sectors in each region.

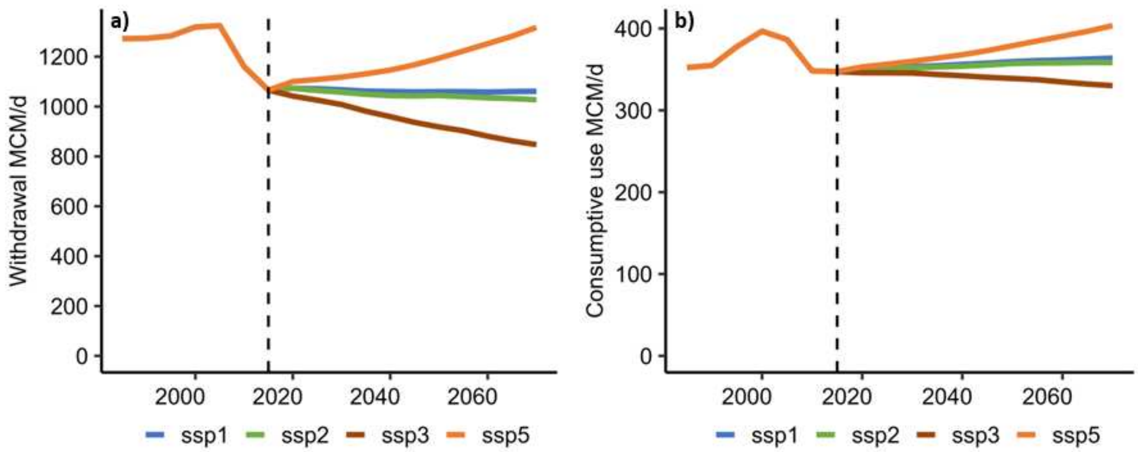

Figure 4.10. Total withdrawal (a) and consumptive use (b) projection in CONUS.

The irrigated agriculture sector is projected to remain the primary consumer of water, while the thermoelectric sector consistently exhibits the lowest consumptive use across all SSPs (Figure 4.11b). Despite a projected doubling of the West's population in 2070 under SSP5, total consumptive use in the West is anticipated to decline across all SSPs. This decline is primarily attributed to reductions in irrigation and domestic withdrawal rates, coupled with a decrease in irrigated areas. Similarly, the Midwest is expected to experience a decline due to decreases in irrigation withdrawal rates and slow population growth. Conversely, the South is projected to witness a consumptive use increase of at least 50% compared to 2015. This rise is driven by projected increases in irrigated areas, irrigation withdrawal rates, and a doubled population by 2070.

The Northeast, historically having the lowest share of consumptive use, is expected to see an increase under all SSPs (Figure 4.11a). The Northeast historically maintains low withdrawal rates in domestic, industrial, and thermoelectric sectors, and these rates are not projected to experience significant reductions. Hence, the increase in consumptive use is primarily driven by population and economic growth, further amplified by a projected increase in irrigation depth. Figure 4.12 displays the subregions' consumptive use historical mean (1991 to 2015) and the percentage change of the mid-future mean (2046 to 2070) consumptive use from the historical values under each SSP.

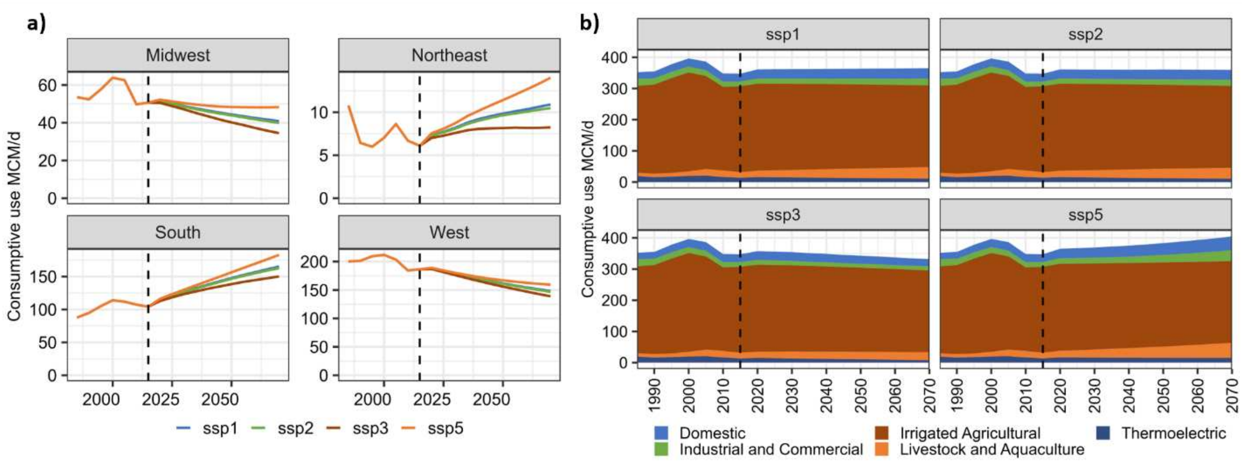

Figure 4.11. Annual historical and projected consumptive use in CONUS. a) total consumptive use in each region colored by SSPs 1,2,3, and 5. b) total consumptive use in CONUS for each SSP colored by the demand sector.

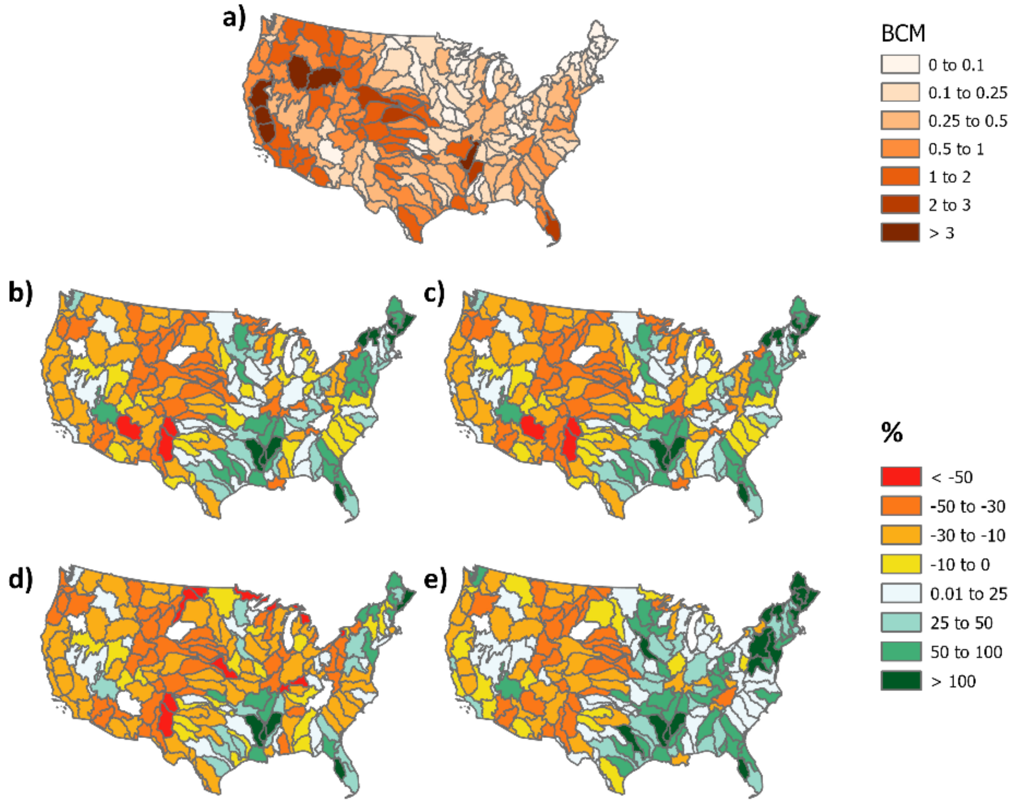

Figure 4.12. Total consumptive use in each sub-region. a) historical mean. b to e: the percentage change between the mid-future mean form the historical mean. b) SSP1, c) SSP2, d) SSP3, and e) SSP5.

4.3.2. Baseline Future Water Shortage Metrics

This section presents the results of the baseline future scenario that includes the modeled withdrawal rates for the water demand calculations and accounts only for the sustainable groundwater in the future as simulated by the VIC model (scenario 1 in Table 4.5). The historical aggregate annual shortage in CONUS ranges between 2 and 12 BCM/y (Figure 4.13). Going into the future, the aggregate annual shortage across the 20 simulated scenarios spans from 2.4 to 12.7 BCM/year (Figure 4.13). However, when considering the mean annual across the 20 scenarios, the range is reduced to have a minimum of 4.7 BCM/y and a maximum of 7.2 BCM/y (Figure 4.13).

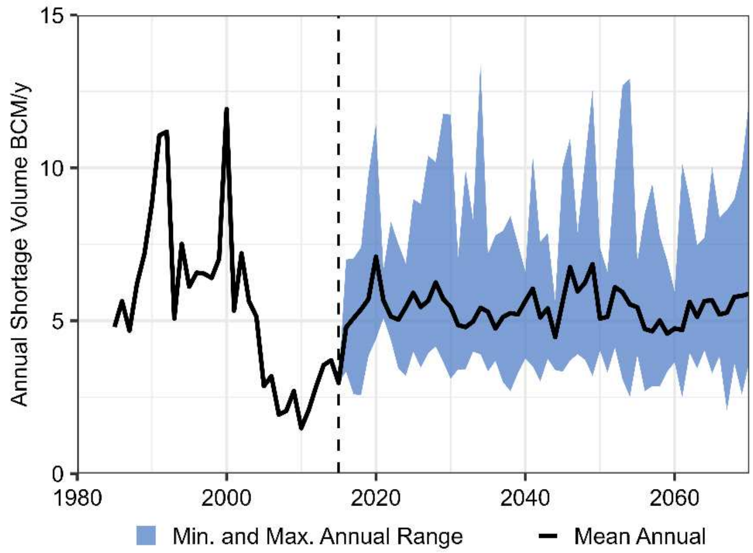

Figure 4.13. annual shortage volume for all the 20 simulated scenarios for the baseline scenarios (Scenario 1 in Table 4.5). The black line presents the historical shortage and the mean future shortage across the simulated scenarios. The shaded blue area shows the minimum and maximum shortage range across the simulated scenarios.

Considering two 25-year periods of 1991 to 2015 representing the historical and 2046 to 2070 representing the mid-future conditions, several shortage metrics are calculated as follows. The historical mean annual shortage is reported at 5.3 BCM/y and the 95th annual shortage percentile reached 11 BCM/y (Figure 4.14a,b). The Dry climate scenario records the highest shortage under all simulated SSPs for the mean and the 95th percentile annual shortage. The Wet and the Least Warm climate scenarios record the minimum across all scenarios. Otherwise, the Middle and Hot climate scenarios have intermediate shortages (Figure 4.14a,b).

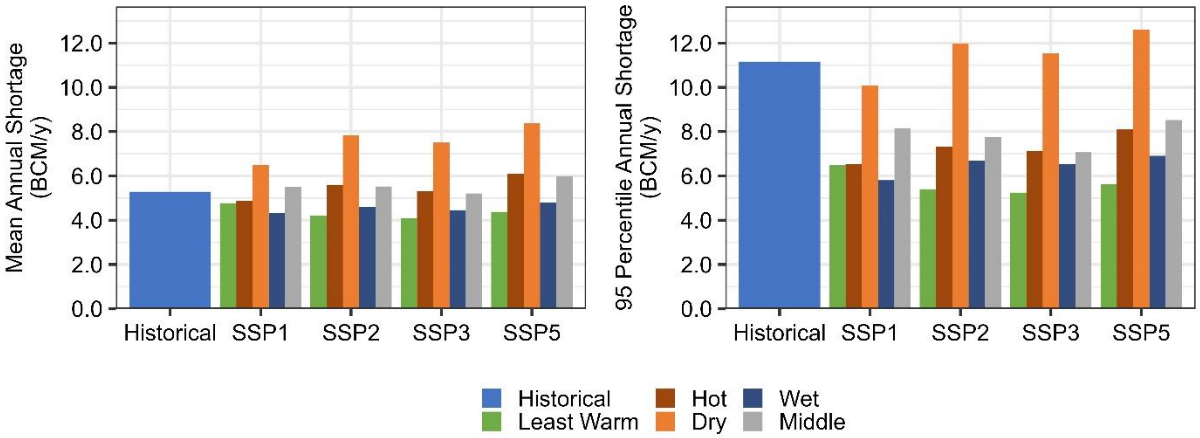

Figure 4.14. 25-year mean and 95th percentile shortage volumes for the baseline scenarios (Scenario 1 in Table 4.5) for the historical and the mid-future periods for all the simulated scenarios.

Limiting the results to the basins with shortages, Figure 4.15 shows the box plot for all scenarios (Figure 4.15), and a geographical representation is shown for selected scenarios in Figure 4.15. The number of basins with shortages in the historical period is 24 with medians of 0.1 for the mean annual shortage ratio (Figure 4.15a), 0.4 for the 95th percentile annual shortage ratio (Figure 4.15b), and 0.1 for the shortage frequency (Figure 4.15). The SSP2 and SSP3 scenarios under the least warm climate conditions report only 17 basins with shortage. However, the dry climate scenario generates a shortage in 30 basins under SSP1 and 28 under the other SSPs (Figure 4.15a-c).

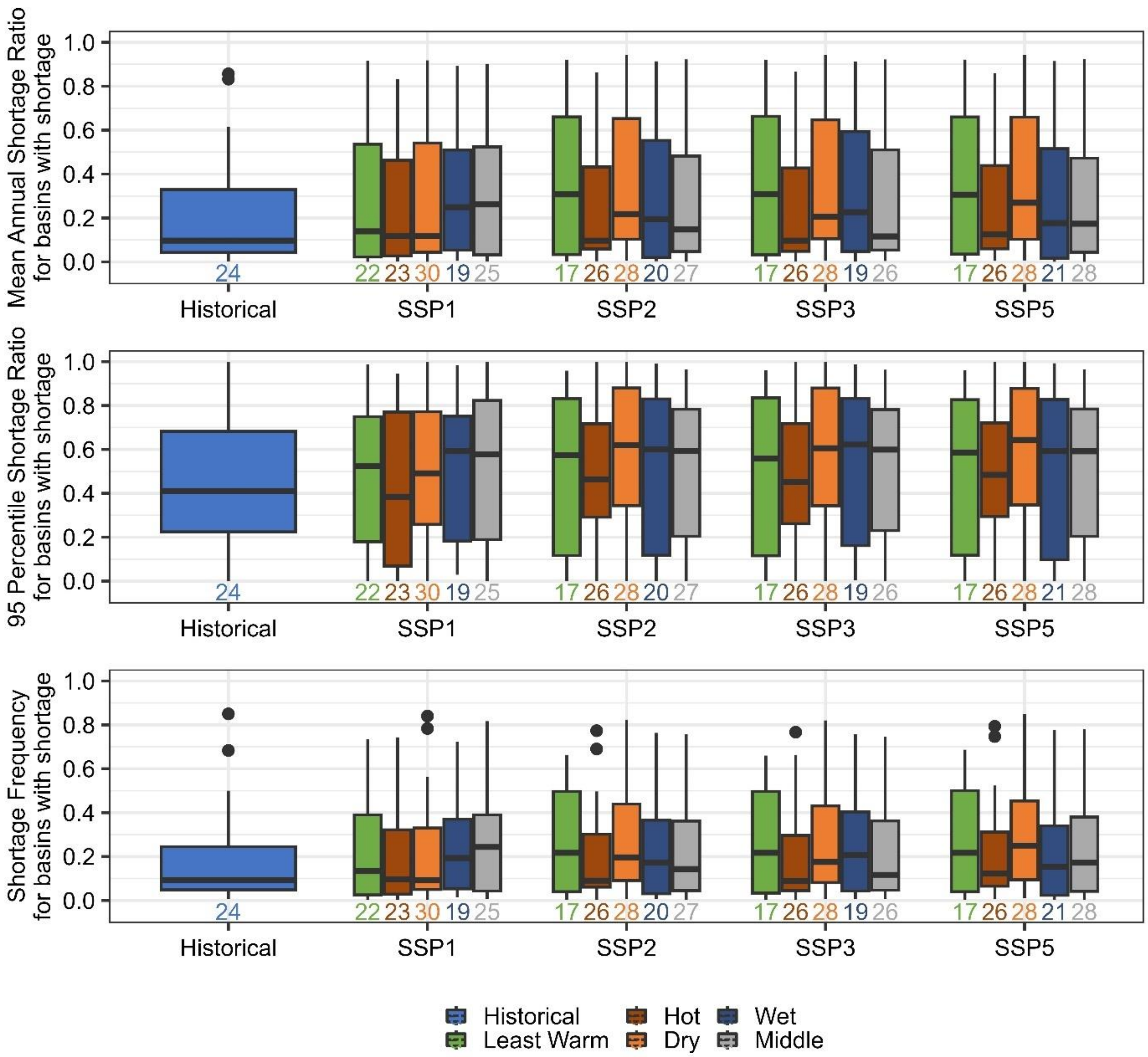

Figure 4.15. 25-year mean shortage ratio, 95th percentile, and shortage frequency for the baseline scenarios (Scenario 1 in Table 4.5) for the historical and the mid-future periods for all the simulated scenarios.

From the historical simulation, shortages have been located along the borders between the West with both the Midwest and the South regions (Figure 4.16 a,d,g). In addition to the states of Arizona and Florida, and the Center Valley in California. Under the Dry RCP8.5 SSP5 scenarios in the mid-future, these regions face increased shortage ratios and frequencies (Figure 4.16 b,e,h), adding threats to major agricultural production areas and fast-growing urban basins. Under the least warm conditions, no observed shortage in Center Valley California, and shortages in Arizona significantly reduced (Figure 4.16 c,f,i).

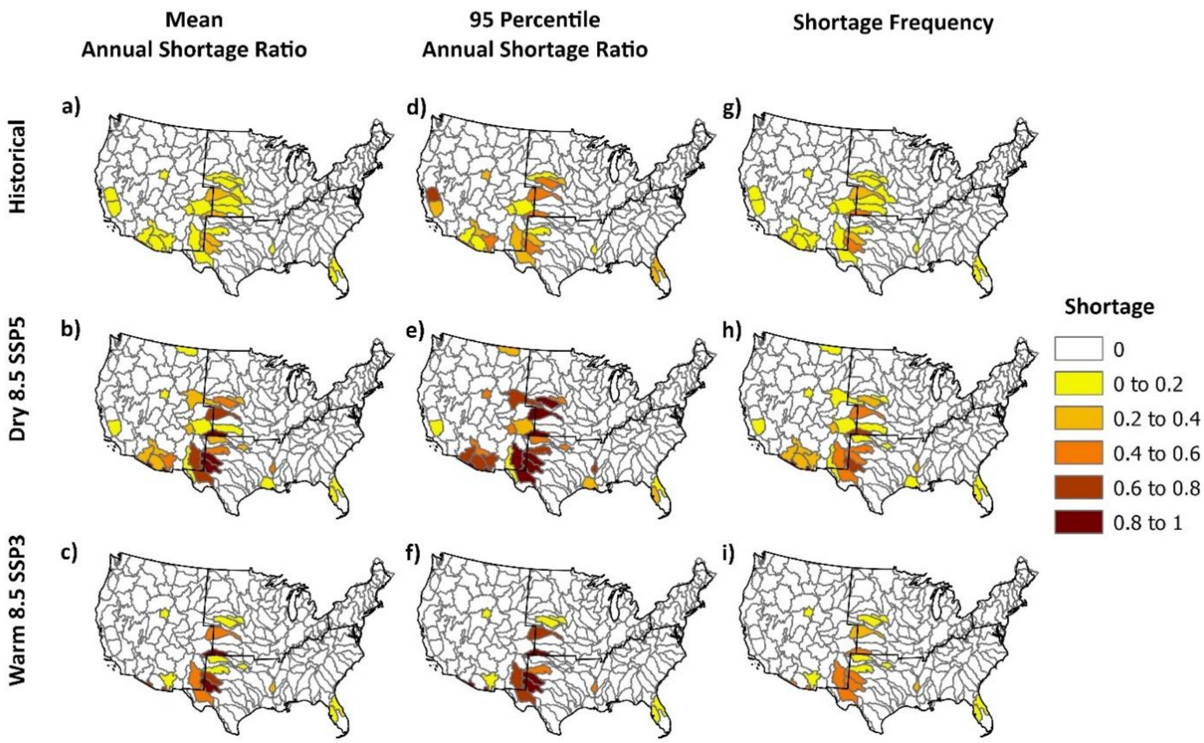

Figure 4.16. 25-year mean shortage shortage ratio, 95th percentile, and shortage frequency for the historical and the mid-future for Dry8.5-SSP5, and Warm4.5-SSP3 scenarios.

4.3.3. Groundwater pumping rates and demand reduction for water shortage mitigation

In this section, two demand models (Figure 4.17) and two future groundwater policies are presented to get a wider range of potential water shortages while focusing on the mean annual conditions as described in Table 4.5. The demand model with the constant historical withdrawal projects more consumptive demand into the future compared to the modeled withdrawal rates and the historical demands (Figure 4.17).

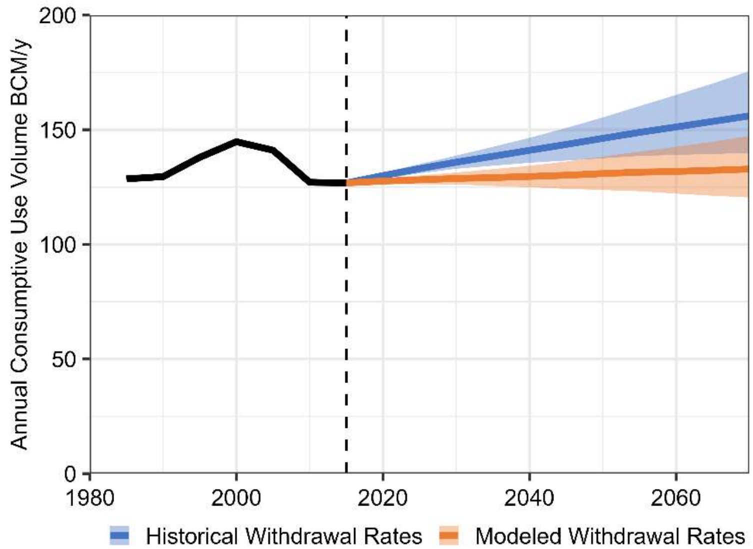

Figure 4.17. Annual consumptive uses across all SSPs using the modeled withdrawal rates in orange and the historical withdrawal rates in blue.

If we switch from sustainable groundwater pumping (only pumping renewable groundwater) to groundwater mining (pumping from non-renewable groundwater that causes groundwater depletion), the simulated water shortage significantly decreases (Figure 4.18). However, additional groundwater mining is required or additional demand reduction strategies should take place to fully mitigate water shortages (Figure 4.18). As groundwater depletion has several consequences for the environment and diminishes groundwater in several basins, demand reduction strategies have to be considered to ensure the groundwater pumping rate is lower than the recharge rate to allow for sustainable groundwater pumping.

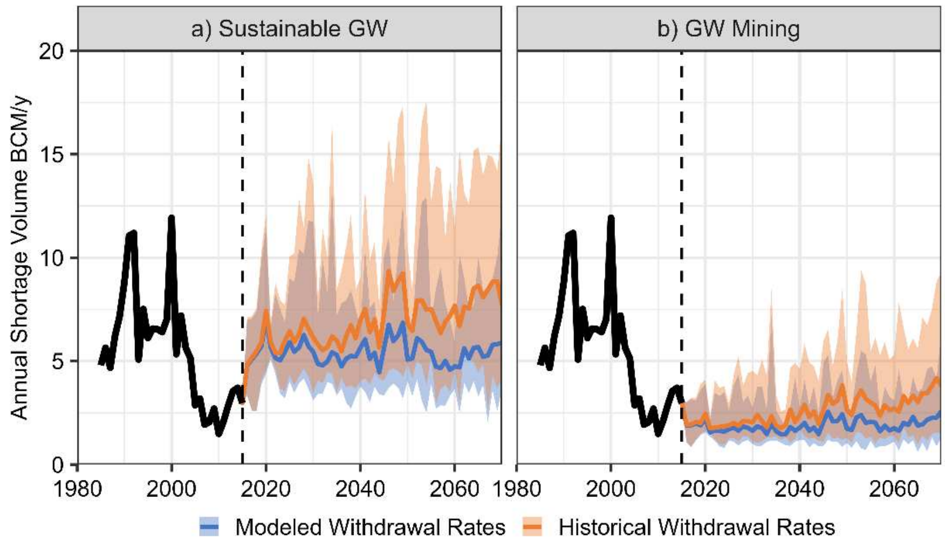

Figure 4.18. annual shortage volume for the four scenarios presented in Table 4.5

4.4. Conclusions

Firstly, this study develops a methodology for projecting water withdrawals and consumptive uses in the Contiguous United States (CONUS) under different Shared Socioeconomic Pathways (SSPs). The water withdrawal rates of 5 demand sectors are modeled for the four CENSUS regions and then applied to the 204 hydrologic unit sub-regions. The results indicate a projected decrease in the weighted average regional domestic, thermoelectric, and industrial/commercial/mining withdrawal rates, while irrigated agriculture withdrawal rates exhibit variation trends across regions.

The consumptive use ratio, marked as the most important factor in demand modeling, was the least investigated in the literature. We calculate the weighted average consumptive use for each demand sector in each region and assume these values continue as the latest available. The consumptive use projections reveal that the irrigated agriculture sector is the primary consumer of water, while thermoelectric has the lowest consumptive use among all SSPs. Despite a projected doubling of the population in the West by 2070, total consumptive use in the region is expected to decline due to reductions in irrigated agriculture and domestic withdrawal rates, coupled with a decrease in irrigated areas. In contrast, the South is anticipated to experience a significant increase in consumptive use, driven by an expansion in irrigated areas, irrigation withdrawal rates, and population growth.

The study further explores the future baseline shortage ratio and frequency projections under combined SSPs and climate models. The analysis reveals historical shortages in some sub-regions, and future projections indicate an increase in the number of sub-regions with shortages under certain SSPs. Shortages are predicted at the sub-regions crossing the borders of the West region with the Midwest and South regions and the states of Arizona, California, and Florida.

Additionally, the study investigates the effects of two groundwater strategies; relying only on sustainable groundwater (pumping rates less than percolation rates) and including groundwater mining (pumping rates above percolation rates). The simulated shortages under the latter scenario are lower than the first one, however, some shortages are still predicted. Hence, more demand reduction strategies have to be applied to reduce the predicted shortages. Finally, relying only on sustainable groundwater pumping is preferred to reduce the consequences of depleting groundwater aquifers but puts more pressure on demand reduction strategies.

CHAPTER 5.

CLOSING REMARKS

Integrated water resource management continues to receive substantial interest, as water is the most essential resource for life. Advancing technology enables modeling more factors in simulations, leveraging increased computing power. High-resolution, basin-specific models with fine time steps effectively capture reservoir operations, deliveries, and return flows to evaluate local strategies like groundwater pumping or reservoir operation. These local models answer key questions not addressable in lower resolution, larger scale models. However, national models highlight overall supply and demand conditions, guiding the investigation of concerning regions. Research benefits from both localized and national modeling approaches.

Hadjimichael et al., (2023) conducted a comparative analysis between large-scale hydrologic modeling and node-based representations of water systems in the Upper Colorado River Basin to identify the distinctions in their analytical approaches. The study revealed that both models effectively captured the overall monthly impacts of various water management processes within the basin. This implies that, in addition to offering a regionally consistent model of hydrologic and other processes, the large-scale model has the potential to bridge aggregate dynamics between interacting basins lacking high-resolution models. However, the study identified a limitation of the large-scale model when it comes to concluding water availability and vulnerability for smaller areas within the catchment (Hadjimichael et al., 2023).

This dissertation applied integrated management allocation modeling at two scales, providing unique findings. Specifically, the first two analyses of this dissertation focused on the South Platte River Basin (SPRB) in Colorado, a snow-driven system with mixed agriculture and urban water demands and growing communities. SPRB relies on inter-basin transfers and has complex water rights and active water market rights, representing the western United States. A detailed water allocation model was developed with a half-monthly time step to capture the effects of climate change on the water supply and water demands. More than 3000 scenarios were simulated to capture a range of climate models, water rights institutions, supply and demand management, population densities, and land use policies, and calculate water shortages and their economic values. Additionally, an integrated land use planning and water management framework was developed.

In the third analysis, we employed a water allocation model for the CONUS at the sub-region level with monthly timestep. Firstly, we updated the water demand projection methodology and then integrated that into the water allocation model with available water supply datasets. Shortage volume, ratio, and frequency were calculated with enhanced shortage metrics. In this analysis, consumption uses ratios and groundwater representations were highlighted as points that require further focus in the future reflecting their importance in the water allocation. Sustainable groundwater pumping can be reached by restricting groundwater pumping to the percolation rates which is essential to reduce groundwater depletion. However, more demand reduction is required to mitigate predicted water shortages while preserving groundwater storage.

A key point of water management and shortages calculations is the data that are used as inputs for the simulations. Hence, investing in data collection (e.g. inter-basin transfers), building tools (e.g. IUWM), and running simulations (e.g. water yield) are always helpful for future actions. Without years of work from previous work within our two scale models in the South Platte River Basin and the United States, presenting this integrated detailed analysis would be impossible. The previous efforts let us focus on the big picture of the water allocation and shortage analysis under several adaptation strategies.

Two important notes should be highlighted regarding the past literature. Firstly, the consumptive use ratio is the most important parameter in the water shortage analysis and should receive more attention in the coming years. The consumptive use ratio is the amount of water that leaves the system while fulfilling the water demands and doesn't appear as surface or groundwater return flow. Second, when actual withdrawal data are used to present the water demand, some adjustments have to be made for shortage calculations. Withdrawals don't represent the full required demand but reflect the demand satisfied. So, investigations have to be for historical water shortage calculations to be added to the simulated shortages.

The integrated water management field is still available for further development. We consider here factors that link components like land use, population density, population locations, groundwater, trends of withdrawal rates, water rights, management strategies, socioeconomic pathways, and climate factors and simulate their effects on the water shortages. Future research directions Throughout the study period, several directions for future research were identified to better quantify water demands and shortage calculations. The recommended areas of future research are outlined below:

1. Including more water rights institutions in the water allocation modeling of SPRB.
2. Update the water withdrawal rate calibration once the 2020 withdrawal data are available.
3. Perform a comprehensive consumptive use ratio analysis by collecting more data.
4. Update the reservoir storage volume to the latest available for a better estimation of the dead storage volume and volume-elevation curve, to account for the active storage volume and the surface area for evaporation calculations.

5. Investigate the historical shortages to correctly model future shortages.

REFERENCES

Abatzoglou, J. T., & Brown, T. J. (2012). A comparison of statistical downscaling methods suited for wildfire applications. *International Journal of Climatology*, *32*(5), 772–780. https://doi.org/10.1002/joc.2312

Aliyari, F., Bailey, R. T., & Arabi, M. (2021). Appraising climate change impacts on future water resources and agricultural productivity in agro-urban river basins. *Science of the Total Environment*, *788*, 147717. https://doi.org/10.1016/j.scitotenv.2021.147717

Alliance for Water Efficiency. (2023). *2022 U.S. State Policy Scorecard for Water Efficiency and Sustainability: Alabama*. https://www.allianceforwaterefficiency.org/sites/default/files/assets/AWE 2022_Scorecard_Alabama.pdf

Angelo, M. J. (2001). Integrating water management and land use planning: uncovering the missing link in the protection of Florida's water resources? *University of Florida Journal of Law and Public Policy*, *12*(spring), 223–249.

Arabi, M., Govindaraju, R. S., Engel, B., & Hantush, M. (2007). Multiobjective sensitivity analysis of sediment and nitrogen processes with a watershed model. *Water Resources Research*, *43*(6), 1–11. https://doi.org/10.1029/2006WR005463

Archfield, S. A., Hirsch, R. M., Viglione, A., & Blöschl, G. (2016). Fragmented patterns of flood change across the United States. *Geophysical Research Letters*, *43*(19), 10,232-10,239. https://doi.org/10.1002/2016GL070590

Arel-Bundock, V. (2022). *Arel-Bundock V (2022). marginaleffects: Marginal Effects, Marginal*

Means, Predictions, and Contrasts. R package version 0.6.0.9000, https://vincentarelbundock.github.io/marginaleffects/.

Ashoori, N., Dzombak, D. A., & Small, M. J. (2017). Identifying water price and population criteria for meeting future urban water demand targets. *Journal of Hydrology*, *555*, 547–556. https://doi.org/10.1016/j.jhydrol.2017.10.047

Baldos, U. L. C., Chepeliev, M., Cultice, B., Huber, M., Meng, S., Ruane, A. C., Suttles, S., & Van Der Mensbrugghe, D. (2023). Global-to-local-to-global interactions and climate change. *Environmental Research Letters*, *18*(5). https://doi.org/10.1088/1748-9326/acc95c

Bareille, F., & Chakir, R. (2023). The impact of climate change on agriculture : A repeat-Ricardian analysis. *Journal of Environmental Economics and Management*, *119*(May), 102822. https://doi.org/10.1016/j.jeem.2023.102822

Barnett, T. P., Pierce, D. W., Hidalgo, H. G., Bonfils, C., Santer, B. D., Das, T., Bala, G., Wood, A. W., Nozawa, T., Mirin, A. a, Cayan, D. R., & Dettinger, M. D. (2008). Human-Induced Changes United States. *Science*, *319*(February), 1080–1083.

Bastidas, L. A., Gupta, H. V., Sorooshian, S., Shuttleworth, W. J., & Yang, Z. L. (1999). Sensitivity analysis of a land surface scheme using multicriteria methods. *Journal of Geophysical Research Atmospheres*, *104*(D16), 19481–19490. https://doi.org/10.1029/1999JD900155

Belete, A. W., & Gezie, W. S. (2017). Assesment on Urban Density and Land Use Efficiency in the Ethiopian Cities. *Civil and Environmental Research*, *9*(10), 7–15. http://land.igad.int/index.php/documents-1/countries/ethiopia/urbanization-1/380-assessment-on-urban-density-and-land-use-efficiency-in-the-ethiopian-cities/file

Biemans, H., Haddeland, I., Kabat, P., Ludwig, F., Hutjes, R. W. A., Heinke, J., Von Bloh, W., & Gerten, D. (2011). Impact of reservoirs on river discharge and irrigation water supply during the 20th century. *Water Resources Research*, *47*(3), 1–15. https://doi.org/10.1029/2009WR008929

Blamey, R., Gordon, J., & Chapman, R. (1999). Choice modelling: Assessing the environmental values of water supply options. *Australian Journal of Agricultural and Resource Economics*, *43*(3), 337–357. https://doi.org/10.1111/1467-8489.00083

Blanc, E., Strzepek, K., Schlosser, A., Jacoby, H., Gueneau, A., Fant, C., Rausch, S., & Reilly, J. (2014). Modeling U.S. water resources under climate change. *Earth's Future*, *2*(4), 197–224. https://doi.org/10.1002/2013ef000214

Bolker, B., Warnes, G. R., & Lumley, T. (2022). *gtools: Various R Programming Tools*. The Comprehensive R Archive Network. https://cran.r-project.org/web/packages/gtools/index.html

Brewer, J., Glennon, R., Ker, A., & Libecap, G. (2008). 2006 Presidential address water markets in the west: Prices, trading, and contractual forms. *Economic Inquiry*, *46*(2), 91–112. https://doi.org/10.1111/j.1465-7295.2007.00072.x

Brown, T. C. (2000). Projecting U.S. freshwater withdrawals. *Water Resources Research*, *36*(3), 769–780. https://doi.org/10.1029/1999WR900284

Brown, T. C. (2006). Trends in water market activity and price in the western United States. *Water Resources Research*, *42*(9), 1–14. https://doi.org/10.1029/2005WR004180

Brown, T. C., Foti, R., & Ramirez, J. A. (2013). Projected freshwater withdrawals in the United States under a changing climate. *Water Resources Research*, *49*(3), 1259–1276.

https://doi.org/10.1002/wrcr.20076

Brown, T. C., Mahat, V., & Ramirez, J. A. (2019). Adaptation to Future Water Shortages in the United States Caused by Population Growth and Climate Change. *Earth's Future*, *7*(3), 219–234. https://doi.org/10.1029/2018EF001091

Burness, B. H. S., & Quirk, J. P. (1979). Appropriative Water Rights and the Efficient Allocation of Resources Author (s): H . Stuart Burness and James P . Quirk Source : The American Economic Review , Mar ., 1979 , Vol . 69 , No . 1 (Mar ., 1979), pp . 25- Published by : American Economic As. *The American Economic Review*, *69*(1), 25–37.

Carleton, T. A., & Hsiang, S. M. (2016). Social and economic impacts of climate. *Science*, *353*(6304). https://doi.org/10.1126/science.aad9837

Carter, N., Kreutzwiser, R. D., & de Loë, R. C. (2005). Closing the circle: Linking land use planning and water management at the local level. *Land Use Policy*, *22*(2), 115–127. https://doi.org/10.1016/j.landusepol.2004.01.004

Chen, D., & Chen, H. W. (2013). Using the Köppen classification to quantify climate variation and change: An example for 1901-2010. *Environmental Development*, *6*(1), 69–79. https://doi.org/10.1016/j.envdev.2013.03.007

Chhipi-Shrestha, G., Hewage, K., & Sadiq, R. (2017). Impacts of neighborhood densification on water-energy-carbon nexus: Investigating water distribution and residential landscaping system. *Journal of Cleaner Production*, *156*, 786–795. https://doi.org/10.1016/j.jclepro.2017.04.113

Chinnasamy, C. V., Arabi, M., Sharvelle, S., Warziniack, T., Furth, C. D., & Dozier, A. (2021). Characterization of Municipal Water Uses in the Contiguous United States. *Water Resources*

Research, *57*(6), 1–18. https://doi.org/10.1029/2020WR028627

Cibin, R., Athira, P., Sudheer, K. P., & Chaubey, I. (2014). Application of distributed hydrological models for predictions in ungauged basins: A method to quantify predictive uncertainty. *Hydrological Processes*, *28*(4), 2033–2045. https://doi.org/10.1002/hyp.9721

Cook, B. I., Smerdon, J. E., Seager, R., & Coats, S. (2014). Global warming and 21st century drying. *Climate Dynamics*, *43*(9–10), 2607–2627. https://doi.org/10.1007/s00382-014-2075-y

CWCB. (2015). *Colorado Water Conservation Board, Colorado Water Plan*. https://cwcb.colorado.gov/colorado-water-plan

CWCB. (2017). *Colorado Water Conservation Board, South Platte River Basin Water Resources Planning Model User's Manual*. https://cdss.colorado.gov/resources/modeling-dataset-documentation

CWCB. (2019a). *Colorado Water Conservation Board, HydroBase, Colorado's Decision Support Systems (CDSS), version:2019-09-10, url: https://cdss.colorado.gov/software/hydrobase*. https://cdss.colorado.gov/software/hydrobase

CWCB. (2019b). Colorado Water Conservation Board, Updated Population Projections for Water Plan Scenarios. In *Analysis and Technical Update to the Colorado Water Plan* (Vol. 2, Issue 2). https://dnrftp.state.co.us/#/CWCB/Technical Update to Water Plan/1. Technical Update Documentation/

Dai, A. (2013). Increasing drought under global warming in observations and models. *Nature Climate Change*, *3*(1), 52–58. https://doi.org/10.1038/nclimate1633

Dalhuisen, J. M., Florax, R. J. G. M., de Groot, H. L. F., & Nijkamp, P. (2003). Price and income elasticities of residential water demand: A meta-analysis. *Land Economics*, *79*(2), 292–308. https://doi.org/10.2307/3146872

Daly, C., Halbleib, M., Smith, J. I., Gibson, W. P., Doggett, M. K., Taylor, G. H., Curtisb, J., & Pasteris, P. P. (2008). Physiographically sensitive mapping of climatological temperature and precipitation across the conterminous United States. *International Journal of Climatology*, *2029*(March 2008), 2011–2029. https://doi.org/10.1002/joc

Degefu, D. M., He, W., Yuan, L., Min, A., & Zhang, Q. (2018). Bankruptcy to Surplus: Sharing Transboundary River Basin's Water under Scarcity. *Water Resources Management*, *32*(8), 2735–2751. https://doi.org/10.1007/s11269-018-1955-z

Del Grosso, S. J., Parton, W. J., Mosier, A. R., Walsh, M. K., Ojima, D. S., & Thornton, P. E. (2006). DAYCENT National-Scale Simulations of Nitrous Oxide Emissions from Cropped Soils in the United States. *Journal of Environmental Quality*, *35*(4), 1451–1460. https://doi.org/10.2134/jeq2005.0160

Del Grosso, S. J., Parton, W., Mosier, A. R., Ojima, D. S., Kulmala, A. E., & Phongpan, S. (2000). General model for N2O and N2 gas emissions from soils. *Global Biogeochemical Cycles*, *14*(4), 1045–1060.

Dettinger, M., Udall, B., & Georgakakos, A. (2015). Western water and climate change. *Ecological Applications*, *25*(8), 2069–2093. https://doi.org/10.1890/15-0938.1

Dieter, C. A., Maupin, M. A., Caldwell, R. R., Harris, M. A., Ivahnenko, T. I., Lovelace, J. K., Barber, N. L., & Linsey, K. S. (2017). Estimated Use of Water in the United States in 2015. *U.S. Geological Survey Circular 1441*, *1441*. https://pubs.usgs.gov/publication/cir1441

DOLA. (2020). *Colorado Department of Local Affairs, State Demography Office*.

https://demography.dola.colorado.gov/population/

Dozier, A., Arabi, M., Wostoupal, B. C., Goemans, C. G., Zhang, Y., & Paustian, K. (2017). Declining agricultural production in rapidly urbanizing semi-arid regions: Policy tradeoffs and sustainability indicators. *Environmental Research Letters*, *12*(8). https://doi.org/10.1088/1748-9326/aa7287

Duan, K., Caldwell, P. V., Sun, G., McNulty, S. G., Zhang, Y., Shuster, E., Liu, B., & Bolstad, P. V. (2019). Understanding the role of regional water connectivity in mitigating climate change impacts on surface water supply stress in the United States. *Journal of Hydrology*, *570*(December 2018), 80–95. https://doi.org/10.1016/j.jhydrol.2019.01.011

Dudley, R. W., Hodgkins, G. A., McHale, M. R., Kolian, M. J., & Renard, B. (2017). Trends in snowmelt-related streamflow timing in the conterminous United States. *Journal of Hydrology*, *547*, 208–221. https://doi.org/10.1016/j.jhydrol.2017.01.051

EPA. (2017). U.S. Environmental Protection Agency. Updates To The Demographic And Spatial Allocation Models To Produce Integrated Climate And Land Use Scenarios (Iclus) (Final Report, Version 2). U.S. Environmental Protection Agency, Washington, DC, EPA/600/R-16/366F. In *Report* (Issue January).

EPA. (2020). *U.S. Environmental Protection Agency. ICLUS V2.1.1.* https://www.epa.gov/gcx/iclus-downloads

Espey, M., Espey, J., & Shaw, W. D. (1997). Price elasticity of residential demand for water: A meta-analysis. *WATER RESOURCES RESEARCH, VOL.*, *33*(6), 1369-1374,. https://doi.org/10.1029/97WR00571

Ferrara, I. (2008). Residential Water Use. *OECD Journal: General Papers*, *2008*(2), 153–180.

https://doi.org/10.1787/gen_papers-v2008-art14-en

Finger, R. (2013). Expanding risk consideration in integrated models - The role of downside risk aversion in irrigation decisions. *Environmental Modelling and Software*, *43*, 169–172. https://doi.org/10.1016/j.envsoft.2013.02.001

Fleck, J. (2016). *Water is for Fighting Over and Other Myths about Water in the West*. Island Press. https://islandpress.org/books/water-fighting-over

Flörke, M., Schneider, C., & McDonald, R. I. (2018). Water competition between cities and agriculture driven by climate change and urban growth. *Nature Sustainability*, *1*(1), 51–58. https://doi.org/10.1038/s41893-017-0006-8

Foti, R., Ramirez, J. A., & Brown, T. C. (2012). *Vulnerability of U.S. water supply to shortage: a technical document supporting the Forest Service 2010 RPA Assessment* (Vol. 295). http://www.treesearch.fs.fed.us/pubs/42363

Foti, R., Ramirez, J. A., & Brown, T. C. (2014a). A probabilistic framework for assessing vulnerability to climate variability and change: The case of the US water supply system. *Climatic Change*, *125*(3–4), 413–427. https://doi.org/10.1007/s10584-014-1111-6

Foti, R., Ramirez, J. A., & Brown, T. C. (2014b). Response surfaces of vulnerability to climate change: The Colorado River Basin, the High Plains, and California. *Climatic Change*, *125*(3–4), 429–444. https://doi.org/10.1007/s10584-014-1178-0

Frigyik, B. A., Kapila, A., & Gupta, M. R. (2010). Introduction to the Dirichlet Distribution and Related Processes. In *UWEE Technical Report, UWEETR-2010-0006*. https://vannevar.ece.uw.edu/techsite/papers/documents/UWEETR-2010-0006.pdf

Fry, J. A., Coan, M. J., Homer, C. G., Meyer, D. K., & Wickham, J. D. (2009). Completion of the

National Land Cover Database (NLCD) 1992 – 2001 Land Cover Change Retrofit Product. *U.S. Geological Survey Open-File Report*, 18. http://pubs.usgs.gov/of/2008/1379/pdf/ofr2008-1379.pdf

Garrick, D., Whitten, S. M., & Coggan, A. (2013). Understanding the evolution and performance of water markets and allocation policy: A transaction costs analysis framework. *Ecological Economics*, *88*, 195–205. https://doi.org/10.1016/j.ecolecon.2012.12.010

GebreEgziabher, M., Jasechko, S., & Perrone, D. (2022). Widespread and increased drilling of wells into fossil aquifers in the USA. *Nature Communications*, *13*(1). https://doi.org/10.1038/s41467-022-29678-7

Gharib, A. A., Blumberg, J., Manning, D. T., Goemans, C., & Arabi, M. (2023). Assessment of vulnerability to water shortage in semi-arid river basins: The value of demand reduction and storage capacity. *The Science of the Total Environment*, *871*(January), 161964. https://doi.org/10.1016/j.scitotenv.2023.161964

Gilligan, J. M., Wold, C. A., Worland, S. C., Nay, J. J., Hess, D. J., & Hornberger, G. M. (2018). Urban Water Conservation Policies in the United States. *Earth's Future*, *6*(7), 955–967. https://doi.org/10.1029/2017EF000797

Gleick, P., Bielawski, A., & Cooley, H. (2021). *The U.S. Infrastructure Plan: Water Components - Pacific Institute*. https://pacinst.org/the-u-s-infrastructure-plan-water-components/

Gleick, P. H. (2002). *Gleick Soft paths water*. *418*(July), 2002.

Glennon, R. (2005). Water scarcity, marketing, and privatization. *Texas Law Review*, *83*(7), 1873–1902.

Golfam, P., Ashofteh, P. S., & Loáiciga, H. A. (2021). Modeling adaptation policies to increase the synergies of the water-climate-agriculture nexus under climate change. *Environmental Development*, *37*(May 2020). https://doi.org/10.1016/j.envdev.2021.100612

Grafton, R. Q., Pittock, J., Davis, R., Williams, J., Fu, G., Warburton, M., Udall, B., Mckenzie, R., Yu, X., Che, N., Connell, D., Jiang, Q., Kompas, T., Lynch, A., Norris, R., Possingham, H., & Quiggin, J. (2013). Global insights into water resources, climate change and governance. *Nature Climate Change*, *3*(4), 315–321. https://doi.org/10.1038/nclimate1746

Gutzler, D. S., & Robbins, T. O. (2011). Climate variability and projected change in the western United States: Regional downscaling and drought statistics. *Climate Dynamics*, *37*(5), 835–849. https://doi.org/10.1007/s00382-010-0838-7

Haddeland, I., Heinke, J., Biemans, H., Eisner, S., Flörke, M., Hanasaki, N., Konzmann, M., Ludwig, F., Masaki, Y., Schewe, J., Stacke, T., Tessler, Z. D., Wada, Y., & Wisser, D. (2014). Global water resources affected by human interventions and climate change. *Proceedings of the National Academy of Sciences of the United States of America*, *111*(9), 3251–3256. https://doi.org/10.1073/pnas.1222475110

Hadjimichael, A., Yoon, J., Reed, P., Voisin, N., & Xu, W. (2023). Exploring the Consistency of Water Scarcity Inferences between Large-Scale Hydrologic and Node-Based Water System Model Representations of the Upper Colorado River Basin. *Journal of Water Resources Planning and Management*, *149*(2), 1–16. https://doi.org/10.1061/jwrmd5.wreng-5522

Hallegatte, S. (2009). Strategies to adapt to an uncertain climate change. *Global Environmental Change*, *19*(2), 240–247. https://doi.org/10.1016/j.gloenvcha.2008.12.003

Hammond, J. C., Simeone, C., Hecht, J. S., Hodgkins, G. A., Lombard, M., McCabe, G., Wolock, D., Wieczorek, M., Olson, C., Caldwell, T., Dudley, R., & Price, A. N. (2022). Going Beyond

Low Flows: Streamflow Drought Deficit and Duration Illuminate Distinct Spatiotemporal Drought Patterns and Trends in the U.S. During the Last Century. *Water Resources Research*, *58*(9), 1–20. https://doi.org/10.1029/2022WR031930

Heidari, H., Arabi, M., & Warziniack, T. (2021). Vulnerability to Water Shortage Under Current and Future Water Supply-Demand Conditions Across U.S. River Basins. *Earth's Future*, *9*(10). https://doi.org/10.1029/2021EF002278

Heidari, H., Arabi, M., Warziniack, T., & Kao, S. C. (2020). Assessing Shifts in Regional Hydroclimatic Conditions of U.S. River Basins in Response to Climate Change over the 21st Century. *Earth's Future*, *8*(10), 1–14. https://doi.org/10.1029/2020EF001657

Heidari, H., Arabi, M., Warziniack, T., & Kao, S. C. (2021). Shifts in hydroclimatology of us megaregions in response to climate change. *Environmental Research Communications*, *3*(6). https://doi.org/10.1088/2515-7620/ac0617

Hering, J. G., Waite, T. D., Luthy, R. G., Drewes, J. E., & Sedlak, D. L. (2013). A changing framework for urban water systems. *Environmental Science and Technology*, *47*(19), 10721–10726. https://doi.org/10.1021/es4007096

Herrera, P. A., Marazuela, M. A., & Hofmann, T. (2022). Parameter estimation and uncertainty analysis in hydrological modeling. *Wiley Interdisciplinary Reviews: Water*, *9*(1), 1–23. https://doi.org/10.1002/wat2.1569

Howe, C., Alexander, P., & Moses, R. (1982). The Performance of Appropriative Water Rights Systems in the Western United States During Drought. *Natural Resources*, *22*(April), 381–389.

Huang, Z., Liu, X., Sun, S., Tang, Y., Yuan, X., & Tang, Q. (2021). Global assessment of future sectoral water scarcity under adaptive inner-basin water allocation measures. *Science of the Total Environment*, *783*, 146973. https://doi.org/10.1016/j.scitotenv.2021.146973

Hutson, S. S., Barber, N. L., Kenny, J. F., Linsey, K. S., Lumia, D. S., & Maupin, M. A. (2004). Estimated use of water in the United States in 2000. *U.S. Geological Survey Circular 1268*, *1268*, 1–44. https://pubs.usgs.gov/circ/2004/circ1268/pdf/circular1268.pdf

Iglesias, A., & Garrote, L. (2015). Adaptation strategies for agricultural water management under climate change in Europe. *Agricultural Water Management*, *155*, 113–124. https://doi.org/10.1016/j.agwat.2015.03.014

IPCC. (2014). *Climate change 2014, synthesis report. In Core Writing Team, R. K. Pachauri, & L.A. Meyer (Eds.), Contribution of working groups I, II and III to the fifth assessment report of the intergovernmental panel on climate change (p. 151). IPCC. https://www.ipcc*.

IPCC. (2022). Fact Sheets | Climate Change 2022: Impacts, Adaptation and Vulnerability. In *Fact Sheet*. https://www.ipcc.ch/report/ar6/wg2/about/factsheets/%0Ahttps://www.ipcc.ch/report/ar6/wg2/about/factsheets

Jaeger, W. K., Amos, A., Bigelow, D. P., Chang, H., Conklin, D. R., Haggerty, R., Langpap, C., Moore, K., Mote, P. W., Nolin, A. W., Plantinga, A. J., Schwartz, C. L., Tullos, D., & Turner, D. P. (2017). Finding water scarcity amid abundance using human–natural system models. *Proceedings of the National Academy of Sciences of the United States of America*, *114*(45), 11884–11889. https://doi.org/10.1073/pnas.1706847114

Joyce, L. A., & Coulson, D. (2020). Climate Scenarios and Projections: A technical document supporting the USDA Forest Service 2020 RPA Assessment. Gen. Tech. Rep. RMRS-GTR-

413. Fort Collins, CO: U.S. Department of Agriculture, Forest Service, Rocky Mountain Research Station. 85 p. https://. In *USDA Forest Service - General Technical Report RMRS-GTR* (Vol. 2020, Issue 413). https://doi.org/10.2737/RMRS-GTR-413

Kenny, J. F., Barber, N. L., Hutson, S. S., Linsey, K. S., Lovelace, J. K., & Maupin, M. A. (2009). Estimated Use of Water in the United States in 2005. *U.S. Geological Survey Circular 1344*, *1344*, 52. https://pubs.usgs.gov/publication/cir1344

Khanmohammadi, S., Kizilkan, O., & Musharavati, F. (2021). Multiobjective optimization of a geothermal power plant. In *Thermodynamic Analysis and Optimization of Geothermal Power Plants*. Elsevier Inc. https://doi.org/10.1016/B978-0-12-821037-6.00011-1

Kim, D., Eum, H. Il, Kaluarachchi, J. J., & Chun, J. A. (2019). A sensitivity-based analysis for managing storage capacity of a small agricultural reservoir under drying climate. *Agricultural Water Management*, *213*(November 2018), 410–418. https://doi.org/10.1016/j.agwat.2018.10.040

Kirshen, P., Aytur, S., Hecht, J., Walker, A., Burdick, D., Jones, S., Fennessey, N., Bourdeau, R., & Mather, L. (2018). Integrated urban water management applied to adaptation to climate change. *Urban Climate*, *24*(August 2017), 247–263. https://doi.org/10.1016/j.uclim.2018.03.005

Knoben, W. J. M., Freer, J. E., & Woods, R. A. (2019). Technical note: Inherent benchmark or not? Comparing Nash-Sutcliffe and Kling-Gupta efficiency scores. *Hydrology and Earth System Sciences*, *23*(10), 4323–4331. https://doi.org/10.5194/hess-23-4323-2019

Kolokytha, E., & Malamataris, D. (2020). Integrated Water Management Approach for Adaptation to Climate Change in Highly Water Stressed Basins. *Water Resources Management*, *34*(3), 1173–1197. https://doi.org/10.1007/s11269-020-02492-w

Konikow, L. F. (2011). Contribution of global groundwater depletion since 1900 to sea-level rise. *Geophysical Research Letters*, *38*. https://doi.org/https://doi.org/10.1029/2011GL048604

Konikow, L. F. (2013). Groundwater depletion in the United States (1900−2008): U.S. Geological Survey Scientific Investigations Report 2013−5079, 63 p. *U.S. Department of the Interior U.S. Geological Survey*. http://pubs.usgs.gov/sir/2013/5079

Konikow, L. F. (2015). Long-Term Groundwater Depletion in the United States. *Groundwater*, *53*(1), 2–9. https://doi.org/10.1111/gwat.12306

Langner, L. L., Joyce, L. A., Wear, D. N., Prestemon, J. P., Coulson, D., & O'Dea, C. B. (2020). A technical document supporting the USDA forest service 2020 RPA assessment. *USDA Forest Service - General Technical Report RMRS-GTR*, *2020*(412), 1–34. https://doi.org/10.2737/RMRSGTR-412

Legaria, U., Mota, S., Martinez, S., Cobá, A., Chable, A., & Neme, A. (2023). Anomaly detection in the probability simplex under different geometries. *Information Geometry*, *6*(2), 385–412. https://doi.org/10.1007/s41884-023-00107-y

Leng, G., Huang, M., Voisin, N., Zhang, X., Asrar, G. R., & Leung, L. R. (2016). Emergence of new hydrologic regimes of surface water resources in the conterminous United States under future warming. *Environmental Research Letters*, *11*(11). https://doi.org/10.1088/1748-9326/11/11/114003

Leonard, B., & Libecap, G. D. (2019). Collective action by contract: Prior appropriation and the development of irrigation in the Western United States. *Journal of Law and Economics*, *62*(1), 67–115. https://doi.org/10.1086/700934

Liang, X., Lettenmaier, D. P., Wood, E. F., & Burges, S. J. (1994). A simple hydrologically based model of land surface water and energy fluxes for general circulation models. *Journal of Geophysical Research*, *99*(D7). https://doi.org/10.1029/94jd00483

Liu, D., Guo, S., Shao, Q., Liu, P., Xiong, L., Wang, L., Hong, X., Xu, Y., & Wang, Z. (2018). Assessing the effects of adaptation measures on optimal water resources allocation under varied water availability conditions. *Journal of Hydrology*, *556*, 759–774. https://doi.org/10.1016/j.jhydrol.2017.12.002

Lucero, L., & Dan Tarlock, A. (2003). Water supply and urban growth in New Mexico: Same old, same old or a new Era? *Natural Resources Journal*, *43*(3), 803–834.

Lukas, J., Barsugli, J., Doesken, N., Rangwala, I., & Wolter, K. (2014). Climate change in Colorado: A synthesis to support water resources management and adaptation. A report for the Colorado Water Conservation Board, 2nd ed. Western Water Assessment, Cooperative Institute for Research in Environmental Sciences, University of. In *University of Colorado Boulder*.

Ma, X. (Cissy), Xue, X., González-Mejía, A., Garland, J., & Cashdollar, J. (2015). Sustainable water systems for the city of tomorrow-A conceptual framework. *Sustainability (Switzerland)*, *7*(9), 12071–12105. https://doi.org/10.3390/su70912071

Maas, A., Dozier, A., & Manning, D. T. (2016). *Allocation Institutions on Value*. 1–16. https://doi.org/10.1002/2016WR019239.Received

Makropoulos, C. K., Natsis, K., Liu, S., Mittas, K., & Butler, D. (2008). Decision support for sustainable option selection in integrated urban water management. *Environmental Modelling and Software*, *23*(12), 1448–1460. https://doi.org/10.1016/j.envsoft.2008.04.010

Martinsen, G., Liu, S., Mo, X., & Bauer-Gottwein, P. (2019). Joint optimization of water allocation and water quality management in Haihe River basin. *Science of the Total Environment*, *654*, 72–84. https://doi.org/10.1016/j.scitotenv.2018.11.036

Maupin, M. A., Kenny, J. F., Hutson, S. S., Lovelace, J. K., Barber, N. L., & Linsey, K. S. (2014). Estimated Use of Water in the United States in 2010. *U.S. Geological Survey Circular 1405*, *November*, 64. https://doi.org/10.3133/cir765

Megdal, S. B., Gerlak, A. K., Varady, R. G., & Huang, L. Y. (2015). Groundwater Governance in the United States: Common Priorities and Challenges. *Groundwater*, *53*(5), 677–684. https://doi.org/10.1111/gwat.12294

Mekonnen, M. M., & Hoekstra, A. Y. (2016). Four billion people facing severe water scarcity. *Science Advances*, *2*(2), e1500323–e1500323. https://doi.org/10.1126/sciadv.1500323

Mesinger, F., DiMego, G., Kalnay, E., Mitchell, K., Shafran, P. C., Ebisuzaki, W., Jović, D., Woollen, J., Rogers, E., Berbery, E. H., Ek, M. B., Fan, Y., Grumbine, R., Higgins, W., Li, H., Lin, Y., Manikin, G., Parrish, D., & Shi, W. (2006). North American regional reanalysis. *Bulletin of the American Meteorological Society*, *87*(3), 343–360. https://doi.org/10.1175/BAMS-87-3-343

Miller, A. (2023). *Smart Housing Policy Is a Climate Strategy for Colorado*. https://www.nrdc.org/bio/alana-miller/smart-housing-policy-climate-strategy-colorado

Miller, K. A., Rhodes, S. L., & Macdonnell, L. J. (1997). Water allocation in a changing climate: Institutions and adaptation. *Climatic Change*, *35*(2), 157–177. https://doi.org/10.1023/A:1005300529862

Miller, O. L., Putman, A. L., Alder, J., Miller, M., Jones, D. K., & Wise, D. R. (2021). Changing climate drives future streamflow declines and challenges in meeting water demand across the southwestern United States. *Journal of Hydrology X*, *11*(December 2020), 100074. https://doi.org/10.1016/j.hydroa.2021.100074

Mitchell, B. (2005). Integrated water resource management, institutional arrangements, and land-use planning. *Environment and Planning A*, *37*(8), 1335–1352. https://doi.org/10.1068/a37224

Momblanch, A., Papadimitriou, L., Jain, S. K., Kulkarni, A., Ojha, C. S. P., Adeloye, A. J., & Holman, I. P. (2019). Untangling the water-food-energy-environment nexus for global change adaptation in a complex Himalayan water resource system. *Science of the Total Environment*, *655*, 35–47. https://doi.org/10.1016/j.scitotenv.2018.11.045

Moore, F. C., & Lobell, D. B. (2015). The fingerprint of climate trends on european crop yields. *Proceedings of the National Academy of Sciences of the United States of America*, *112*(9), 2970–2975. https://doi.org/10.1073/pnas.1409606112

Moriasi, D. N., Gitau, M. W., Pai, N., & Daggupati, P. (2015). Hydrologic and water quality models: Performance measures and evaluation criteria. *Transactions of the ASABE*, *58*(6), 1763–1785. https://doi.org/10.13031/trans.58.10715

Muratoglu, A., Iraz, E., & Ercin, E. (2022). Water resources management of large hydrological basins in semi-arid regions: Spatial and temporal variability of water footprint of the Upper Euphrates River basin. *Science of the Total Environment*, *846*(April), 157396. https://doi.org/10.1016/j.scitotenv.2022.157396

Naz, B. S., Kao, S. C., Ashfaq, M., Rastogi, D., Mei, R., & Bowling, L. C. (2016). Regional hydrologic response to climate change in the conterminous United States using high-resolution hydroclimate simulations. *Global and Planetary Change*, *143*, 100–117. https://doi.org/10.1016/j.gloplacha.2016.06.003

Neale, M. R., Sharvelle, S., Arabi, M., Dozier, A., & Goemans, C. (2020). Assessing tradeoffs of strategies for urban water conservation and fit for purpose water. *Journal of Hydrology X*, *8*(June), 100059. https://doi.org/10.1016/j.hydroa.2020.100059

NOAA. (2021). *NOAA National Centers for Environmental information, Climate at a Glance: Statewide Mapping, retrieved on August, 2021*. https://www.ncdc.noaa.gov/cag/statewide/

Nouri, H., Stokvis, B., Galindo, A., Blatchford, M., & Hoekstra, A. Y. (2019). Water scarcity alleviation through water footprint reduction in agriculture: The effect of soil mulching and drip irrigation. *Science of the Total Environment*, *653*, 241–252. https://doi.org/10.1016/j.scitotenv.2018.10.311

Ogle, S. M., Jay Breidt, F., Easter, M., Williams, S., Killian, K., & Paustian, K. (2010). Scale and uncertainty in modeled soil organic carbon stock changes for US croplands using a process-based model. *Global Change Biology*, *16*(2), 810–822. https://doi.org/10.1111/j.1365-2486.2009.01951.x

Olmstead, S. M., Michael Hanemann, W., & Stavins, R. N. (2007). Water demand under alternative price structures. *Journal of Environmental Economics and Management*, *54*(2), 181–198. https://doi.org/10.1016/j.jeem.2007.03.002

Oubeidillah, A. A., Kao, S. C., Ashfaq, M., Naz, B. S., & Tootle, G. (2014). A large-scale, high-resolution hydrological model parameter data set for climate change impact assessment for the conterminous US. *Hydrology and Earth System Sciences*, *18*(1), 67–84. https://doi.org/10.5194/hess-18-67-2014

Palmer, M. A., Reidy Liermann, C. A., Nilsson, C., Flörke, M., Alcamo, J., Lake, P. S., & Bond, N. (2008). Climate change and the world's river basins: Anticipating management options. *Frontiers in Ecology and the Environment*, *6*(2), 81–89. https://doi.org/10.1890/060148

Parton, W. J., Hartman, M., Ojima, D., & Schimel, D. (1998). *Daycent description and testing*. 35–48.

Paterson, W., Rushforth, R., Ruddell, B. L., Konar, M., Ahams, I. C., Gironás, J., Mijic, A., & Mejia, A. (2015). Water footprint of cities: A review and suggestions for future research. *Sustainability (Switzerland)*, *7*(7), 8461–8490. https://doi.org/10.3390/su7078461

Payne, M. T., Smith, M. G., & Landry, C. J. (2014). Price Determination and Efficiency in the Market for South Platte Basin Ditch Company Shares. *Journal of the American Water Resources Association*, *50*(6), 1488–1500. https://doi.org/10.1111/jawr.12215

Plummer, R., De Grosbois, D., De Loë, R., & Velaniškis, J. (2011). Probing the integration of land use and watershed planning in a shifting governance regime. *Water Resources Research*, *47*(9), 1–13. https://doi.org/10.1029/2010WR010213

Qin, Y., Abatzoglou, J. T., Siebert, S., Huning, L. S., AghaKouchak, A., Mankin, J. S., Hong, C., Tong, D., Davis, S. J., & Mueller, N. D. (2020). Agricultural risks from changing snowmelt. *Nature Climate Change*, *10*(5), 459–465. https://doi.org/10.1038/s41558-020-0746-8

Räsänen, A., Nygren, A., Monge Monge, A., Käkönen, M., Kanninen, M., & Juhola, S. (2018). From divide to nexus: Interconnected land use and water governance changes shaping risks related to water. *Applied Geography*, *90*(November 2017), 106–114. https://doi.org/10.1016/j.apgeog.2017.11.005

Rateb, A., Scanlon, B. R., Pool, D. R., Sun, A., Zhang, Z., Chen, J., Clark, B., Faunt, C. C., Haugh,

C. J., Hill, M., Hobza, C., McGuire, V. L., Reitz, M., Müller Schmied, H., Sutanudjaja, E. H., Swenson, S., Wiese, D., Xia, Y., & Zell, W. (2020). Comparison of Groundwater Storage Changes From GRACE Satellites With Monitoring and Modeling of Major U.S. Aquifers. *Water Resources Research*, *56*(12), 1–19. https://doi.org/10.1029/2020WR027556

Rathnayaka, K., Malano, H., & Arora, M. (2016). Assessment of sustainability of urban water supply and demand management options: A comprehensive approach. *Water (Switzerland)*, *8*(12). https://doi.org/10.3390/w8120595

Renard, B., Kavetski, D., Kuczera, G., Thyer, M., & Franks, S. W. (2010). Understanding predictive uncertainty in hydrologic modeling: The challenge of identifying input and structural errors. *Water Resources Research*, *46*(5), 1–22. https://doi.org/10.1029/2009WR008328

Richter, B. D. (2023). Decoupling Urban Water Use from Population Growth in the Colorado River Basin. *Journal of Water Resources Planning and Management*, *149*(2), 1–9. https://doi.org/10.1061/jwrmd5.wreng-5887

Richter, B. D., Abell, D., Bacha, E., Brauman, K., Calos, S., Cohn, A., Disla, C., O'Brien, S. F., Hodges, D., Kaiser, S., Loughran, M., Mestre, C., Reardon, M., & Siegfried, E. (2013). Tapped out: How can cities secure their water future? *Water Policy*, *15*(3), 335–363. https://doi.org/10.2166/wp.2013.105

Rijsberman, F. R. (2006). Water scarcity: Fact or fiction? *Agricultural Water Management*, *80*(1-3 SPEC. ISS.), 5–22. https://doi.org/10.1016/j.agwat.2005.07.001

Rob J. Hyndman, & Yeasmin Khandakar. (2008). Automatic Time Series Forecasting: The forecast Package for R. *Journal of Statistical Software*, *27*(3), 22.

http://www.jstatsoft.org/%0Ahttp://www.jstatsoft.org/v27/i03/paper

Robertson, A. D., Zhang, Y., Sherrod, L. A., Rosenzweig, S. T., Ma, L., Ahuja, L., & Schipanski, M. E. (2018). Climate Change Impacts on Yields and Soil Carbon in Row Crop Dryland Agriculture. *Journal of Environmental Quality*, *47*(4), 684–694. https://doi.org/10.2134/jeq2017.08.0309

Rosegrant, M. W., & Ringler, C. (2000). Impact on food security and rural development of transferring water out of agriculture. *Water Policy*, *1*(6), 567–586. https://doi.org/10.1016/S1366-7017(99)00018-5

Roy, S. B., Chen, L., Girvetz, E. H., Maurer, E. P., Mills, W. B., & Grieb, T. M. (2012). Projecting water withdrawal and supply for future decades in the U.S. under climate change scenarios. *Environmental Science and Technology*, *46*(5), 2545–2556. https://doi.org/10.1021/es2030774

Rudd, M. A., & Fleishman, E. (2014). Policymakers' and scientists' ranks of research priorities for resource-management policy. *BioScience*, *64*(3), 219–228. https://doi.org/10.1093/biosci/bit035

Russell, S., & Fielding, K. (2010). Water demand management research: A psychological perspective. *Water Resources Research*, *46*(5), 1–12. https://doi.org/10.1029/2009WR008408

Sankarasubramanian, A., Sabo, J. L., Larson, K. L., Seo, S. B., Sinha, T., Bhowmik, R., Vidal, A. R., Kunkel, K., Mahinthakumar, G., Berglund, E. Z., & Kominoski, J. (2017). Synthesis of public water supply use in the United States: Spatio-temporal patterns and socio-economic controls. *Earth's Future*, *5*(7), 771–788. https://doi.org/10.1002/2016EF000511

Scheierling, S. M., Loomis, J. B., & Young, R. A. (2006). Irrigation water demand: A meta-analysis of price elasticities. *Water Resources Research*, *42*(1), 1–9. https://doi.org/10.1029/2005WR004009

Schoengold, K., Sunding, D. L., & Moreno, G. (2006). Price elasticity reconsidered: Panel estimation of an agricultural water demand function. *Water Resources Research*, *42*(9), 1–10. https://doi.org/10.1029/2005WR004096

Seager, R., Ting, M., Li, C., Naik, N., Cook, B., Nakamura, J., & Liu, H. (2013). Projections of declining surface-water availability for the southwestern United States. *Nature Climate Change*, *3*(5), 482–486. https://doi.org/10.1038/nclimate1787

Shandas, V., Lehman, R., Larson, K. L., Bunn, J., & Chang, H. (2015). Stressors and strategies for managing Urban water scarcity: Perspectives from the field. *Water (Switzerland)*, *7*(12), 6775–6787. https://doi.org/10.3390/w7126659

Shandas, V., & Parandvash, G. H. (2010). Integrating urban form and demographics in water-demand management: An empirical case study of Portland, Oregon. *Environment and Planning B: Planning and Design*, *37*(1), 112–128. https://doi.org/10.1068/b35036

Sharvelle, S., Dozier, A., Arabi, M., & Reichel, B. (2017). A geospatially-enabled web tool for urban water demand forecasting and assessment of alternative urban water management strategies. *Environmental Modelling and Software*, *97*, 213–228. https://doi.org/10.1016/j.envsoft.2017.08.009

Siddik, M. A. B., Dickson, K. E., Rising, J., Ruddell, B. L., & Marston, L. T. (2023). Inter-basin water transfers in the United States and Canada. *Scientific Data*, *10*(1), 1–9. https://doi.org/10.1038/s41597-023-01935-4

Solley, W. B., Merk, C. F., & Pierce, R. R. (1988). Estimated use of water in the United States in 1985. *U.S. Geological Survey Circular 1004*, *1004*. https://pubs.usgs.gov/publication/cir1004

Solley, W. B., Pierce, R. R., & Perlman, H. A. (1993). Estimated Use of Water in the United States in 1990. *U.S. Geological Survey Circular 1081*, *1081*. https://pubs.usgs.gov/publication/cir1081

Solley, W. B., Pierce, R. R., & Perlman, H. A. (1998). Estimated use of water in the United States in 1995. *U.S. Geological Survey Circular 1200*, *1200*. https://pubs.usgs.gov/publication/cir1200

Song, X., Zhang, J., Zhan, C., Xuan, Y., Ye, M., & Xu, C. (2015). Global sensitivity analysis in hydrological modeling: Review of concepts, methods, theoretical framework, and applications. *Journal of Hydrology*, *523*(225), 739–757. https://doi.org/10.1016/j.jhydrol.2015.02.013

Stackpoole, S. M., Oelsner, G. P., Stets, E. G., Hecht, J. S., Johnson, Z. C., Tesoriero, A. J., Walvoord, M. A., Chanat, J. G., Dunne, K. A., Goodling, P. J., Lindsey, B. D., Meador, M. R., & Spaulding, S. A. (2023). Integrated water resources trend assessments: State of the science, challenges, and opportunities for advancement. *Journal of the American Water Resources Association*, *May*, 1–17. https://doi.org/10.1111/1752-1688.13137

State of California. (2018). *Assembly Bill No. 1668*. *1668*, 1–26. https://leginfo.legislature.ca.gov/faces/billTextClient.xhtml?bill_id=201720180AB1668

State of Colorado, & State of Nebraska. (1923). *Article 65: South Platte River Compact*.

Stehfest, E., Heistermann, M., Priess, J. A., Ojima, D. S., & Alcamo, J. (2007). Simulation of global crop production with the ecosystem model DayCent. *Ecological Modelling*, *209*(2–4), 203–219. https://doi.org/10.1016/j.ecolmodel.2007.06.028

Stoker, P., Albrecht, T., Follingstad, G., & Carlson, E. (2022). Integrating Land Use Planning and Water Management in U.S. Cities: A Literature Review. *Journal of the American Water Resources Association*, *58*(3), 321–335. https://doi.org/10.1111/1752-1688.13022

Stoker, P., Chang, H., Wentz, E., Crow-Miller, B., Jehle, G., & Bonnette, M. (2019). Building Water-Efficient Cities: A Comparative Analysis of How the Built Environment Influences Water Use in Four Western U.S. Cities. *Journal of the American Planning Association*, *85*(4), 511–524. https://doi.org/10.1080/01944363.2019.1638817

Stoker, P., & Rothfeder, R. (2014). Drivers of urban water use. *Sustainable Cities and Society*, *12*, 1–8. https://doi.org/10.1016/j.scs.2014.03.002

Strzepek, K., Yohe, G., Neumann, J., & Boehlert, B. (2010). Characterizing changes in drought risk for the United States from climate change. *Environmental Research Letters*, *5*(4). https://doi.org/10.1088/1748-9326/5/4/044012

Sun, Y., Liu, N., Shang, J., & Zhang, J. (2017). Sustainable utilization of water resources in China: A system dynamics model. *Journal of Cleaner Production*, *142*, 613–625. https://doi.org/10.1016/j.jclepro.2016.07.110

Sutherland, D. C., & Fenn, C. R. (2000). Assessment of water supply options. *Thematic Review IV.3 Prepared as an Input to the World Commission on Dams, Cape Town*. https://citeseerx.ist.psu.edu/document?repid=rep1&type=pdf&doi=1c2db257b37bfe982a81b03591b1471e07c83c4b

Thaw, M., GebreEgziabher, M., Villafañe-Pagán, J. Y., & Jasechko, S. (2022). Modern groundwater reaches deeper depths in heavily pumped aquifer systems. *Nature*

Communications, *13*(1). https://doi.org/10.1038/s41467-022-32954-1

Thornton, P., Dinesh, D., Cramer, L., Loboguerrero, A. M., & Campbell, B. (2018). Agriculture in a changing climate: Keeping our cool in the face of the hothouse. *Outlook on Agriculture*, *47*(4), 283–290. https://doi.org/10.1177/0030727018815332

Thornton, P. E., Running, S. W., & White, M. A. (1997). Generating surfaces of daily meteorological variables over large regions of complex terrain. *Journal of Hydrology*, *190*(3–4), 214–251. https://doi.org/10.1016/S0022-1694(96)03128-9

Tidwell, V. C., Moreland, B. D., Zemlick, K. M., Roberts, B. L., Passell, H. D., Jensen, D., Forsgren, C., Sehlke, G., Cook, M. A., King, C. W., & Larsen, S. (2014). Mapping water availability, projected use and cost in the western United States. *Environmental Research Letters*, *9*(6). https://doi.org/10.1088/1748-9326/9/6/064009

Ty, T. Van, Sunada, K., Ichikawa, Y., & Oishi, S. (2012). Scenario-based Impact Assessment of Land Use/Cover and Climate Changes on Water Resources and Demand: A Case Study in the Srepok River Basin, Vietnam-Cambodia. *Water Resources Management*, *26*(5), 1387–1407. https://doi.org/10.1007/s11269-011-9964-1

United States Census Bureau. (2020). *COLORADO: 2020 Census*. https://www.census.gov/library/stories/state-by-state/colorado-population-change-between-census-decade.html

Villarini, G., & Wasko, C. (2021). Humans, climate and streamflow. *Nature Climate Change*, *11*(9), 725–726. https://doi.org/10.1038/s41558-021-01137-z

Wang, H., Bracciano, D., & Asefa, T. (2020). Evaluation of Water Saving Potential for Short-Term Water Demand Management. *Water Resources Management*, *34*(10), 3317–3330.

https://doi.org/10.1007/s11269-020-02615-3

Wang, X. (2001). Integrating water-quality management and land-use planning in a watershed context. *Journal of Environmental Management*, *61*(1), 25–36. https://doi.org/10.1006/jema.2000.0395

Wang, Y. (2020). Urban land and sustainable resource use: Unpacking the countervailing effects of urbanization on water use in China, 1990–2014. *Land Use Policy*, *90*(October 2019). https://doi.org/10.1016/j.landusepol.2019.104307

Warziniack, T., Arabi, M., Brown, T. C., Froemke, P., Ghosh, R., Rasmussen, S., & Swartzentruber, R. (2022). Projections of Freshwater Use in the United States Under Climate Change. *Earth's Future*, *10*(2). https://doi.org/10.1029/2021EF002222

Warziniack, T., & Brown, T. C. (2019). The importance of municipal and agricultural demands in future water shortages in the United States. *Environmental Research Letters*, *14*(8). https://doi.org/10.1088/1748-9326/ab2b76

Wear, D. N., & Prestemon, J. P. (2019). Spatiotemporal downscaling of global population and income scenarios for the United States. *PLoS ONE*, *14*(7), 1–19. https://doi.org/10.1371/journal.pone.0219242

Wehner, M. F., Arnold, J. R., Knutson, T., Kunkel, K. E., & LeGrande, A. N. (2017). Ch. 8: Droughts, Floods, and Wildfires. Climate Science Special Report: Fourth National Climate Assessment, Volume I. *Climate Science Special Report: Fourth National Climate Assessment, Volume I*, *I*, 231–256. https://doi.org/10.7930/J0CJ8BNN.U.S.

Wheeler, K. G., Udall, B., Wang, J., Kuhn, E., Salehabadi, H., & Schmidt, J. C. (2022). What will it take to stabilize the Colorado River? *Science*, *377*(6604), 373–375.

https://doi.org/10.1126/science.abo4452

Williams, A. P., Cook, B. I., & Smerdon, J. E. (2022). Rapid intensification of the emerging southwestern North American megadrought in 2020–2021. *Nature Climate Change*, *12*(3), 232–234. https://doi.org/10.1038/s41558-022-01290-z

Womble, P., & Hanemann, W. M. (2020). Legal Change and Water Market Transaction Costs in Colorado. *Water Resources Research*, *56*(4). https://doi.org/10.1029/2019WR025508

Wong, T.-T. (1998). Generalized Dirichlet distribution in Bayesian analysis. *Applied Mathematics and Computation*, *97*(2–3), 165–181. https://doi.org/10.1016/s0096-3003(97)10140-0

Yan, D., Yao, M., Ludwig, F., Kabat, P., Huang, H. Q., Hutjes, R. W. A., & Werners, S. E. (2006). Water Allocation Strategies. *Sharing Water in Times of Scarcity*, 102–110. https://doi.org/10.1061/9780784408469.ch05

Yates, D., Sieber, J., Purkey, D., & Huber-Lee, A. (2005). WEAP21 - A demand-, priority-, and preference-driven water planning model. Part 1: Model characteristics. *Water International*, *30*(4), 487–500. https://doi.org/10.1080/02508060508691893

Yigzaw, W., & Hossain, F. (2016). Water sustainability of large cities in the United States from the perspectives of population increase, anthropogenic activities, and climate change. *Earth's Future*, *4*(12), 603–617. https://doi.org/10.1002/2016EF000393

Zhang, Y., Gurung, R., Marx, E., Williams, S., Ogle, S. M., & Paustian, K. (2020). DayCent Model Predictions of NPP and Grain Yields for Agricultural Lands in the Contiguous U.S. *Journal of Geophysical Research: Biogeosciences*, *125*(7), 1–15. https://doi.org/10.1029/2020JG005750

APPENDIX A

SUPPORTING INFORMATION FOR CHAPTER 2:

ASSESSMENT OF VULNERABILITY TO WATER SHORTAGE IN SEMI-ARID RIVER BASINS: THE VALUE OF DEMAND REDUCTION AND STORAGE CAPACITY

1. WEAP Schematic

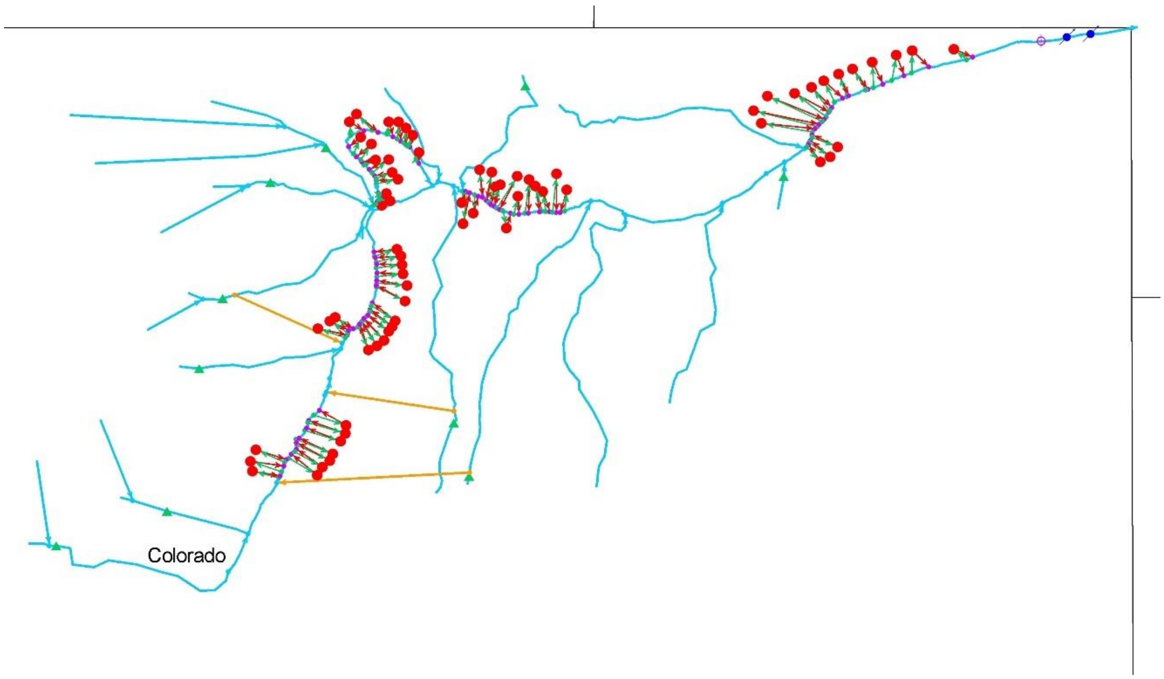

Figure A1. WEAP Schematic

2. Regression models

2.1. Population of Region 3 as a Function of Population of Region 4

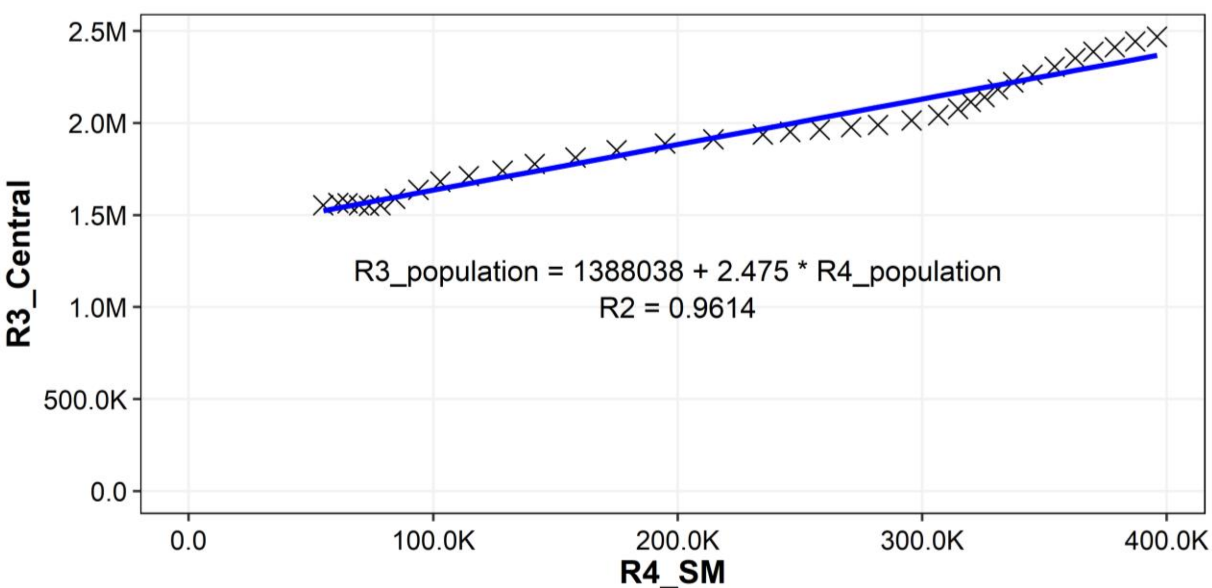

Figure A2. Population in regions 3 and 4 from 1980 to 2015 with the regression model used to split their combined estimated population.

2.2. Households as a Function of Population (Colored by Model Regions)

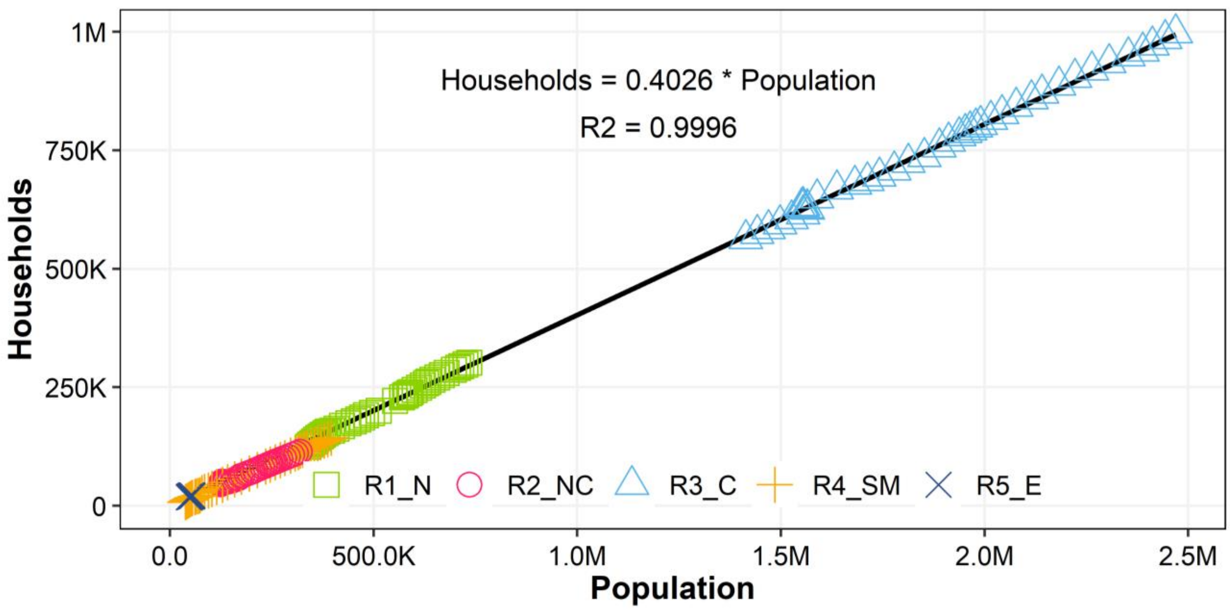

Figure A3. Households and population in each region and the regression model used to estimate the households from the population

2.3. Flood Application Irrigation Efficiency as a Function of Ag Consumptive Demands Per Unit Area.

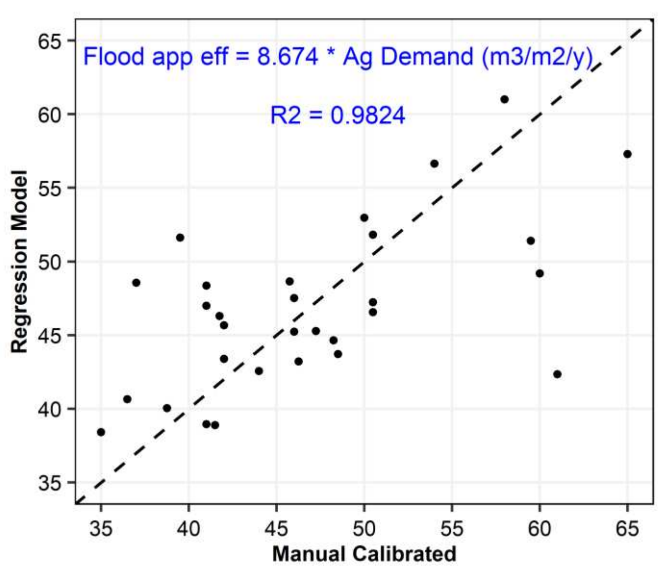

Figure A4. Manual calibrated flood application irrigation and output from the linear regression model with a 1:1 line.

2.4. Outflow Regression Model

$$Outflow = e^{1.44e-6*Water\ Yield(sum\ of\ coming\ 6\ months)+\ 2.36e-6*Water\ Yield\ (sum\ of\ previous\ 10\ months)} \quad (A1)$$

where outflow in cubic feet per second (CFS) and water yield from the VIC model in acre-feet (AF)

$$Outflow = e^{1.16e-9*Water\ Yield\ (sum\ of\ coming\ 6\ months)+1.91e-9*Water\ Yield\ (sum\ of\ previous\ 10\ months)} / 35.315 \quad (A2)$$

where outflow in m^3/s and water yield from the VIC model in m^3

3. Climate Models

Table A1. MACA climate models (Joyce & Coulson, 2020)

Name	RCP	Description	Model agency
HadGEM2-ES365	4.5 and 8.5	HOT	Met Office Hadley Center, U.K.
MRI-CGCM3	4.5 and 8.5	WARM	Meteorological Research Institute, Japan
CNRM-CM5	4.5 and 8.5	WET	National Centre of Meteorological Research, France
IPSL-CM5A-MR	4.5 and 8.5	DRY	Institute Pierre Simon Laplace, France

- Warm means the lowest average increase in temperature.
- Hot means the highest average increase in temperature.
- Wet means the highest average increase in precipitation.
- Dry means the highest average decrease in precipitation.

The Precipitation change (percent) against temperature difference (°C) at mid-century (2041–2070) from the historical period (1971–2000) under RCP 4.5 and RCP 8.5 for 16 climate models at the scale of the conterminous United States are presented in Langner (2022) figure 3 for more details.

Langner, Linda L.; Joyce, Linda A.; Wear, David N.; Prestemon, Jeffrey P.; Coulson, David; O'Dea, Claire B. 2020. Future scenarios: A technical document supporting the USDA Forest Service 2020 RPA Assessment. Gen. Tech. Rep. RMRS-GTR-412. Fort Collins, CO: U.S.

Department of Agriculture, Forest Service, Rocky Mountain Research Station. 34 p. https://doi.org/10.2737/RMRS- GTR-412.

4. Water Supply and Demands Calibration

Table A2 summarizes the supply and demands calibration.

Table A2. Water supply and demands calibration

<table>
<tr><th colspan="2">Model</th><th>Monitored</th><th>Simulated</th><th>Comments</th></tr>
<tr><td colspan="2">Water Supply in BCM/y (VIC + the transferred water)</td><td>2.34</td><td>2.89</td><td>The simulated water supply includes the surface runoff, the baseflow, and the transferred water, while parts of this baseflow are accounted as groundwater withdrawal in the monitored data.</td></tr>
<tr><td rowspan="2">Urban Water Demand in liters per capita per day (IUWM)</td><td>Metro Region</td><td>586.7</td><td>550</td><td rowspan="2">Results are very close</td></tr>
<tr><td>Other regions in SPRB</td><td>711.7</td><td>719.2</td></tr>
<tr><td colspan="2">Irrigation Water Requirements in cm (DayCENT)</td><td>53.6</td><td>50.2</td><td>Results are very close</td></tr>
</table>

4.1. Water supply calibration

The annual mean of water from the VIC model plus the transferred (out-of-basin) water is 2.89 BCM/y over the historical period. The Colorado Water Plan (CWCB, 2015) reports the long-term average water supply in SPRB is 2.34 BCM/y (Table A2). VIC reports higher mean values as it accounts for baseflow, while parts of this baseflow are accounted as groundwater withdrawal in the monitored flow from The Water Plan.

Also, a comparison between the USGS-monitored prominent mouth of canyons of SPRB - in blue- to the VIC results at the outlets of the corresponding HUC8s over the historical period is presented in the two figures below -in orange-. VIC results are higher than the monitored flow because of the more area that contributes to the VIC flow and the accounting for the baseflow. Overall, this half monthly average over the historical period indicates that VIC can imitate the flow in the study area.

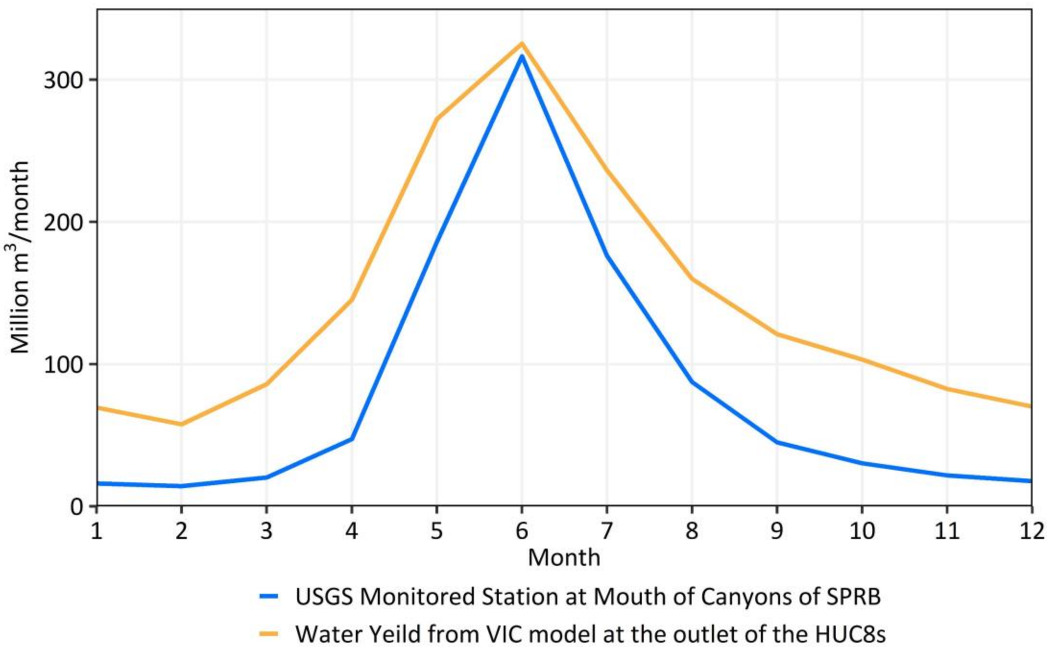

Figure A5. Average historical monthly water supply from VIC at the huc8s outlets, with the monitored monthly average at the mouth of canyons.

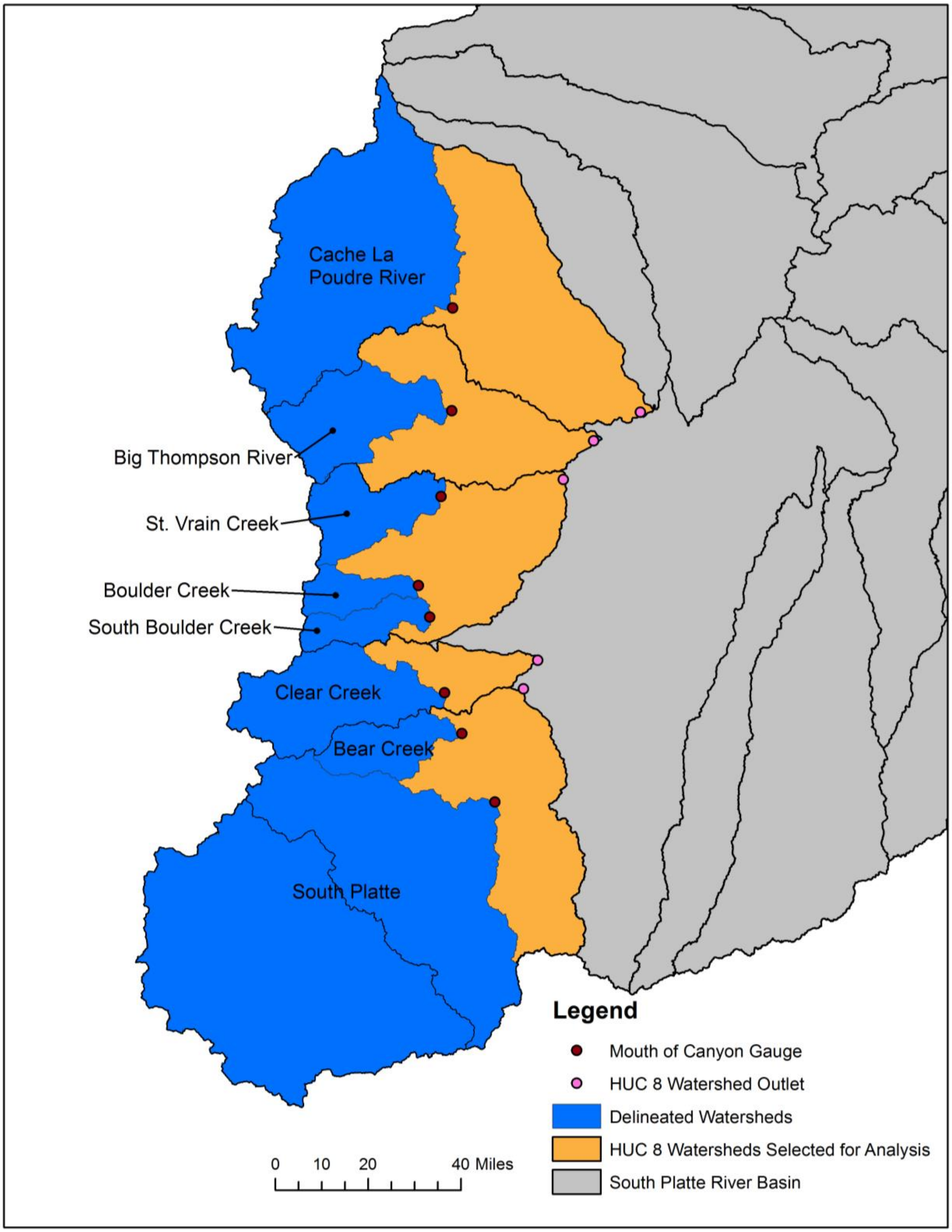

Figure A6. The mouth of major canyons contributing to SPRB water (bule) with the Huc8 areas (grey and orange)

4.2. Urban water demand

The Colorado Water Plan (CWCB, 2015) estimated the 2010 municipal water demand for the metro regions as 586.7 liters per capita per day (lpcd), while IUWM estimate the demand to be 550 lcpd (Table A2). Similarly, for the other regions in SPRB, the plan reports 711.7 lpcd and IUWM estimated it as 719.2 lpcd. These values are very close to the monitored values. Figure A7 shows the annual urban demand simulated by IUWM.

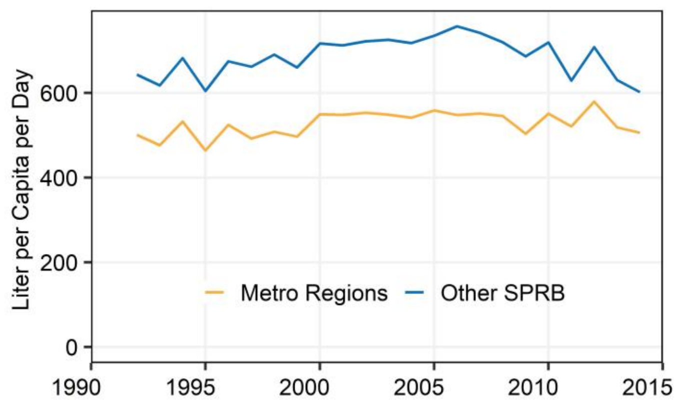

Figure A7. Annual urban water demand from IUWM per capita

4.3. Ag water demand

The technical update of the Colorado Water Plan (Volume 2, Section 3, Table 4) reports the average irrigation water requirement (IWR) in SPRB to be 53.6 cm (CWCB, 2019). The historical mean of the IWR from DayCENT is 50.2 cm as shown in the two figures below, which is very close to the reported values (Table A2).

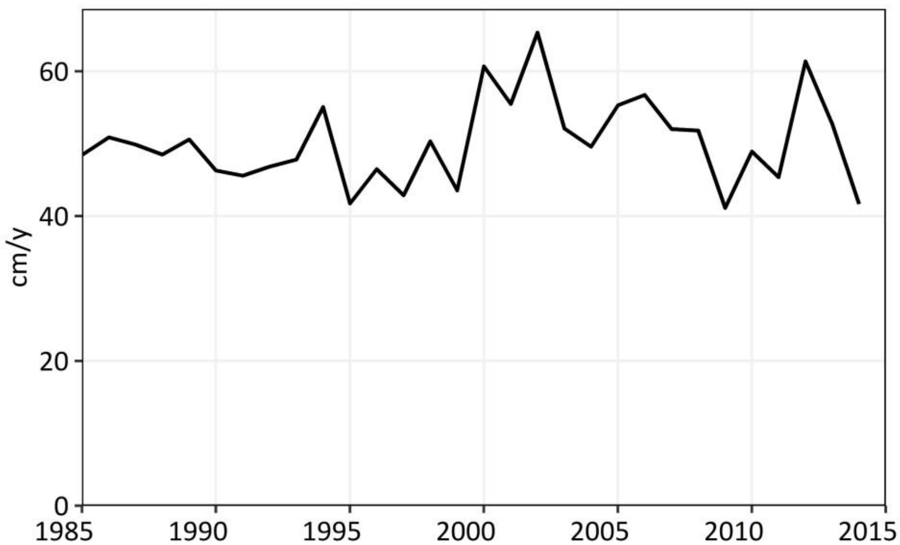

Figure A8. DayCENT historical annual irrigation water requirements

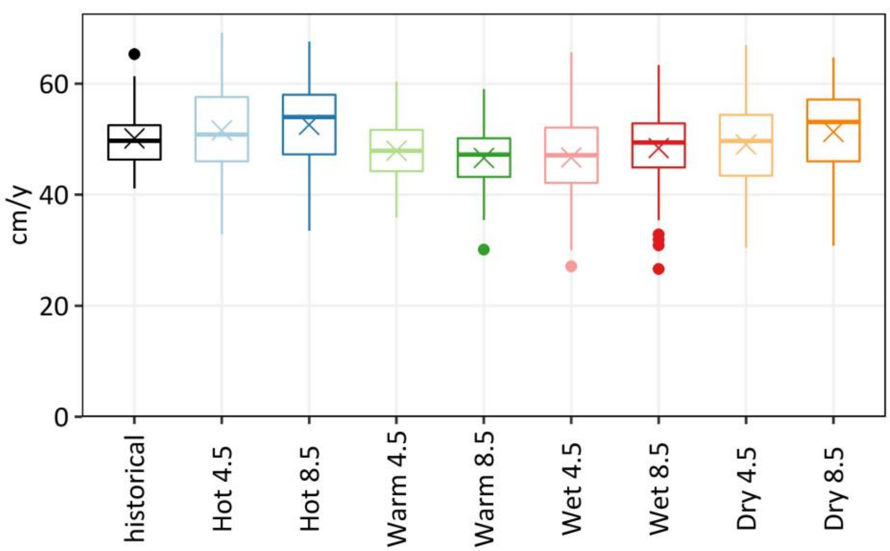

Figure A9. DayCENT annual irrigation requirement box plot for the historical period 1985-2014 and the future scenarios 2015-2099

5. Water Supply

The annual mean of the water yield from VIC for the eight climate scenarios is close to the historical pattern, while more severe and frequent flood and drought years are predicted in the future (Figure A10). In contrast, the results of the ARIMA model show less fluctuation for the out-of-basin water supply over the climate scenarios with an annual mean that is close to the historical (Figure A10).

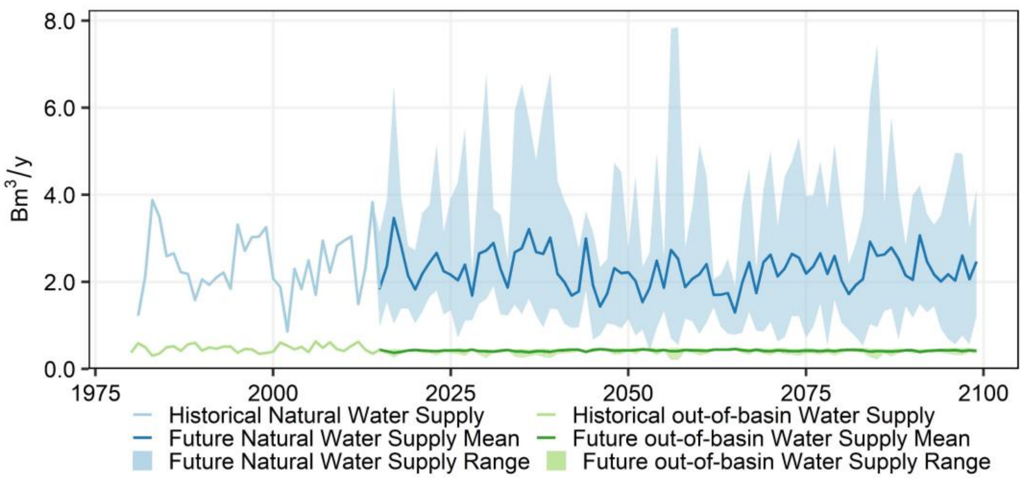

Figure A10. Annual Water Supply

6. 10 years average Consumptive uses

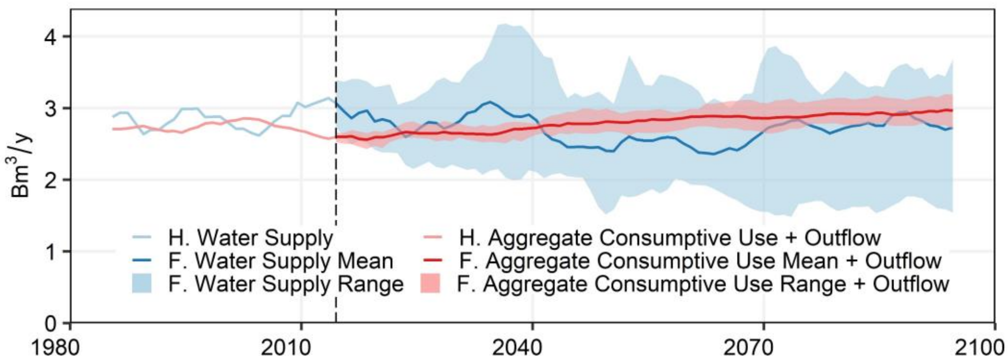

Figure A11. 10-year running mean of annual water supply and aggregate consumptive use. The lighter lines are the historical values, and the darker lines are the means of the future baseline scenarios. The areas around the means present the maximum and minimum values of the future baseline scenarios

7. Annual Required Water Diversions and Shortages: Total, Model Region, and Aggregate Users

To better understand Basin, we aggregate the required water diversion by Ag and Urban in each of the five regions (Figure A12). Figure A12b shows that urban increased water diversion is predicted in the Central region, followed by South Metro and North region. In contrast, the North region has the highest Ag water required diversion, followed by North Central and East regions. Figure A12a illustrates that the total Ag required diversion is approximately 3.08 BCM/y. In comparison, the urban needed diversion is almost doubled by the end of the century, reaching about 1.85 BCM/y, which is still lower than Ag required diversion. Figure A13 shows the required diversion of the aggregate users in each model region, followed by the shortage of these users in Figure A15.

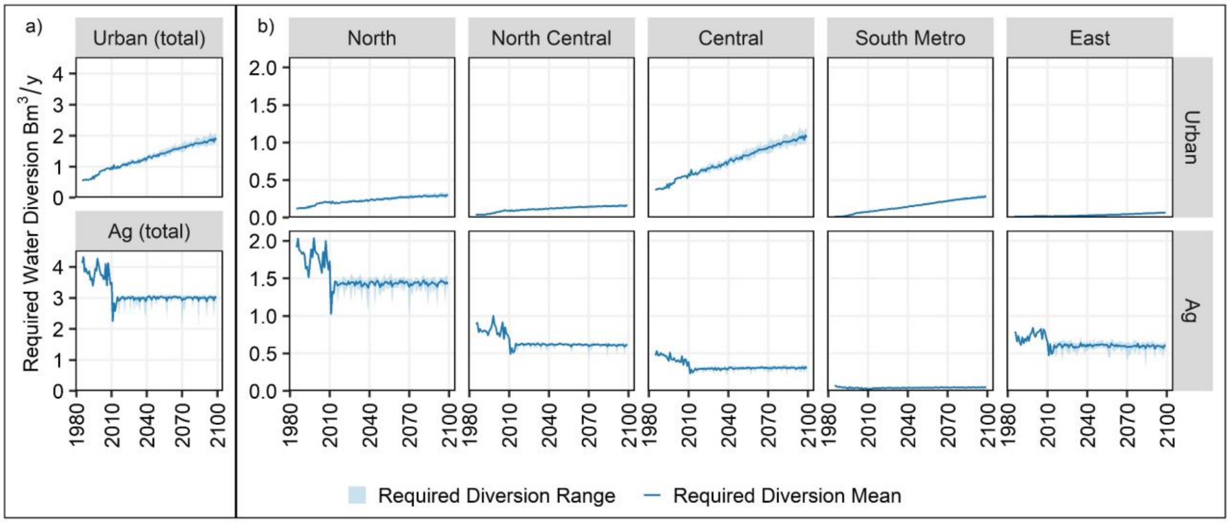

Figure A12: Future baseline Annual Required Water Diversion (Total and by Model Region)

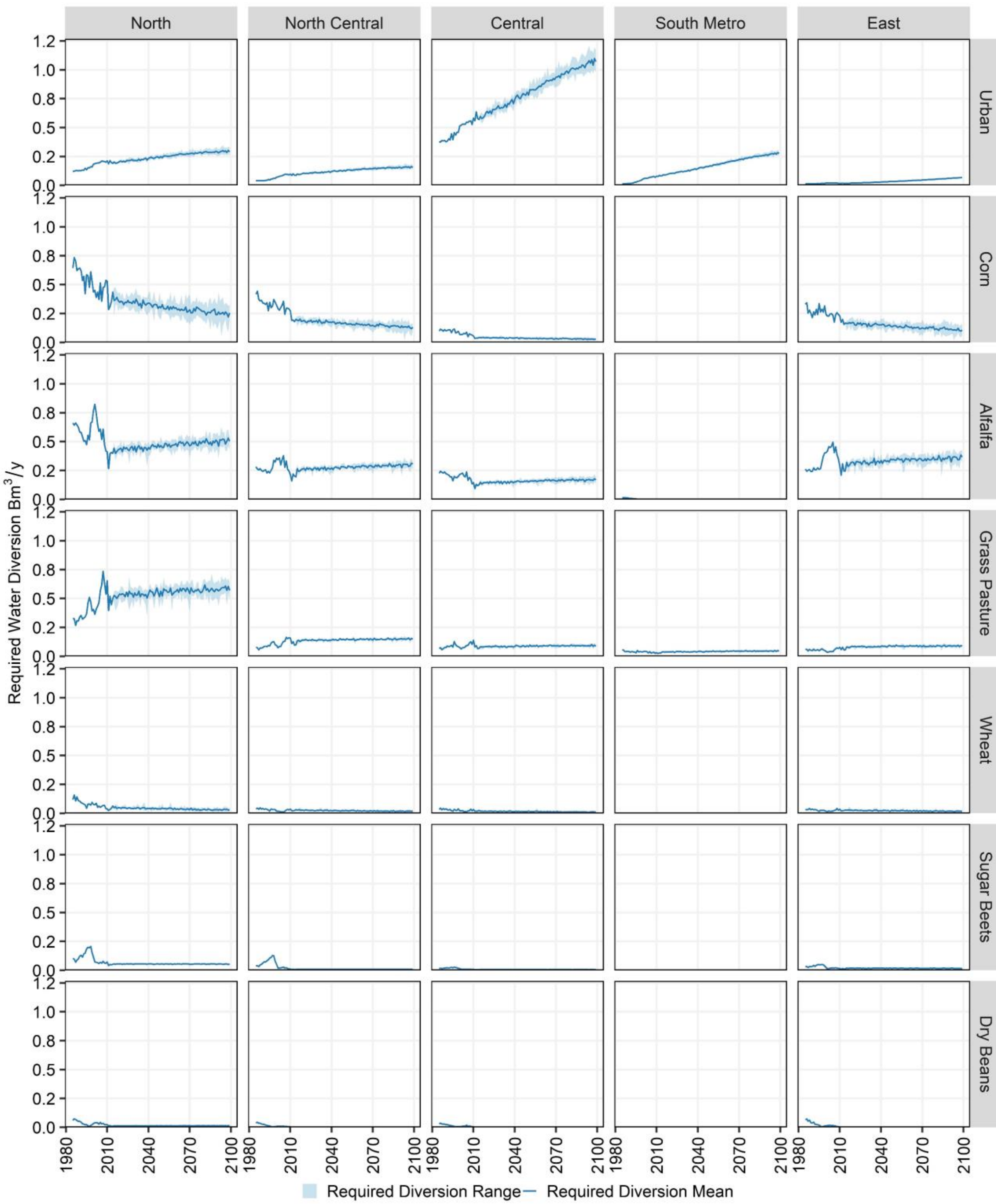

Figure A13: Future baseline Annual Required Diversion for aggregated users in each region.

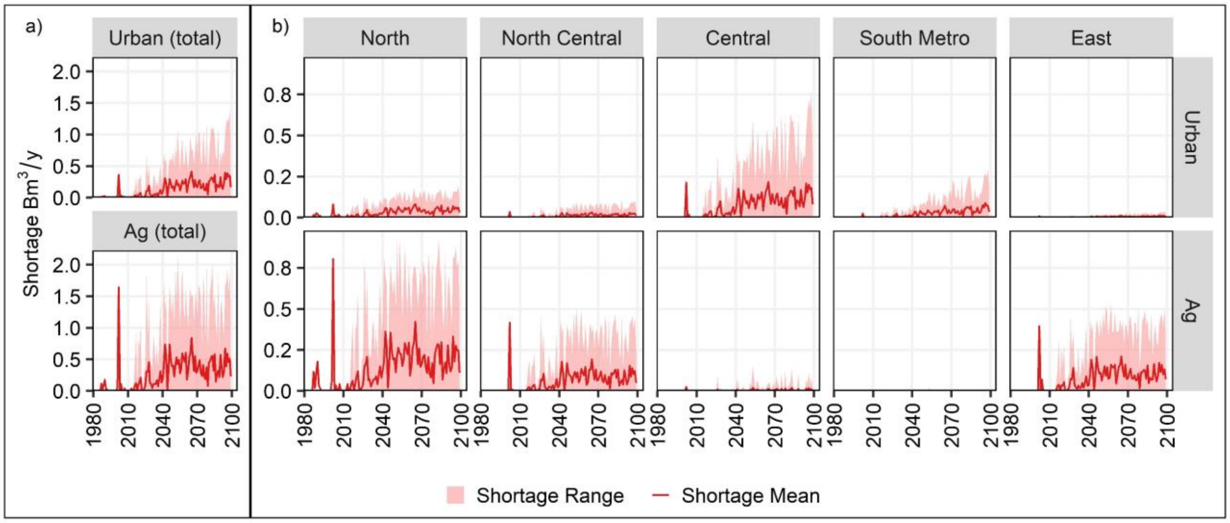

Figure A14. Future baseline annual water shortage (total and by model region)

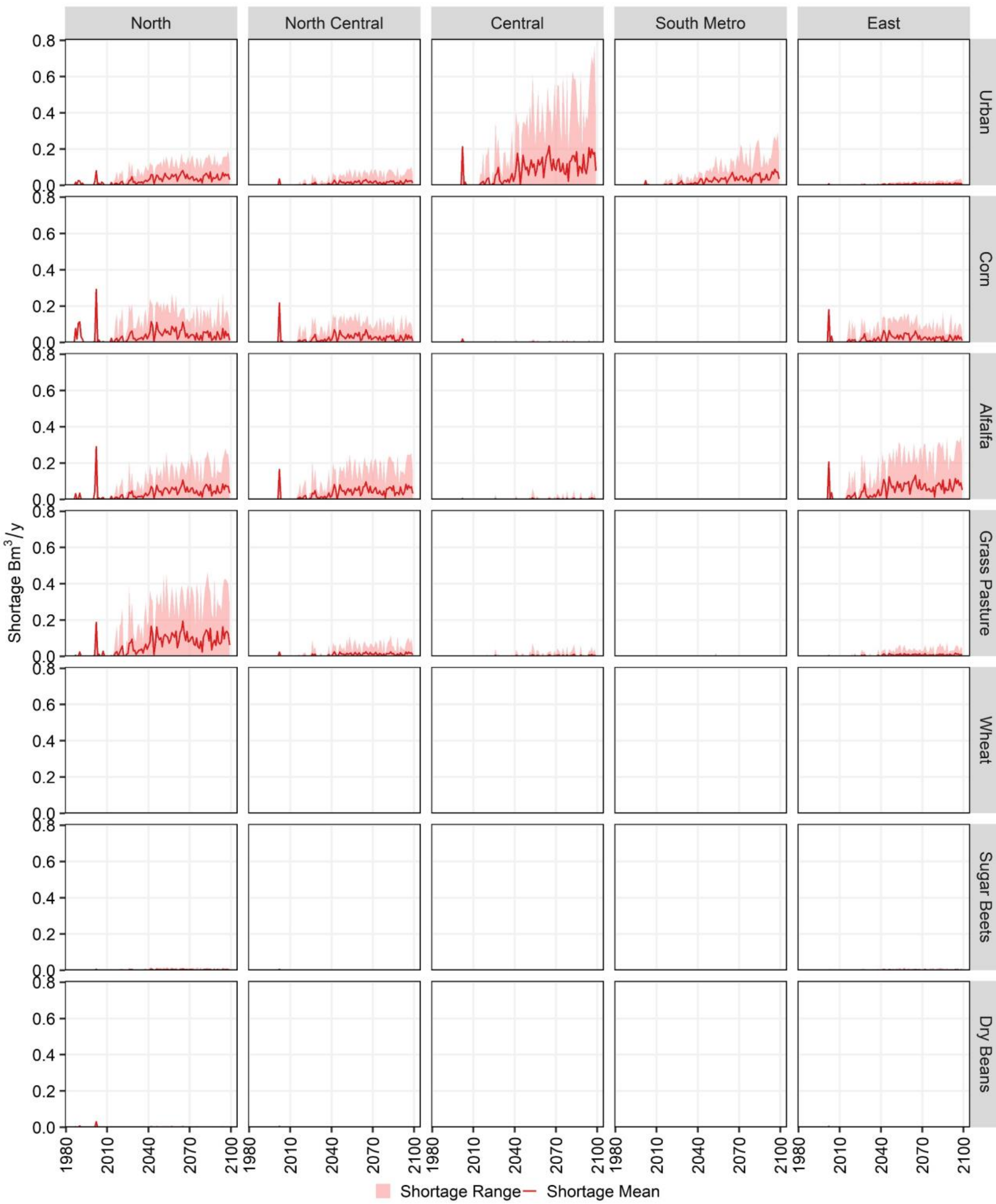

Figure A15. Future baseline Annual Shortage for aggregated users in each region.

8. 30-year annual average results

Table A3. 30-year annual total water supply, required diversion, shortage, and shortage percentage means

Scenario	Historical	Future Scenario	Hot 4.5	Hot 8.5	Warm 4.5	Warm 8.5	Wet 4.5	Wet 8.5	Dry 4.5	Dry 8.5
Total Supply (BCM/y)	2.86	Near	2.66	2.6	2.34	2.85	3.4	2.96	2.71	2.08
		Far	2.71	2.62	3.22	3.06	3.24	3.28	2.54	1.58
Outflow (BCM/y)	0.66	Near	0.69	0.62	0.38	0.71	1.3	0.85	0.75	0.39
		Far	0.6	0.58	0.91	0.72	1.1	1.09	0.47	0.15
Diversion (BCM/y)	4.43	Near	4.3	4.35	4.25	4.23	4.2	4.22	4.25	4.31
		Far	4.8	4.92	4.66	4.72	4.62	4.71	4.71	4.92
Shortage ratio	0.1	Near	0.5	0.62	0.43	0.14	0.13	0.19	0.47	0.95
		Far	0.66	0.95	0.05	0.02	0.27	0.31	0.54	2.05
Shortage (%)	2.2	Near	11.2	13.9	9.9	3.3	2.9	4.3	10.7	21.4
		Far	13.5	19	1	0.5	5.7	6.3	11.3	41.3

9. Effectiveness of Alternative Adaptation Strategies for Reducing Shortages

The conducted analysis in section 3.2 represents sensitivity analysis for water demand, storage capacity, and water supply. Figure 6 in the manuscript represents the range of the results, and Figure A16 represents climate scenarios (a: for the near future, b: for the far future). From this figure, we can conclude that the performance of the tested strategies is the same across the climate scenarios, and we can select some of them to perform a more detailed analysis.

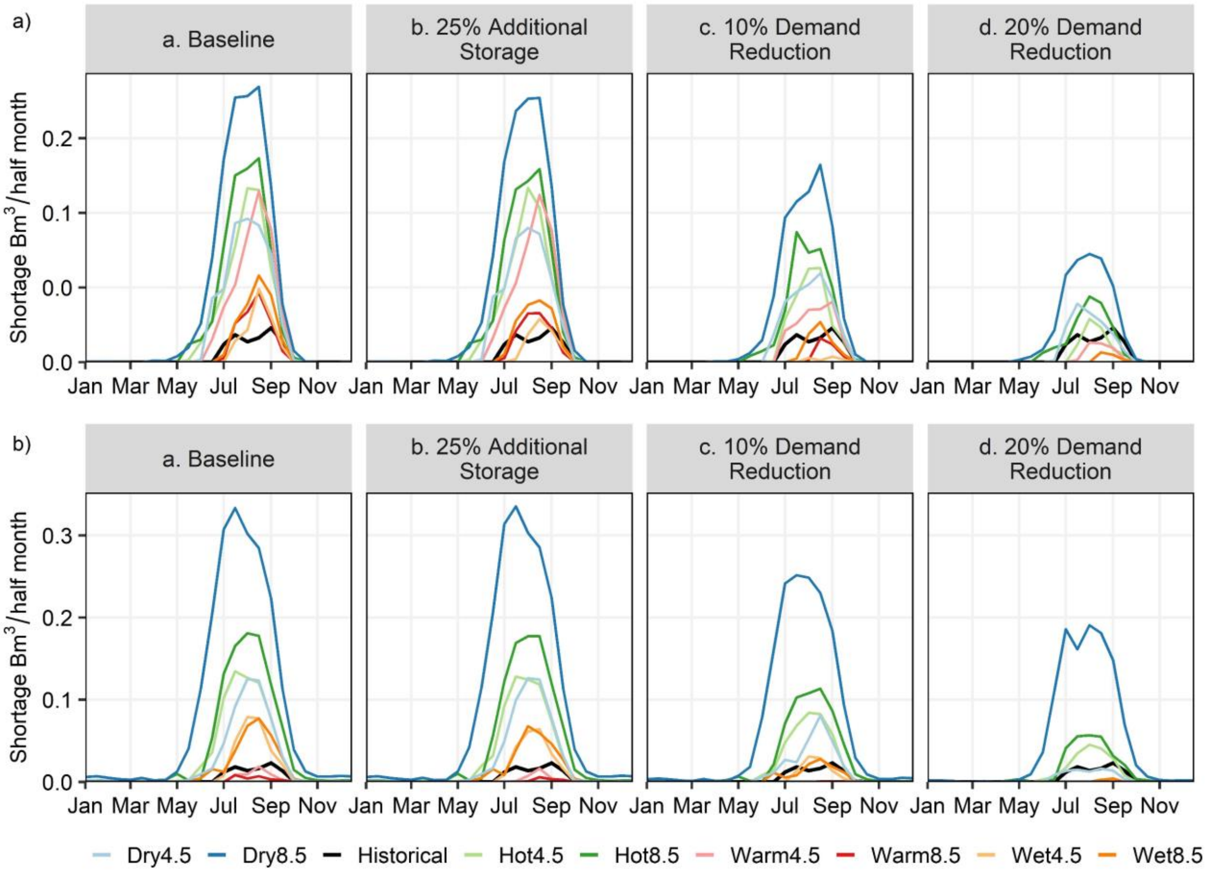

Figure A16. 30-year half-monthly shortage means of future baseline scenarios and the three alternative adaptation strategies with the historical mean. a) near future, b) far future.

10. Uncertainty Analysis

Table A4. WEAP parameters definitions.

Parameter		Mean	Min.	Max.	Calculation	WEAP Definition	Used in the Sobol Analysis
Ag Demand (Net crop irrigation requirements)							
Delivery Efficiency (%)	Ag	80			Manual Calibration and Regression Model	Not a WEAP parameter	
Application Efficiency (%)	Ag Flood	46.4	35	65			
	Ag Sprinkler	71.4	60	90			
Consumption (%)	Ag Flood	37.1	28	52	Del Eff * App Eff	Return Flow = Simulated Diversions * (1 - Consumption)	YES, as latent variable
	Ag Sprinkler	57.1	48	72			YES, as latent variable
Loss Rate (%)	Ag Flood	62.9	48	72	1- Del Eff * App Eff or 1 - Consumption	Required Diversion = Demand / (1 - Loss Rate)	Calculated
	Ag Sprinkler	42.9	28	52			Calculated
Urban Demand (Urban water demand in cities)							
Delivery Efficiency (%)	Urban	75			Manual Calibration	Not a WEAP parameter	YES
Water use Efficiency (%)	Urban Outdoor	71					NO (Fixed in IUWM simulations)
	Urban Indoor	20					YES
Consumption (%)	Urban Indoor	15			Del Eff * Water use Eff	Return Flow = Simulated Diversion * (1 - Consumption)	Calculated
	Urban Outdoor	53.3					Calculated
Loss Rate (%)	Urban Indoor	25			1 - Del Eff	Required Diversion = Demand / (1 - Loss Rate)	Calculated
	Urban Outdoor	25					Calculated
Losses from return flow from demand locations							
Loss from return flow (%)	Ag Flood	10			Manual Calibration	Evaporative and leakage losses specified as a percentage of the flow passing through the link	YES
	Ag Sprinkler	13					YES
	Urban Indoor	15					YES
	Urban Outdoor	35					YES

Table A5. Sobol parameter range and first and total indices results

Parameter	minimum	maximum	S1	ST
Loss from return flow (Ag Flood)	5	15	0.4380	0.4754
Consumption (Ag flood), as latent variable	0.9	1.1	0.4356	0.5136
Deliver efficiency (urban)	65	85	0.0273	0.0506
Water use efficiency (urban indoor)	10	30	0.0206	0.0165
Consumption (Ag sprinkler), as latent variable	0.9	1.1	0.0110	0.0063
Loss from return flow (Ag Sprinkler)	8	18	0.0066	0.0065
Loss from return flow (urban indoor)	10	20	0.0043	0.0080
Loss from return flow (urban) outdoor	30	40	0.0005	0.0039

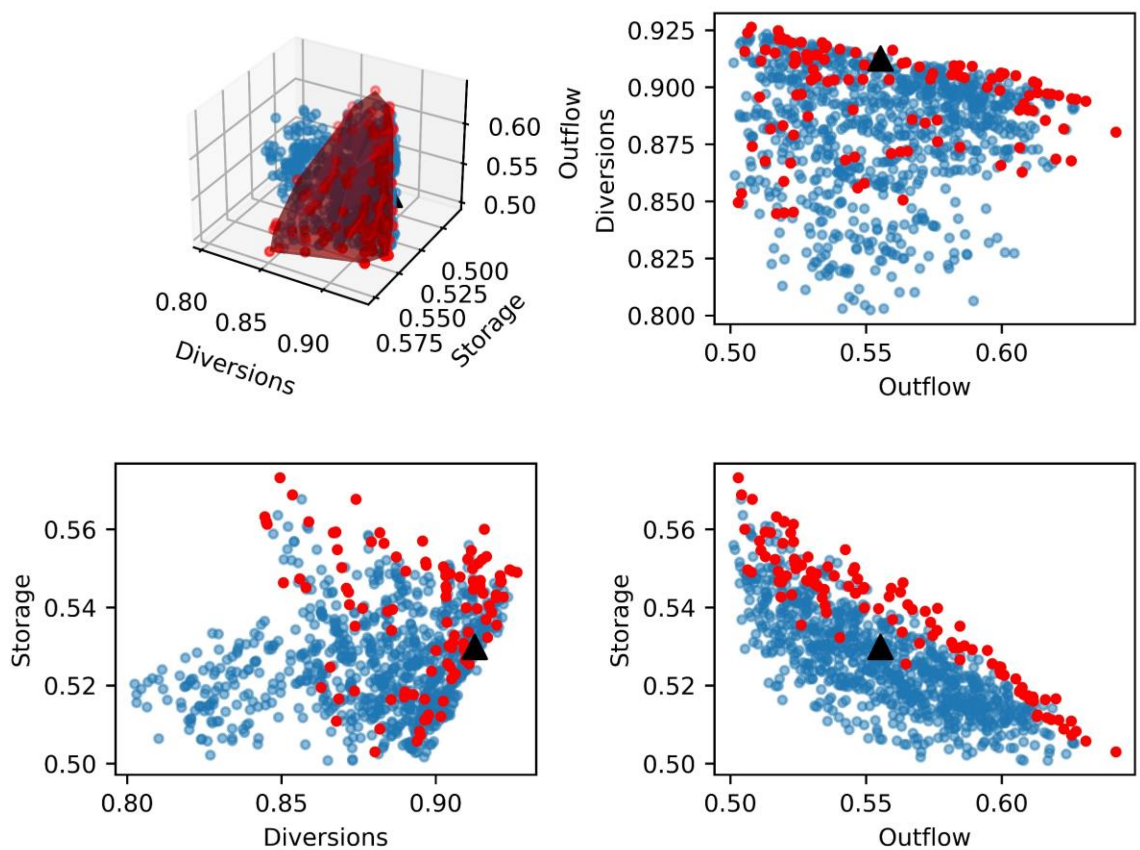

Figure A17. Pareto front for maximizing KGE of the annual diversions, annual outflow and monthly storage.

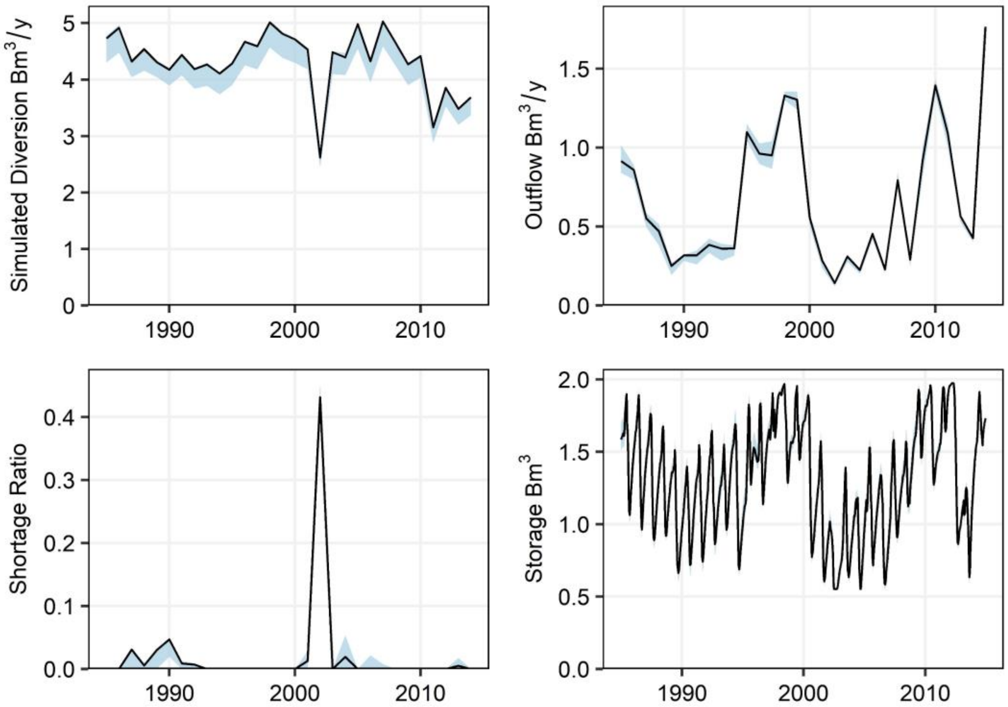

Figure A18. The 95% confidence interval for WEAP historical results for the 108 points on the Pareto front; the black line represents the calibrated parameters' set

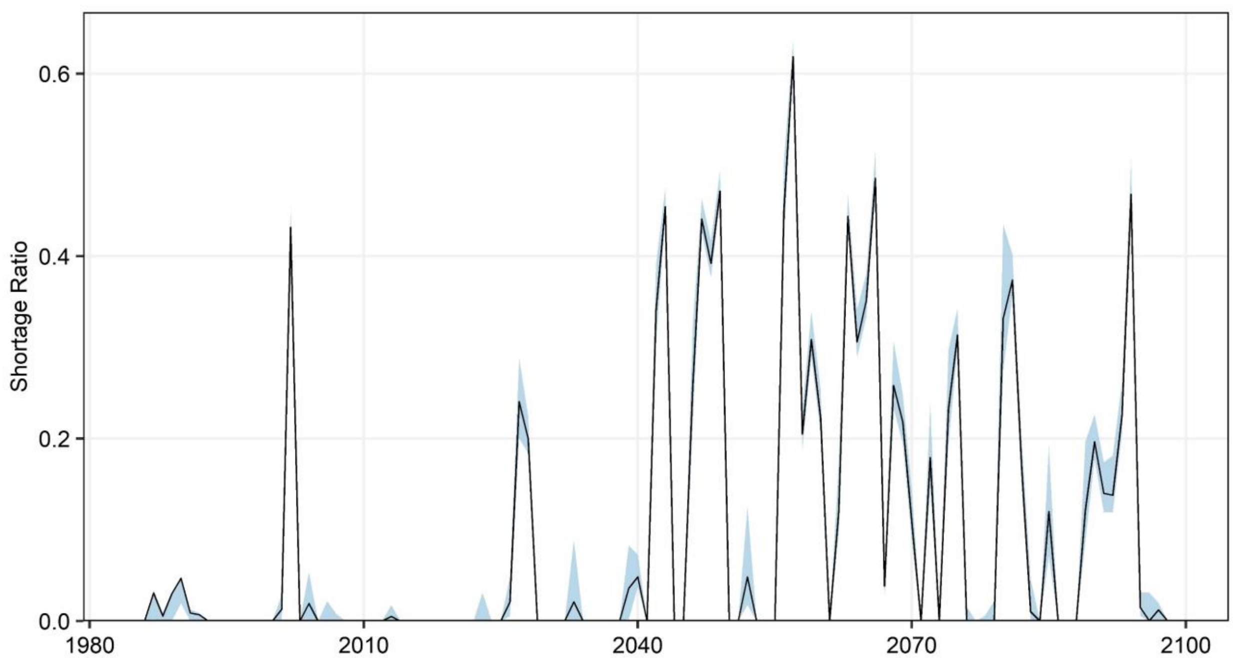

Figure A19. The 95% confidence interval for the shortage ratio (DRY-4.5 scenario) for the 108 points of the Pareto front; the black line represents the calibrated parameters' set.

11. Generalization polynomial model for defining shortage.

From this analysis, we test several regression models to predict y as a function of the three introduced indices. A polynomial regression model (equation A3) suggests that X_1, X_1^2, X_1^3, X_2, and X_3 explain 99.2% of the variation in Y. Figure A20 shows the model residual plot versus predicted y, residual histogram, and normal quantile-quantile plot. These subplots show that this model passes the linearity, homogeneous variance, and normality checks.

This model can be used to predict the y (the 30-year annual shortage mean normalized by the 30-year annual water supply mean) without having to repeat the complete water allocation modeling effort. This model's quadratic and cubic terms highly support the curvilinear relationship between y and X_1, as shown in the manuscript.

$$Y = \beta_1 X_{1\ c,t,i} + \beta_2 X_{1\ c,t,i}^2 + \beta_3 X_{1\ c,t,i}^3 + \beta_4 X_{2\ c,t,i} + \beta_5 X_{3\ c,t,i} \tag{A3}$$

where X_1 is the 30-year annual required diversion mean normalized by the 30-year annual water supply mean (WS), X_2 is the storage capacity normalized by WS, X_3 is the 30-year annual return flow mean normalized by WS, c is for the climate scenario, t is for the simulation period (near or far future), and i for the starting conditions.

Table A6 and Table A7 show other tested models with their parameter estimates and performances.

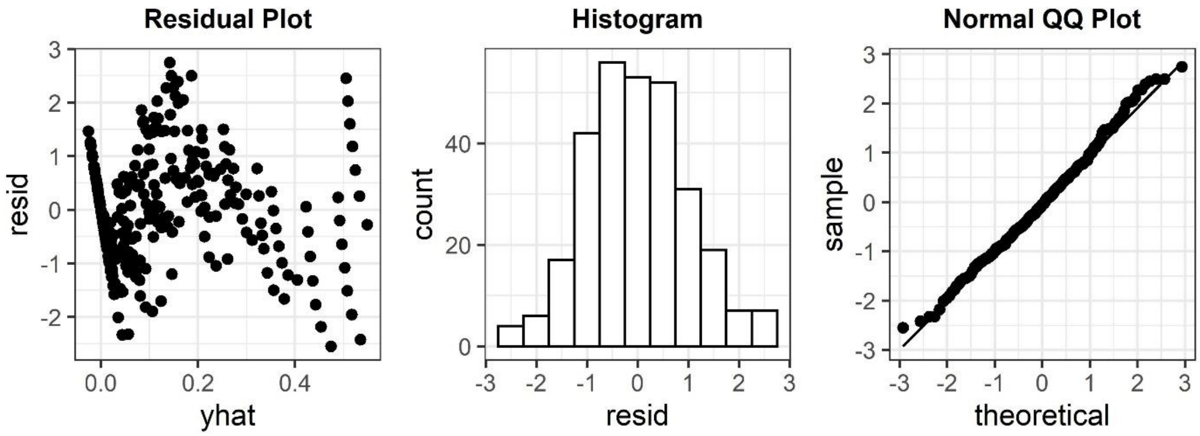

Figure A20. Checking assumptions of the shortage polynomial model

Table A6. Some trails of model fitting showing the best model

Model trail #	AIC*	BIC**	Adjusted R^2	Model
7 (Selected Model)	-1533	-1511	0.9917	$y = \beta_1 x_1 + \beta_2 x_1^2 + \beta_3 x_1^3 + \beta_4 x_2 + \beta_5 x_3$
1	-1348	-1326	0.9724	$y = \beta_0 + \beta_1 x_1 + \beta_2 x_1^2 + \beta_3 x_1^3 + \beta_4 x_2$
8	-1233	-1214	0.9588	$y = \beta_0 + \beta_1 x_1 + \beta_2 x_2 + \beta_3 x_3$
9	-1127	-1112	0.9407	$y = \beta_0 + \beta_1 x_1 + \beta_2 x_2$

* AIC: Akaike Information Criterion

** BIC: Bayesian information criterion

Table A7. P values of some trails of model fitting

Model	Intercept	X_1	X_1^2	X_1^3	X_2	X_3
7 (Selected Model)		1.84E-34	7.19E-25	1.49E-69	6.83E-26	5.62E-50
1	2.84E-10	3.81E-20	1.88E-47	2.89E-44	2.64E-21	
8	2.40E-18	2.25E-135			8.54E-13	8.38E-25
9	1.39E-77	9.04E-176			1.50E-09	

12. Return Flow ratio to water supply.

Water diversions are higher than the water supplies; hence water is used several times to fulfill the required diversions through the return flow. Return flow plays an essential role in fulfilling the required diversions as water is used several times in the basin, which is more than doubled in some conditions (Figure A21). The baseline conditions (shown by the X) range from 0.75 to 1.2, indicating the high dependency of meeting the required diversions on the return water.

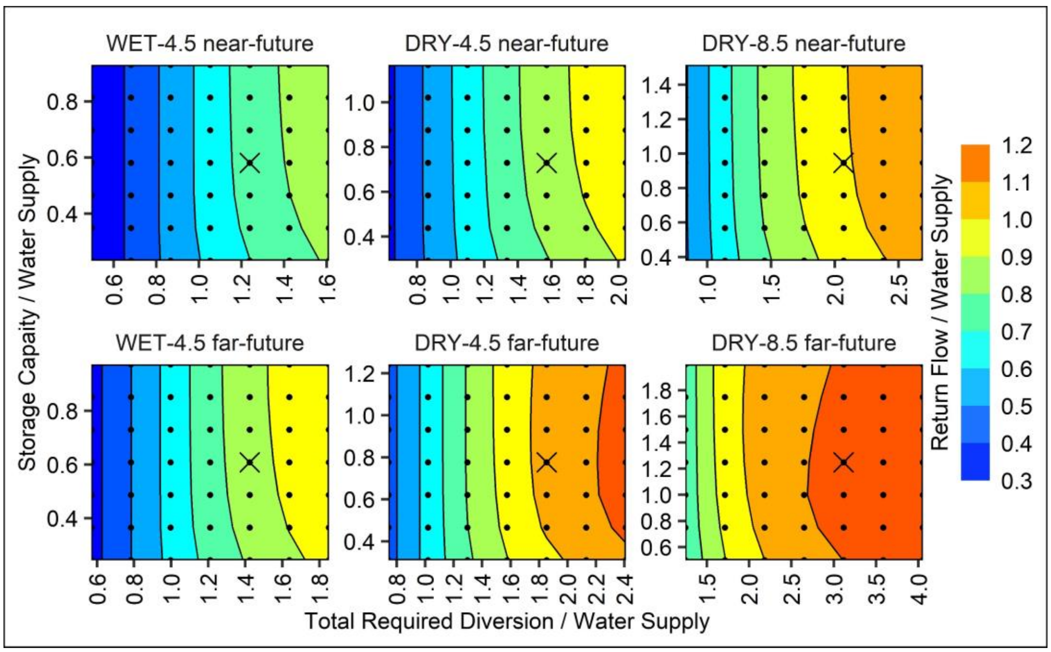

Figure A21. The 30-year return flow ratio to the water supply (X_3) at different starting conditions -the dots- of required diversion (X_1) and storage (X_2); each subplot represents one 30-year period; the cross represents the future baseline conditions for each scenario.

13. Statistical Evidence of Storage Threshold

Equation A4 (linear model1) tests the significance of a dummy variable (D) that indicates a threshold level. D is equal to one if X_2 is greater than a threshold and zero otherwise. Figure A22 shows the β_3 estimates at different threshold runs using equation A3 (with its significant level; significant if P-value is less than 0.05. β_3 is significant if the threshold is below 0.64 with negative values or above 1.26 with positive values. These results match the contour maps in the manuscript.

$$Y_{c,t,i} = \alpha + \beta_1 * X_{1\ c,t,i} + \beta_2 * X_{2\ c,t,i} + \beta_3 * D \quad \text{(A4)}$$

where X_1 is the 30-year annual required diversion mean normalized by the 30-year annual water supply mean (WS), (X_2) the storage capacity normalized by WS, D equals one if X_2 >= threshold and zero otherwise, c is for the climate scenario, t is for the simulation period (near or far future), and i for the starting conditions.

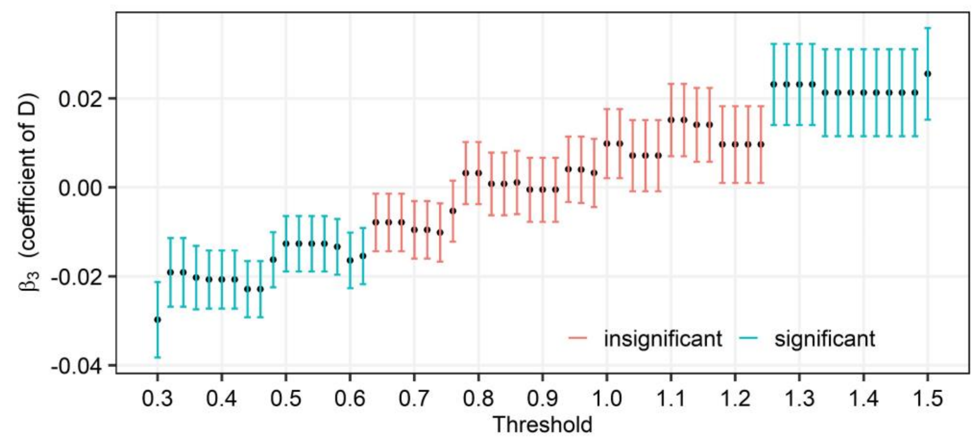

Figure A22. β3 estimates from several thresholds runs 0.3:1.5 using the linear model presented in equation (A3), with colors indicating the significance (Pvalue <0.05) of β3 of each run.

14. Discussion about VIC model bias correction

This section shows the VIC results generated using the historical climate and the MACA downscaled climate datasets and their statistical comparison for the period of 1985-2014. Table A8 shows the Kolmogorov-Smirnov P-values between the annual water yield generated using the historical climate and the MACA downscaled climate datasets. All the scenarios except for the DRY 8.5, have a P-Value greater than 0.05 suggesting that we cannot reject the null hypotheses that they follow the same distribution of the results generated from the historical climate.

Table A8. Kolmogorov-Smirnov P-values between the annual water yield generated using the historical climate and the MACA downscaled climate datasets

Climate Scenario	***KS P-Value***
Hot 4.5	0.3929
Warm 4.5	0.1350
Wet 8.5	0.1350
Hot 8.5	0.1350
Dry 4.5	0.1350
Warm 8.5	0.0709
Wet 4.5	0.0709
Dry 8.5	0.0156

Additionally, Figure A23 presents a graphical representation of the distribution of the VIC results from the historical and climate scenarios. Figure A23a shows the box plots and the distribution density of the half monthly VIC water yield using the historical and downscaled climate datasets. The results support the matching between both data sets except for some extreme events which may be important for flood analyses that is out of the scope of this study. -ggplot package is used in R to compute the box plots and the density graphic-

Figure A23b and Figure A23c show the empirical cumulative distribution function (ECDF) for the half monthly and yearly water yield, highlighting the very close behavior between the historical and downscaled climate datasets except for the Dry 8.5 scenario. -R is used to compute the ecdf-

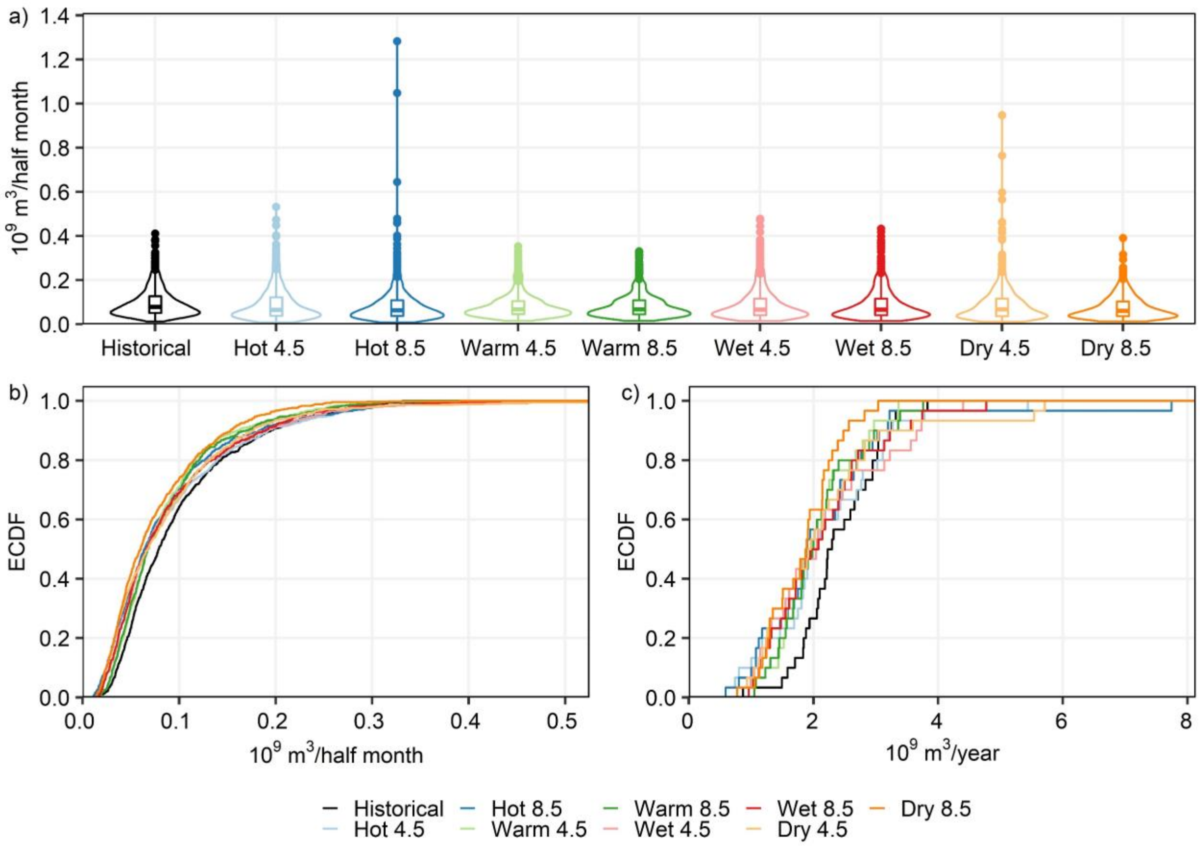

Figure A23. a) The box plots with the distribution density of the half monthly water yield from VIC for the historical and the MACA downscaled climate data sets for the period of 1985-2014. b) The empirical cumulative distribution function (ECDF) of the half monthly water yield from VIC for the historical and the MACA downscaled climate data sets for the period of 1985-2014. c) The ECDF for the yearly water yield from VIC for the historical and the MACA downscaled climate data sets for the period of 1985-2014.

APPENDIX B

SUPPORTING INFORMATION FOR CHAPTER 3:

INTEGRATED LAND USE PLANNING AND WATER MANAGEMENT UNDER DIFFERENT WATER RIGHTS INSTITUTIONS: METHODOLOGY AND APPLICATION

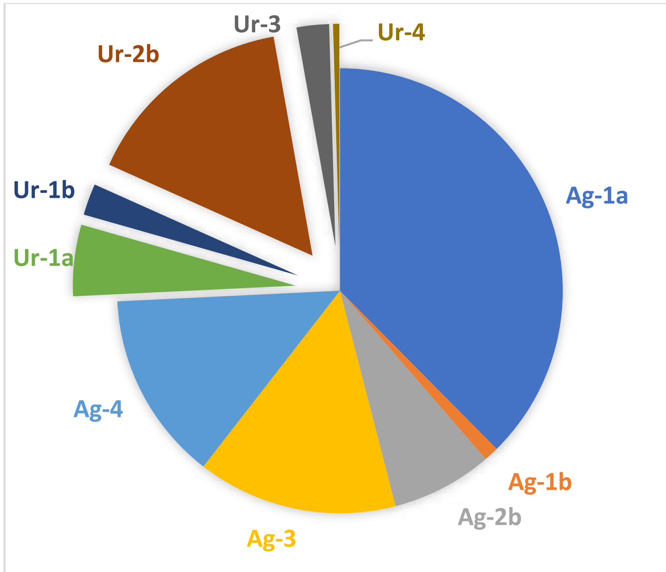

Figure B1. Water Demand percentages by regions and sectors (Ag or Urban) in the 2014 baseline.

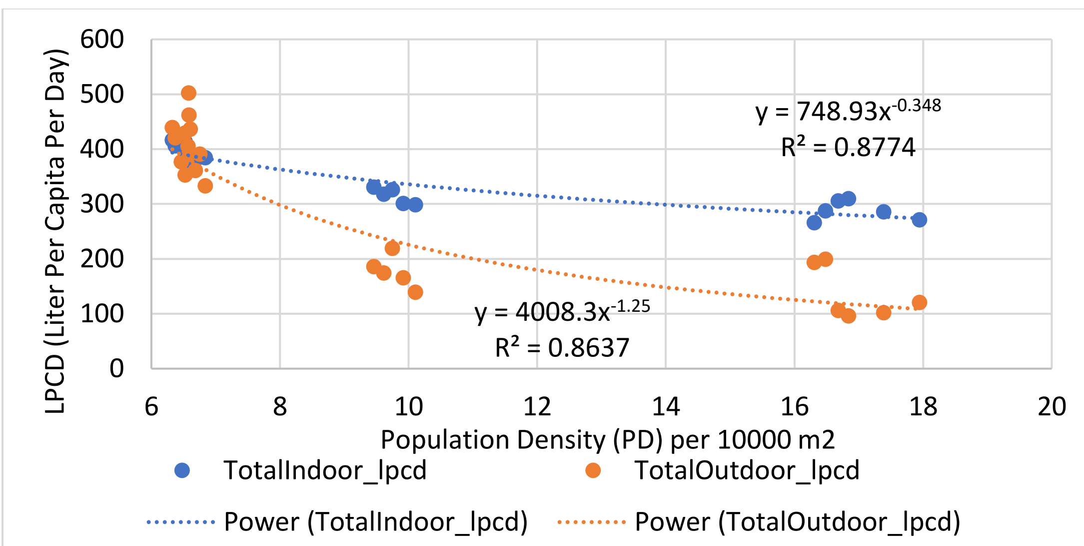

Figure B2. Indoor and outdoor lpcd as a function of population density

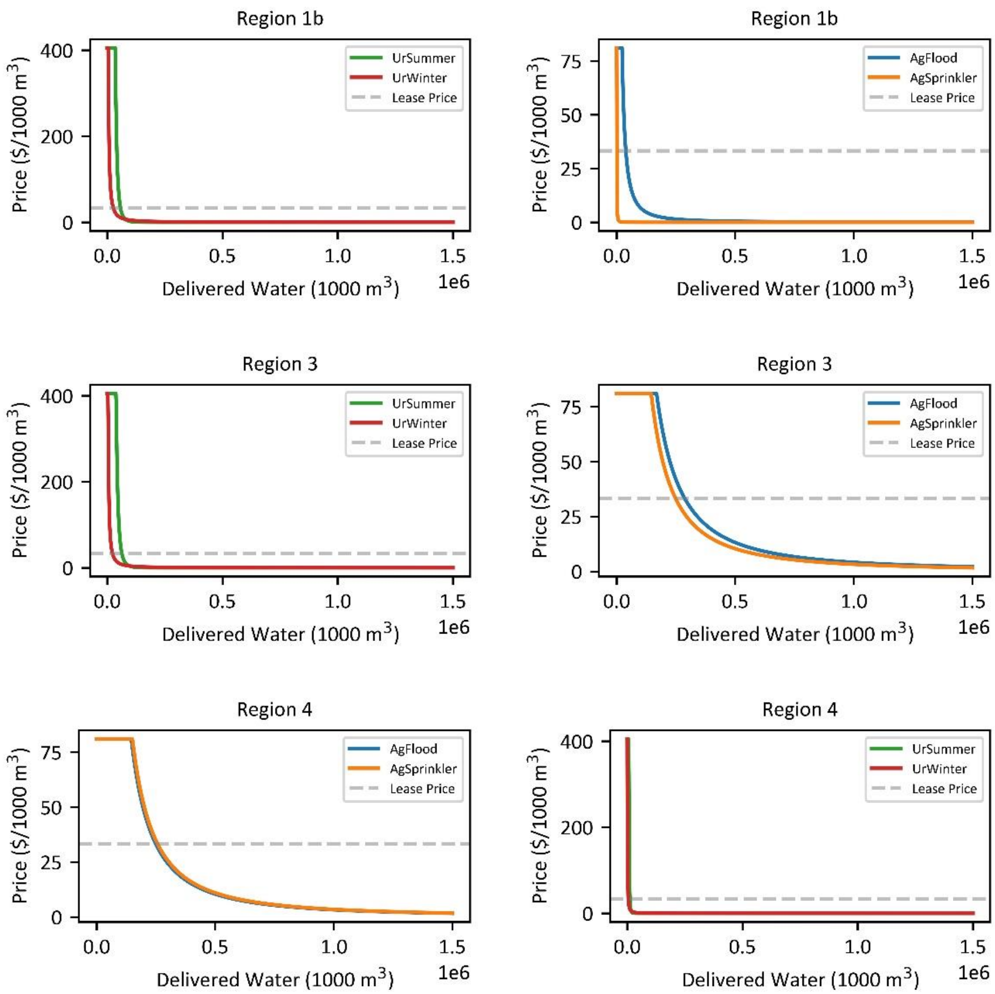

Figure B3. Demand functions for each water demand sector in other regions omitted in the main manuscript.

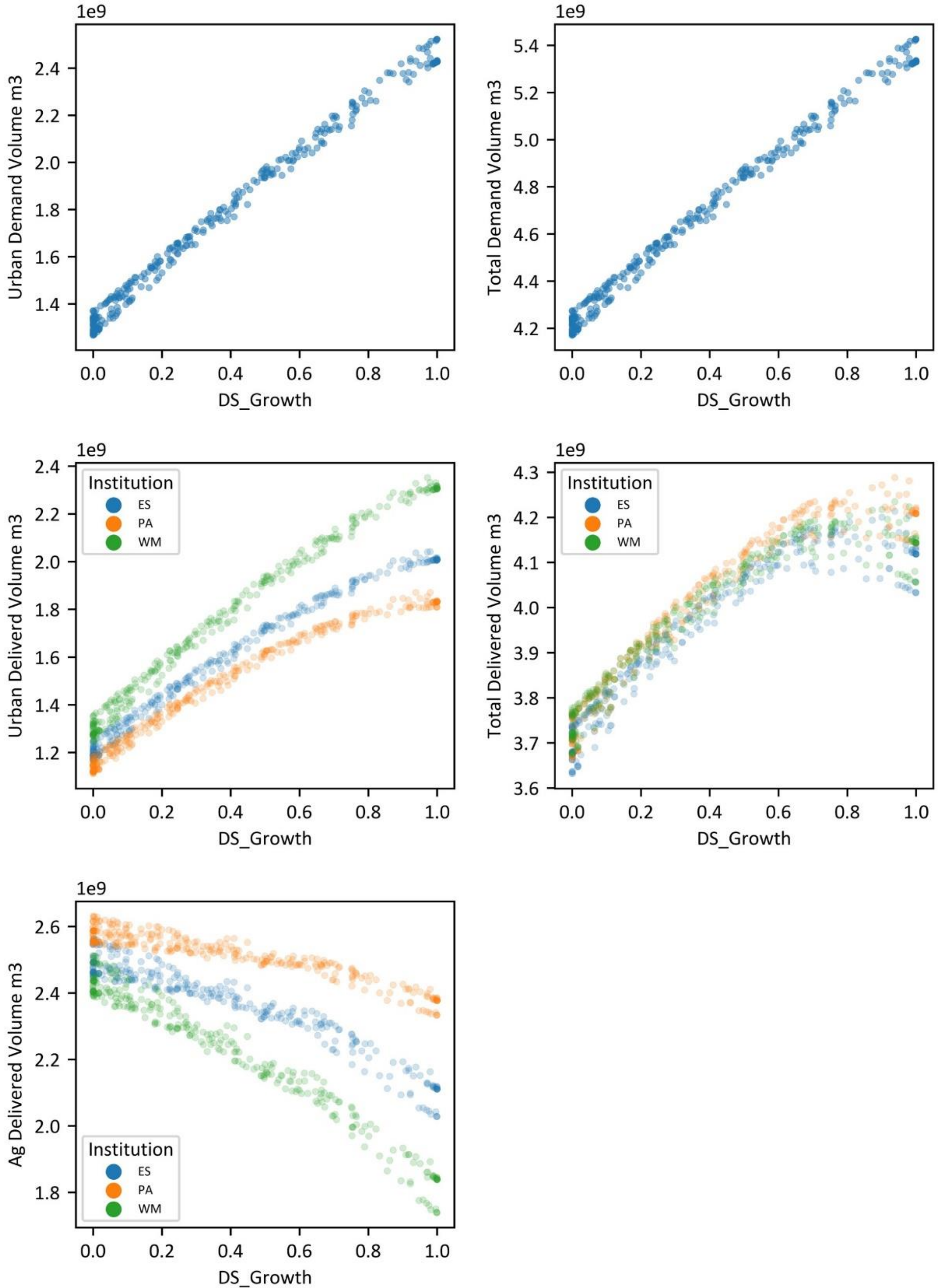

Figure B4. Scenario 2 demands and deliveries.

APPENDIX C

SUPPORTING INFORMATION FOR CHAPTER 4:

WATER DEMAND AND SHORTAGES PROJECTION UNDER SUPPLY MANAGEMENT, CLIMATE CHANGE AND SOCIOECONOMIC PATHWAYS IN THE UNITED STATES

1. CONUS Regions

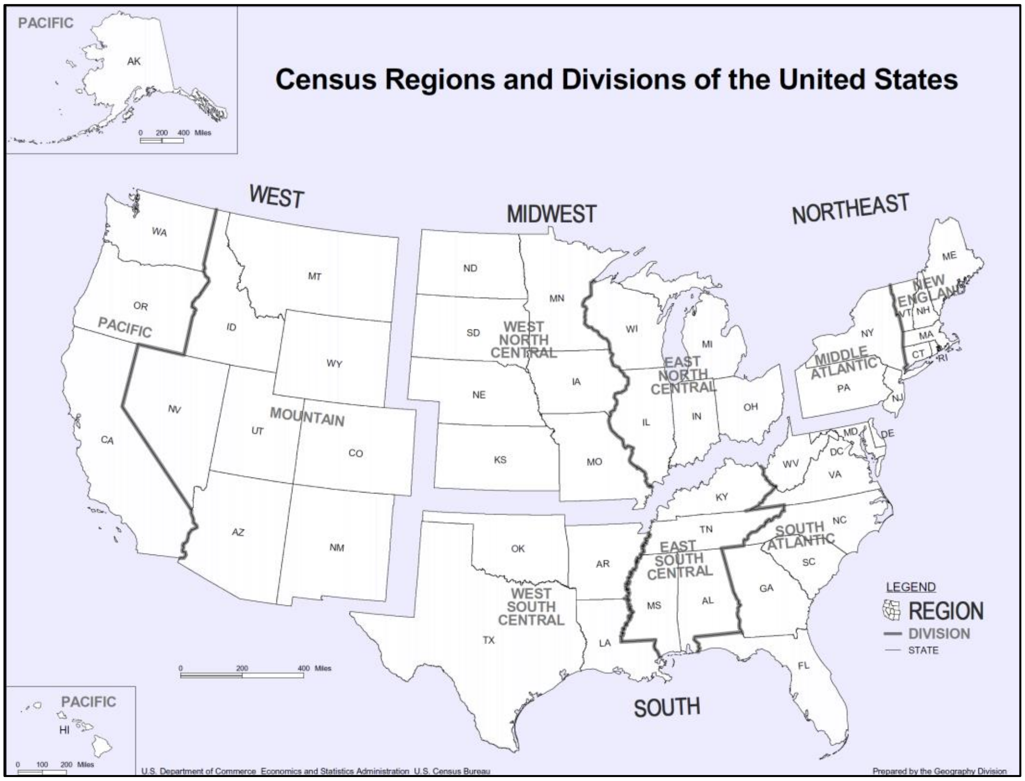

Figure C1. CENSUS regions.

2. Projected drivers by regions.

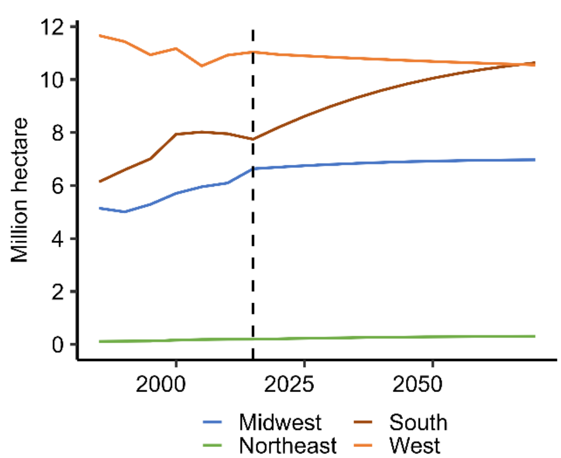

Figure C2. The projected irrigated hectares in each region.

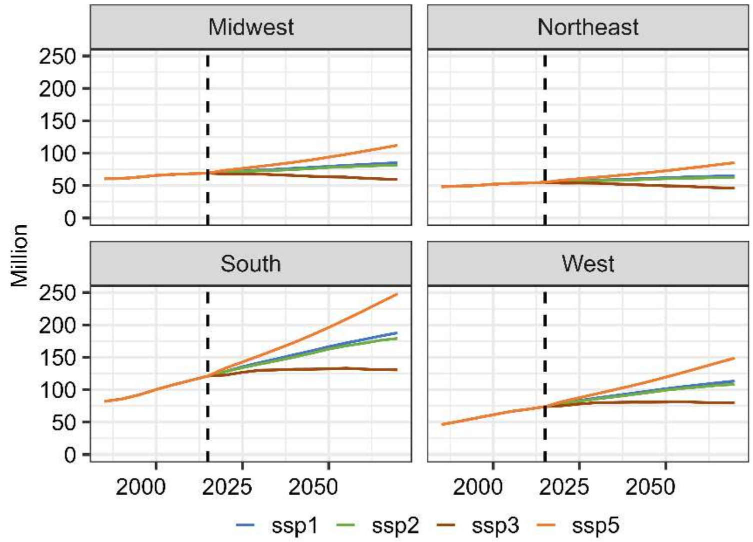

Figure C3. The projected population in each region under SSPs 1, 2, 3, and 5.

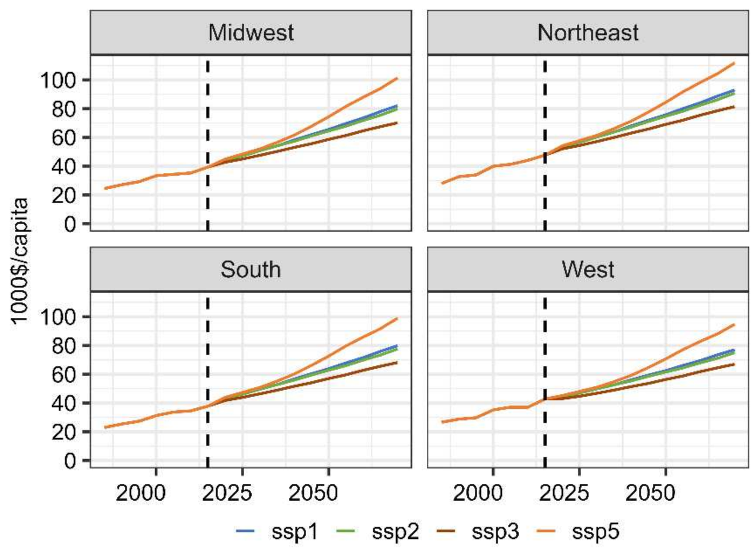

Figure C4. The projected personal per capita income in each region under SSPs 1, 2, 3, and 5 in 2005$.

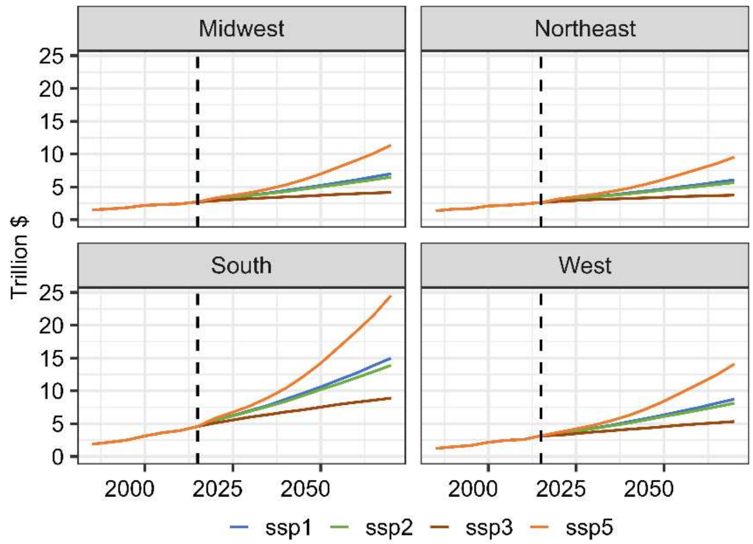

Figure C5. The projected total personal income in each region under SSPs 1, 2, 3, and 5 in 2005$

3. Withdrawals and consumptive use by sectors and regions

3.1. Midwest region projections

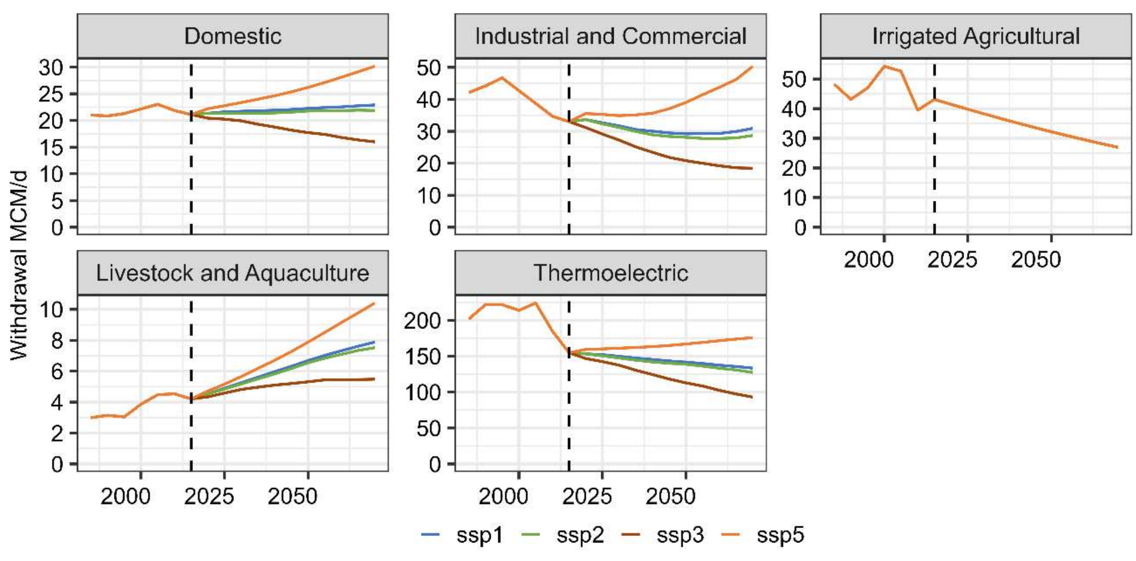

Figure C6. Midwest annual withdrawals

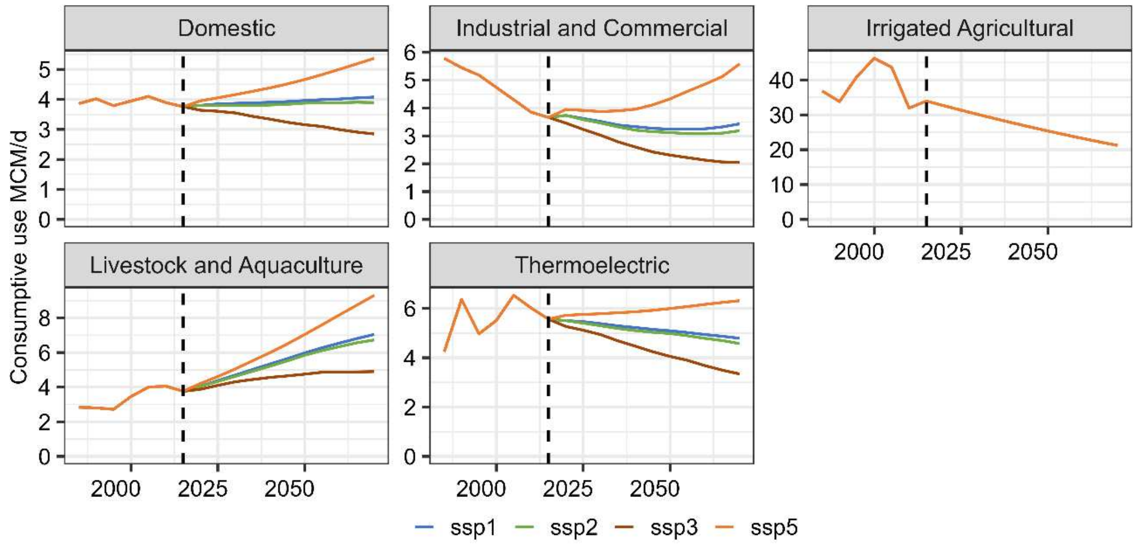

Figure C7. Midwest annual consumptive use

3.2. Northeast region projections

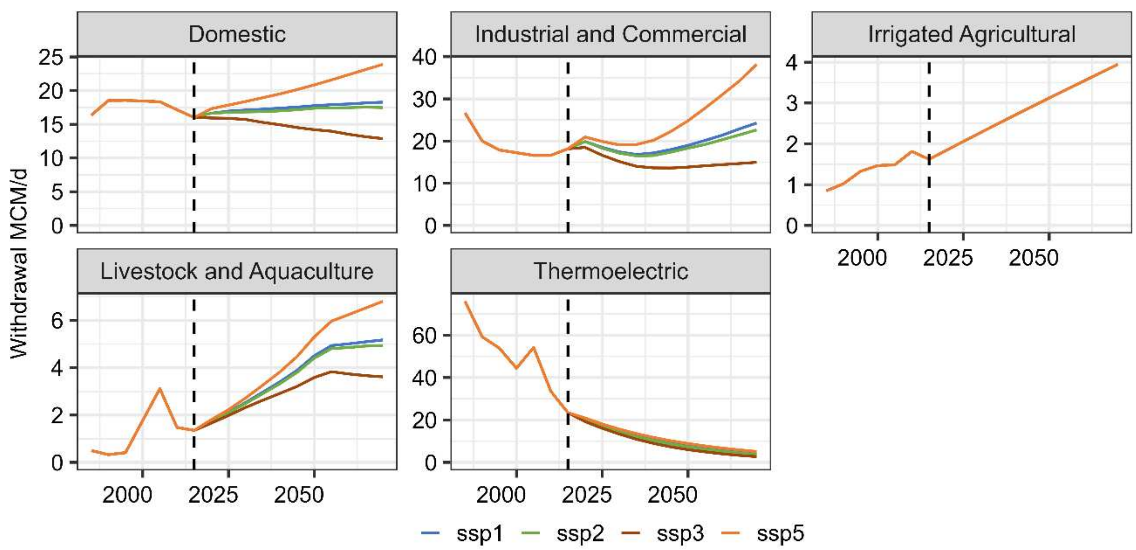

Figure C8. Northeast annual withdrawals

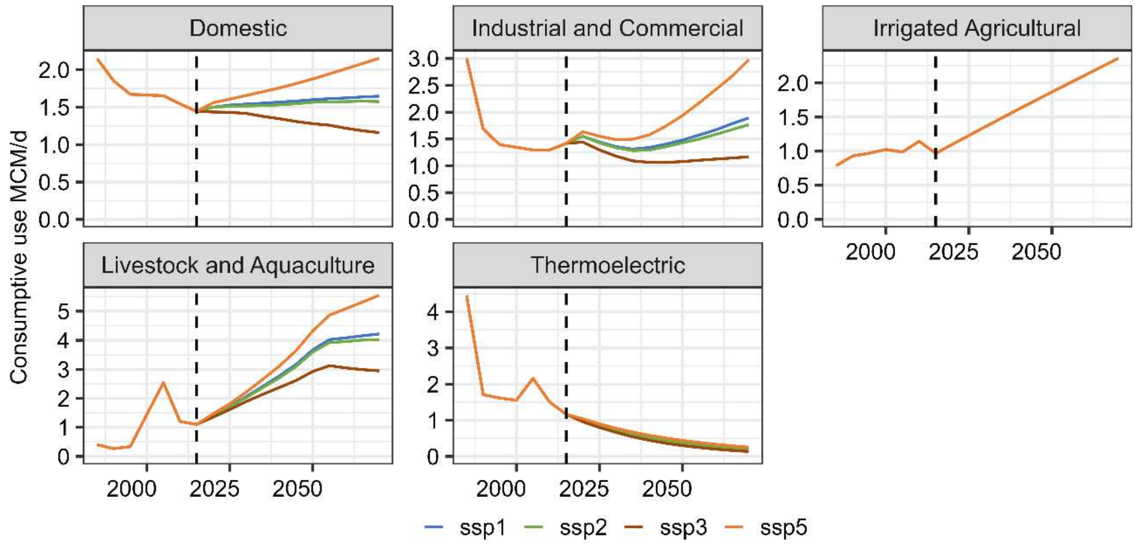

Figure C9. Northeast annual consumptive use

3.3. South region projections

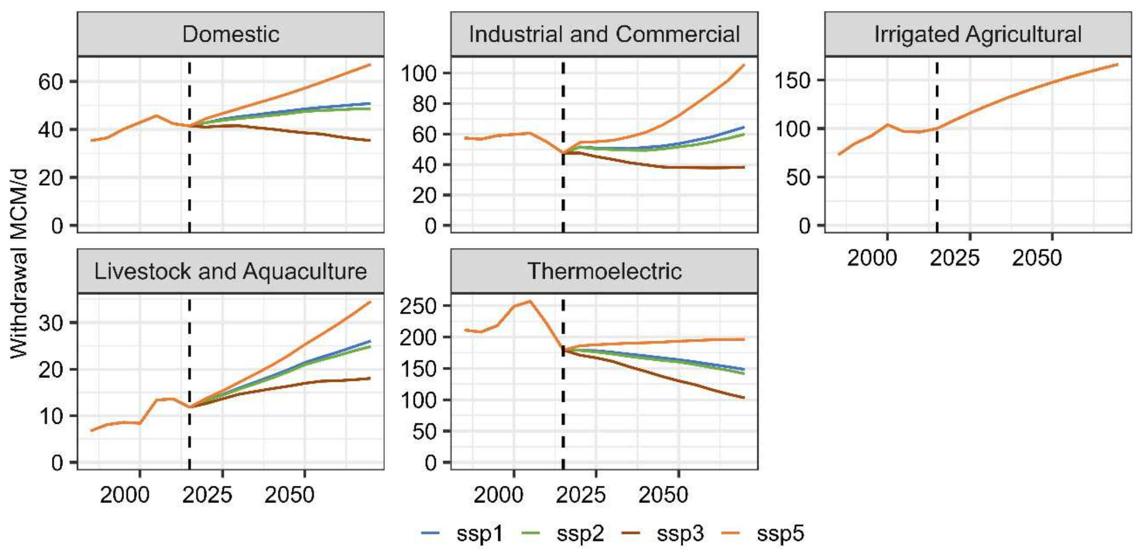

Figure C10. South annual withdrawals

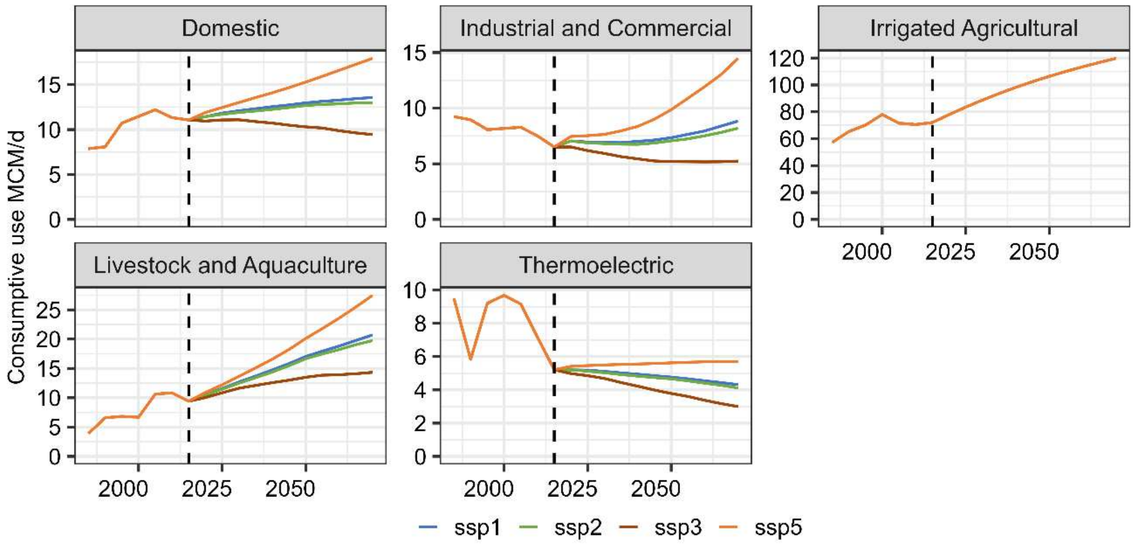

Figure C11. South annual consumptive use

3.4. West region projections

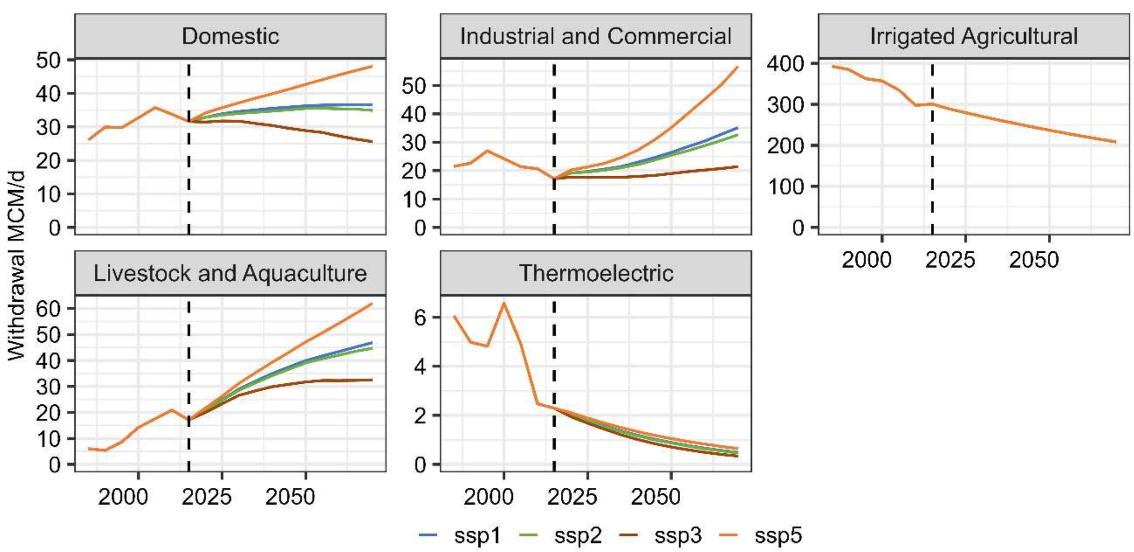

Figure C12. West annual withdrawals

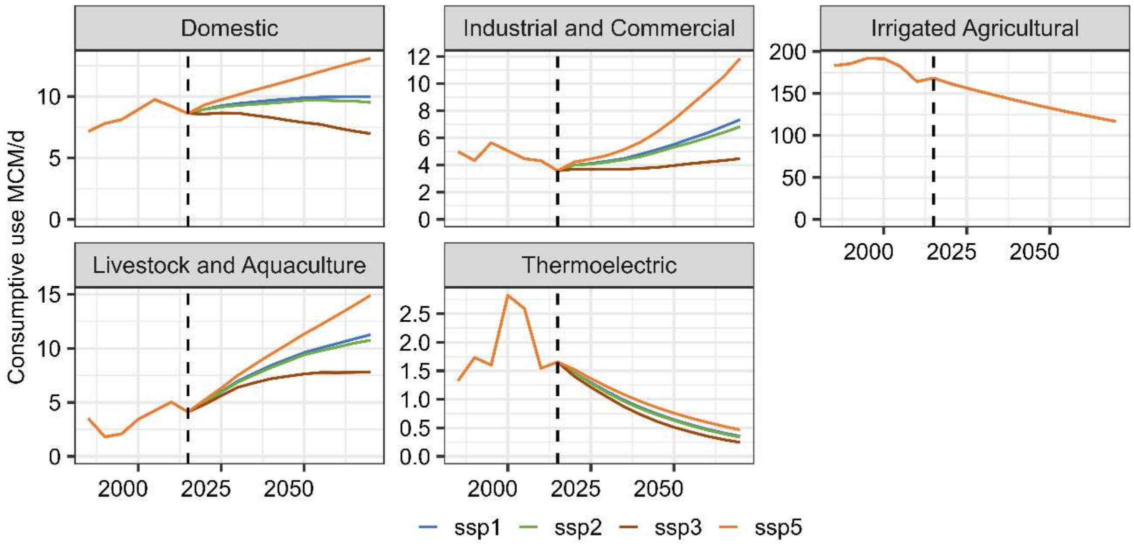

Figure C13. West annual consumptive use